北京大学
PEKING UNIVERSITY

Pion Photoproduction at Low Energies

Yao Ma (马垚)

In collaboration with Wen-Qi Niu, De-Liang Yao and Han-Qing Zheng

10th July, 2020

Contents

1. Backgroud

1.1 Hidden Pole in S_{11} Channel

PKU Representation

[1] Z. G. Xiao and H. Q. Zheng, Nucl. Phys. A695, 273 (2001).
[2] J. Y. He, Z. G. Xiao, and H. Q. Zheng, Phys. Lett. B536, 59 (2002).
[3] H. Q. Zheng et al., Nucl. Phys. A733, 235 (2004).
[4] Z. Y. Zhou et al., JHEP 02, 043 (2005).
[5] Z. Zhou and H. Zheng, Nucl. Phys. A775, 212 (2006).

$$S(s) = \prod_b S_b \prod_v S_v \prod_r S_r \times e^{2i\rho f(s)}$$

$$f(s) = \frac{s}{2\pi \mathrm{i}} \int_L ds' \frac{\mathrm{disc} f\left(s'\right)}{\left(s'-s\right) s'} + \frac{s}{2\pi \mathrm{i}} \int_{\mathrm{R}'} ds' \frac{\mathrm{disc} f\left(s'\right)}{\left(s'-s\right) s'}$$

Subthreshold resonance $N^*(890)$ on the second Riemann sheet

[6] Y. F. Wang, D. L. Yao, and H. Q. Zheng, Chin. Phys. C43, 064110 (2019).
[7] Y. F. Wang, D. L. Yao, and H. Q. Zheng, Front. Phys. 14, 1 (2019).
[8] Y. F. Wang, D. L. Yao, and H. Q. Zheng, Eur. Phys. J. C78, 543 (2018).

Figure 1. PKU representation analysis of πN scattering phase shift.

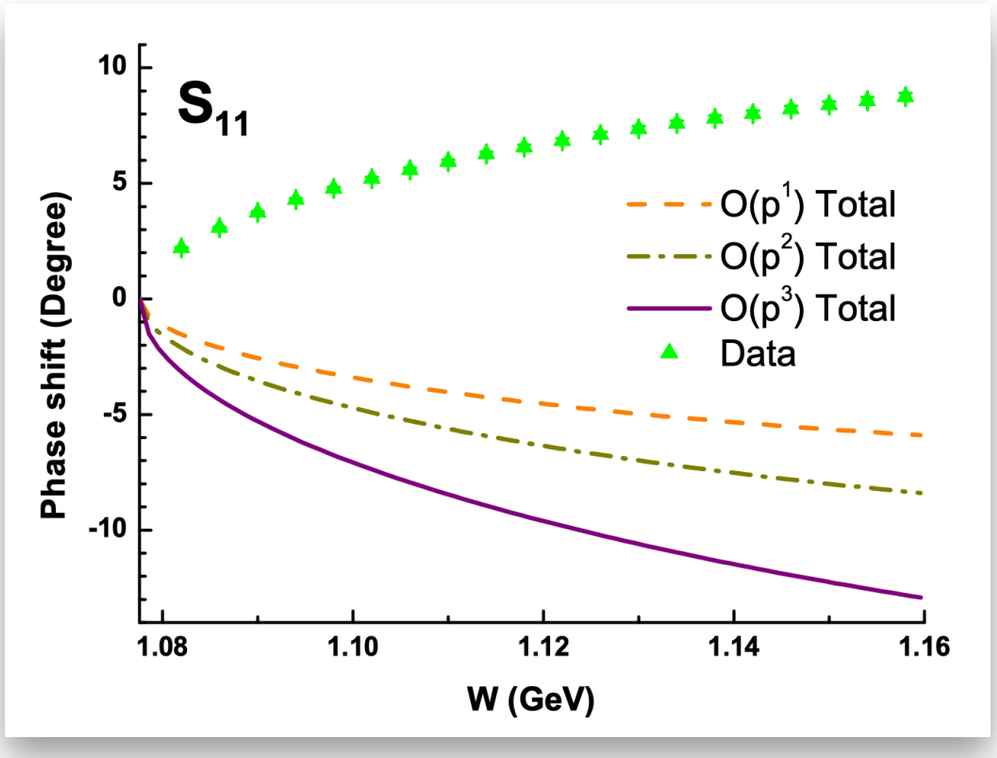

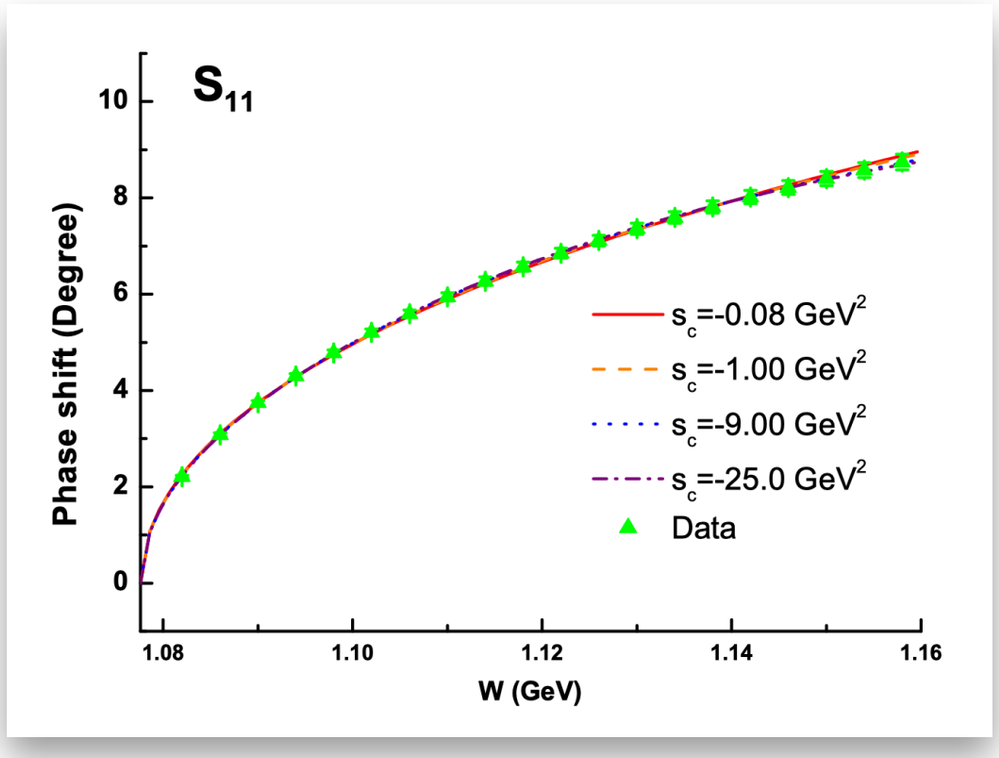

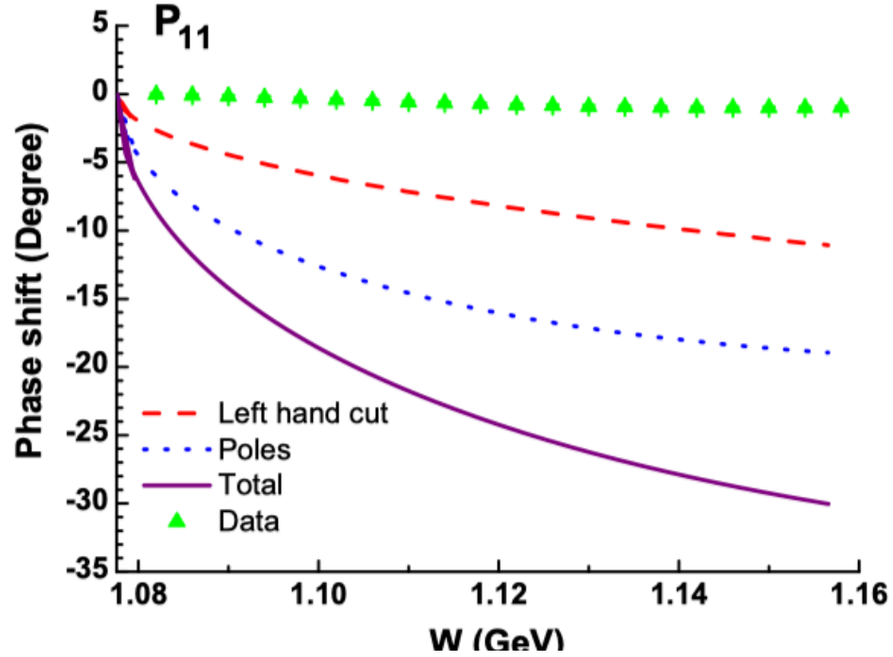

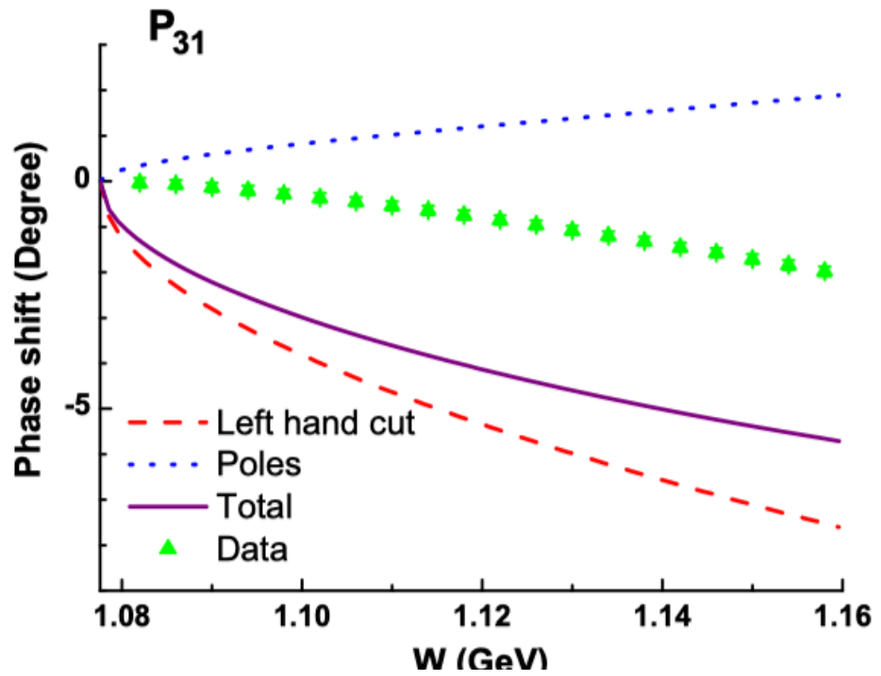

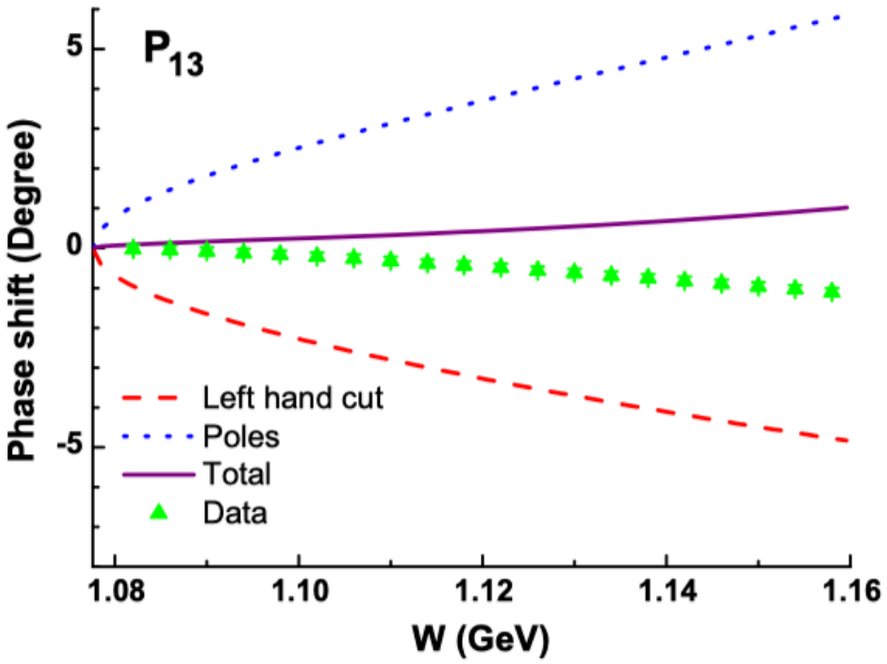

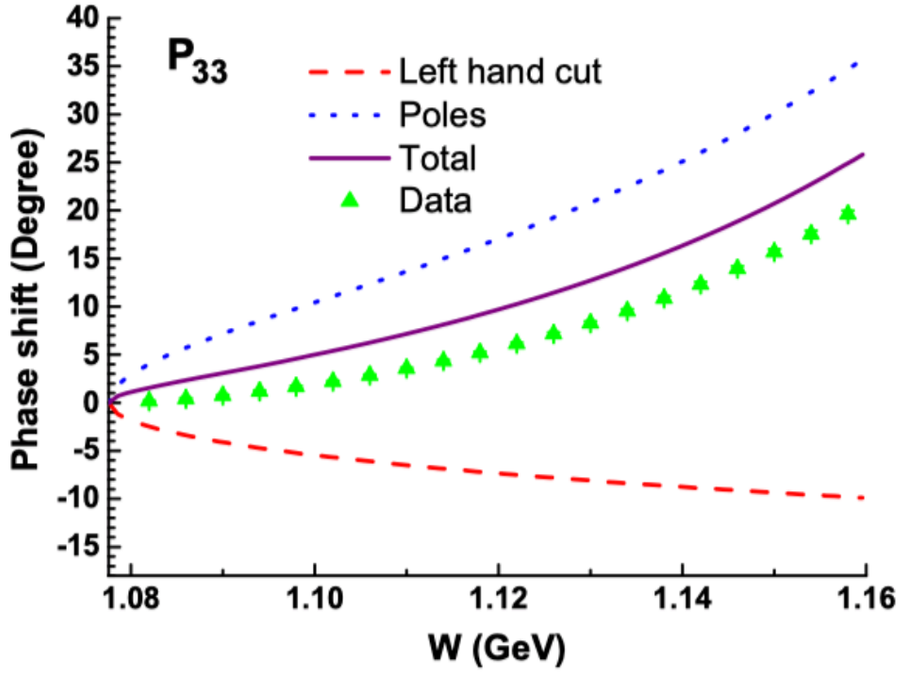

A virtual state in P_{11} channel.

In Ref [9] A. Gasparyan and M. Lutz, Nucl. Phys. A848, 126 (2010)., there also exists a CDD pole in P_{11} channel.

The phases of other channels can be well reproduced.

In Ref [10]M. Doring, and K. Nakayama, Eur. Phys. J. A43, 83 (2010), they considered this kind of pole to be the effects of left hand cuts.

K-matrix Fit [11] Y. Ma, W. Q. Niu, Y. F. Wang, and H. Q. Zheng, (2020).

$$T^{-1} = K^{-1} - \frac{B_0}{\pi} \rightarrow \rho$$

$$B_0(p^2, m_1^2, m_2^2)$$

$$= -16\pi^2 i \int \frac{d^D k \mu^{2\epsilon}}{(2\pi)^D} \frac{1}{(k^2 - m_1^2)[(p+k)^2 - m_2^2]}$$

$$= s \int_R \frac{\rho(s')}{s'(s'-s)} ds'$$

$$K_{ij} = \sum_{\alpha=1,2} \frac{c_{ij}^{\alpha}}{s - M_{\alpha}^2} + P_{ij}^{(2)}(s) + K_{ij}^{t,u-channel}$$

Figure 2. Im$f(s)$ on left hand cuts.

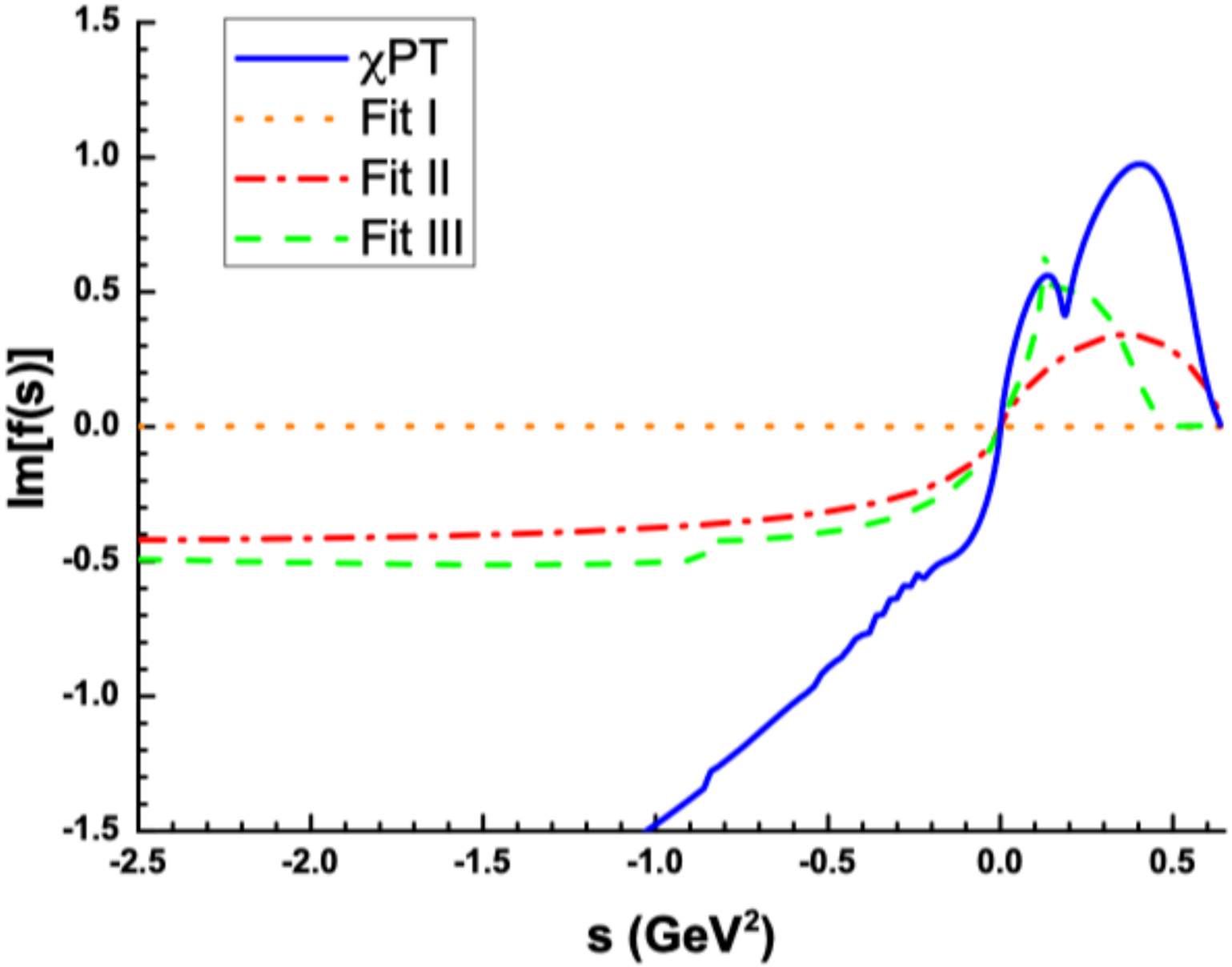

Figure 3. Fit results of K-matrix Fit III.

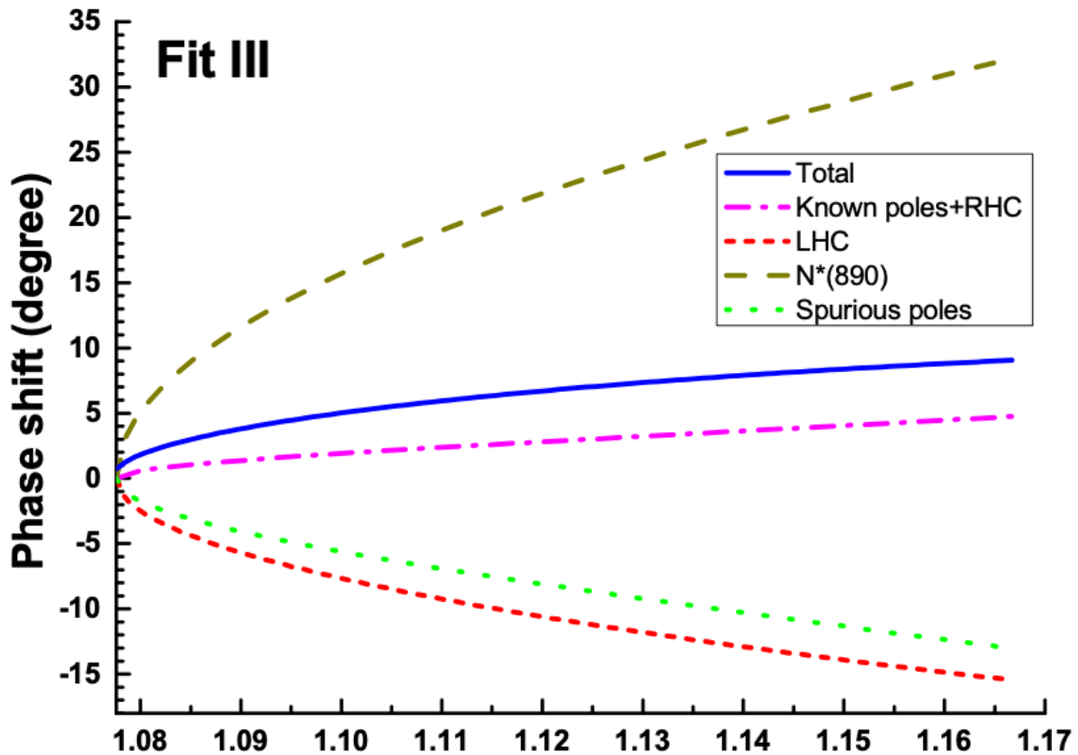

Table 1. Poles of K-matrix.

sheet	$\sqrt{s}(\mathrm{GeV})$
I	$1.35 - 0.58\mathrm{i}$
II	$1.67 - 0.07\mathrm{i}$
	$0.93 - 0.27\mathrm{i}$
III	$1.65 - 0.09\mathrm{i}$
	$1.53 - 0.07\mathrm{i}$
IV	$1.51 - 0.08\mathrm{i}$

1.2 Pion Photoproduciton

Production of mesons by X-rays through carbon slab

[12] E. M. McMillan, J. M. Peterson and R. S. White, Science 110, 579 (1949)

Production of Mesons by X-Rays

Edwin M. McMillan, Jack M. Peterson, and R. Stephen White[1]

Radiation Laboratory, Department of Physics,
University of California, Berkeley

$$\gamma + p \rightarrow \pi^+ + n$$

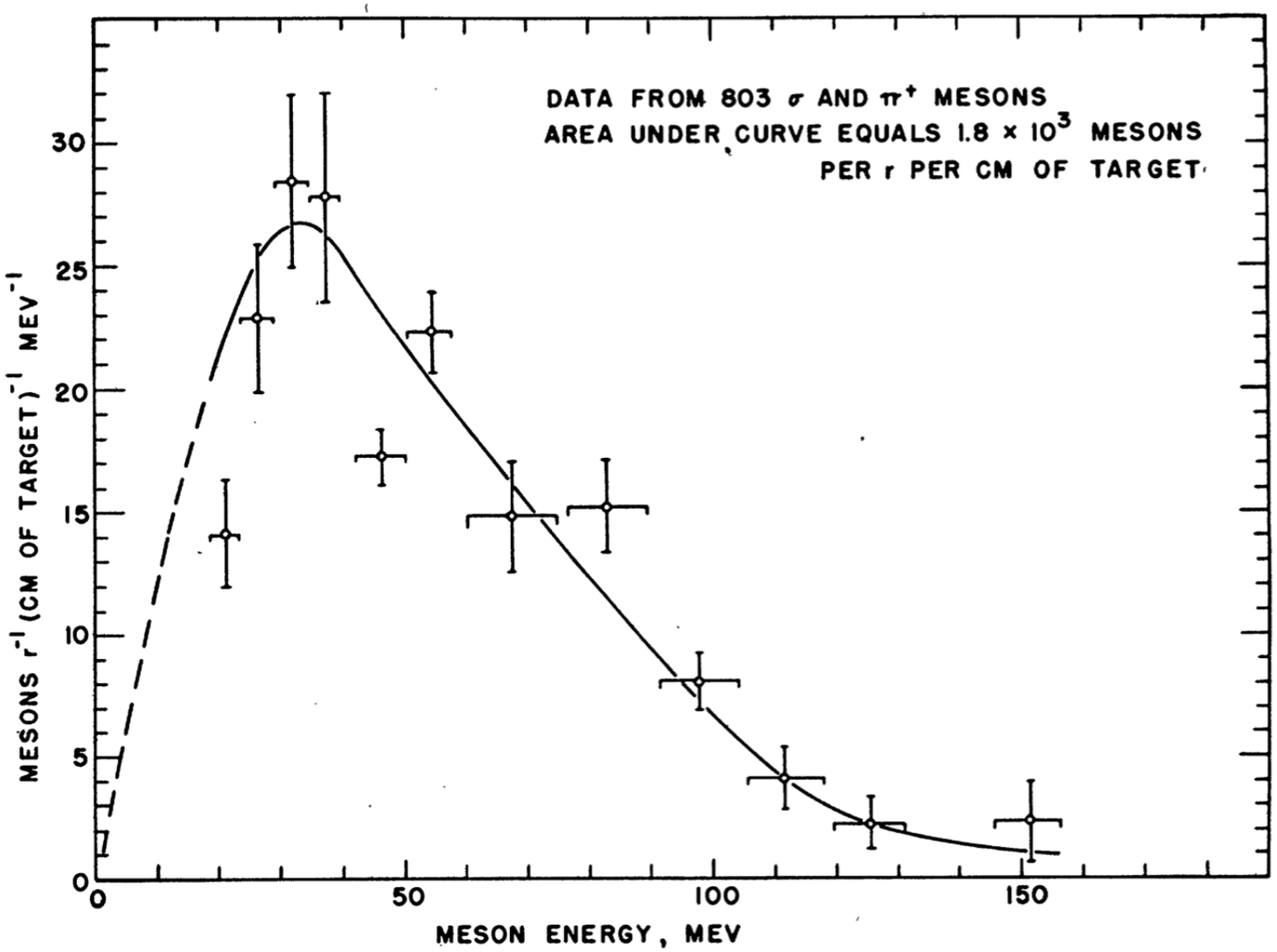

In the bombardment of nuclei, neutral pion photoproduction was found.

[13] J. Steinberger, W. K. H. Panofsky, and J. Steller, Phys. Rev. 78, 802 (1950)

PHYSICAL REVIEW VOLUME 78, NUMBER 6 JUNE 15, 1950

Evidence for the Production of Neutral Mesons by Photons*

J. Steinberger, W. K. H. Panofsky, and J. Steller
Radiation Laboratory, Department of Physics, University of California, Berkeley, California
(Received April 28, 1950)

In the bombardment of nuclei by 330-Mev x-rays, multiple gamma-rays are emitted. From their angular correlation it is deduced that they are emitted in pairs in the disintegration of neutral particles moving with relativistic velocities and therefore of intermediate mass. The neutral mesons are produced with cross sections similar to those for the charged mesons and with an angular distribution peaked more in the forward direction. The production cross section in hydrogen and the production cross section per nucleon in C and Be are comparable.

$$\gamma + p \rightarrow \pi^0 + p$$

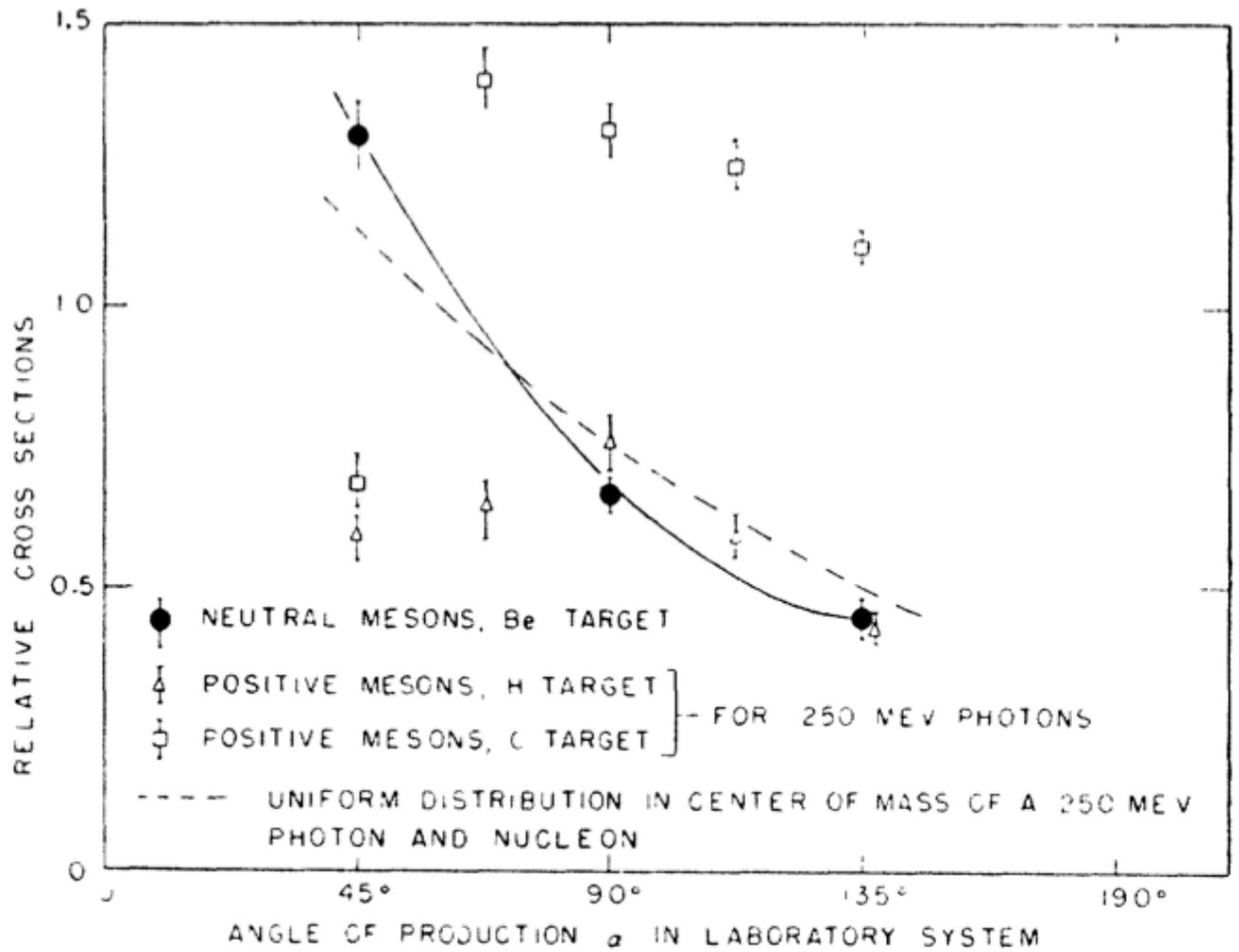

Charged Meson production from hydrogen and deuterium gas

[14] R. S. White, M. J. Jacobson, and A. G. Schulz, Phys. Rev. 88, 836 (1952).

PHYSICAL REVIEW VOLUME 88, NUMBER 4 NOVEMBER 15, 1952

The Production of Charged Photomesons from Deuterium and Hydrogen. I*

R. S. White, M. J. Jacobson,† and A. G. Schulz‡
Radiation Laboratory, Department of Physics, University of California, Berkeley, California
(Received June 30, 1952)

Hydrogen and deuterium gases have been bombarded in a gas target at a temperature of 77°K and at a pressure of about 140 atmospheres by the 318±10 Mev "spread-out" bremsstrahlung photon beam of the Berkeley electron synchrotron. The charged π-mesons which were produced were collimated at angles of 45°, 90°, and 135° to the beam direction. The π^+ mesons were detected with *trans*-stilbene scintillation crystals using $\pi\mu$, $\pi\beta$, and $\pi\mu\beta$ delayed coincidences and π^+ and π^- mesons were detected with Ilford C-2 200-micron nuclear emulsions. The ratios of the numbers of π^- to π^+ mesons produced in deuterium were 0.96±0.10, 1.09±0.12, and 1.21±0.17 for the angles of 45°, 90°, and 135°, respectively. No variation of the ratio with meson energy, outside statistics, was observed. Absolute values for the π^+ meson energy distribution functions from hydrogen and deuterium per "equivalent quantum" have been measured at each of the above production angles. The differential and total cross sections have been obtained by integrating over energy and angle, respectively. The experimental ratios of the deuterium to hydrogen cross sections are in good agreement with the phenomenological theory of Chew and Lewis when the Hulthén deuteron function with $\beta=6\alpha$ is used in the initial state, plane waves are used for the nucleons in the final state, and the bremsstrahlung cutoff is taken into account. The statistics of the data are, however, not sufficient to determine the amount of spin interaction. The excitation functions for hydrogen and deuterium and points on the angular distribution curves in the center-of-mass system have been obtained. An upper limit of 0.08 of the charged π-meson cross section was obtained for μ-meson production from deuterium.

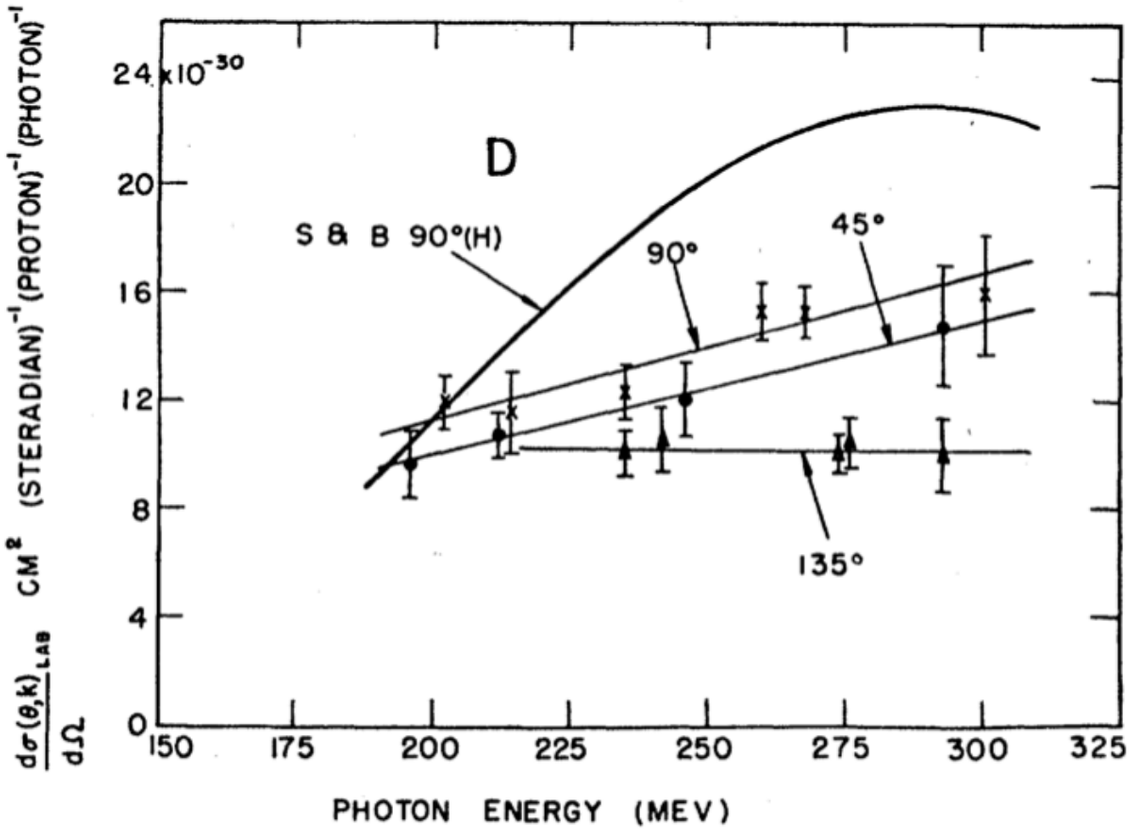

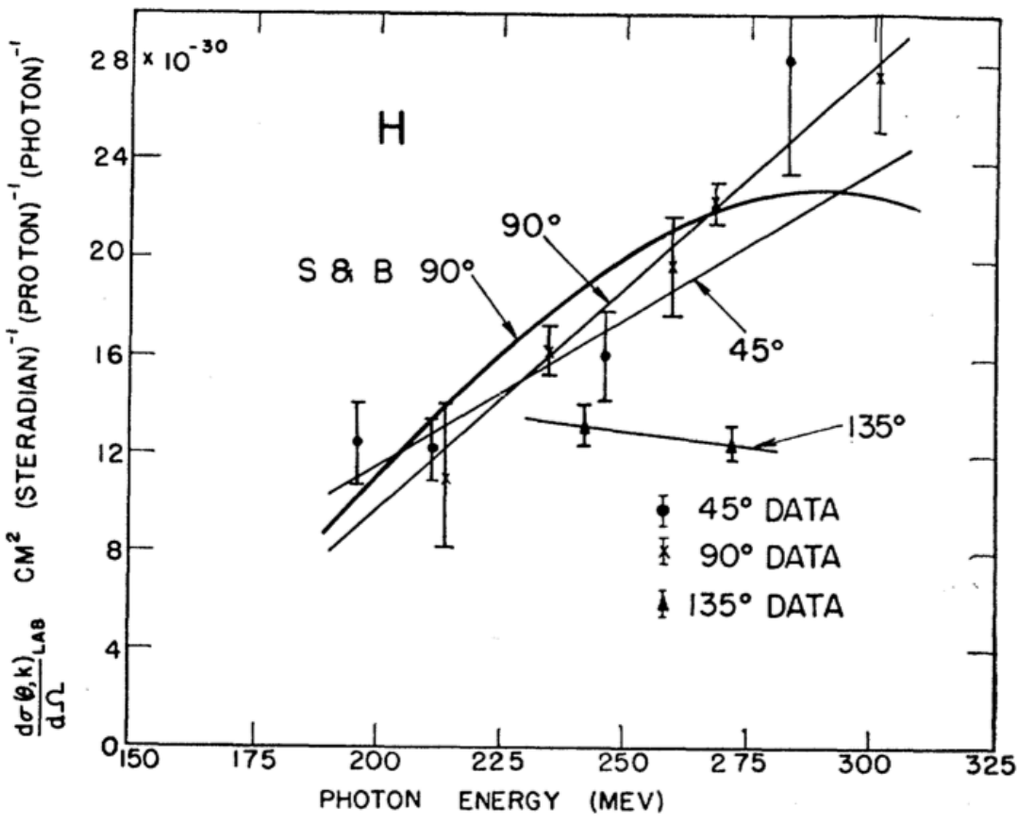

$$\gamma + p \rightarrow \pi^+ + n$$

$$\gamma + n \rightarrow \pi^- + p$$

A wealth of experimental datas, such as recoil nucleon polarization:

$$\mathbf{P} \cdot (\hat{q} \times \hat{q}')$$

$$\gamma + p \to \pi^+ + n$$

[15] K. H. Althoff, H. Piel, W. Wallraff, and G. Wessels, Phys. Lett. B26, 640 (1968)

[16] R. Querzoli, G. Salvini, and A. Silverman, Nuovo Cimento 19, 53 (1961)

[17] J. R. Kenemuth and P. C. Stein, Phys. Rev. 129, 2259 (1963)

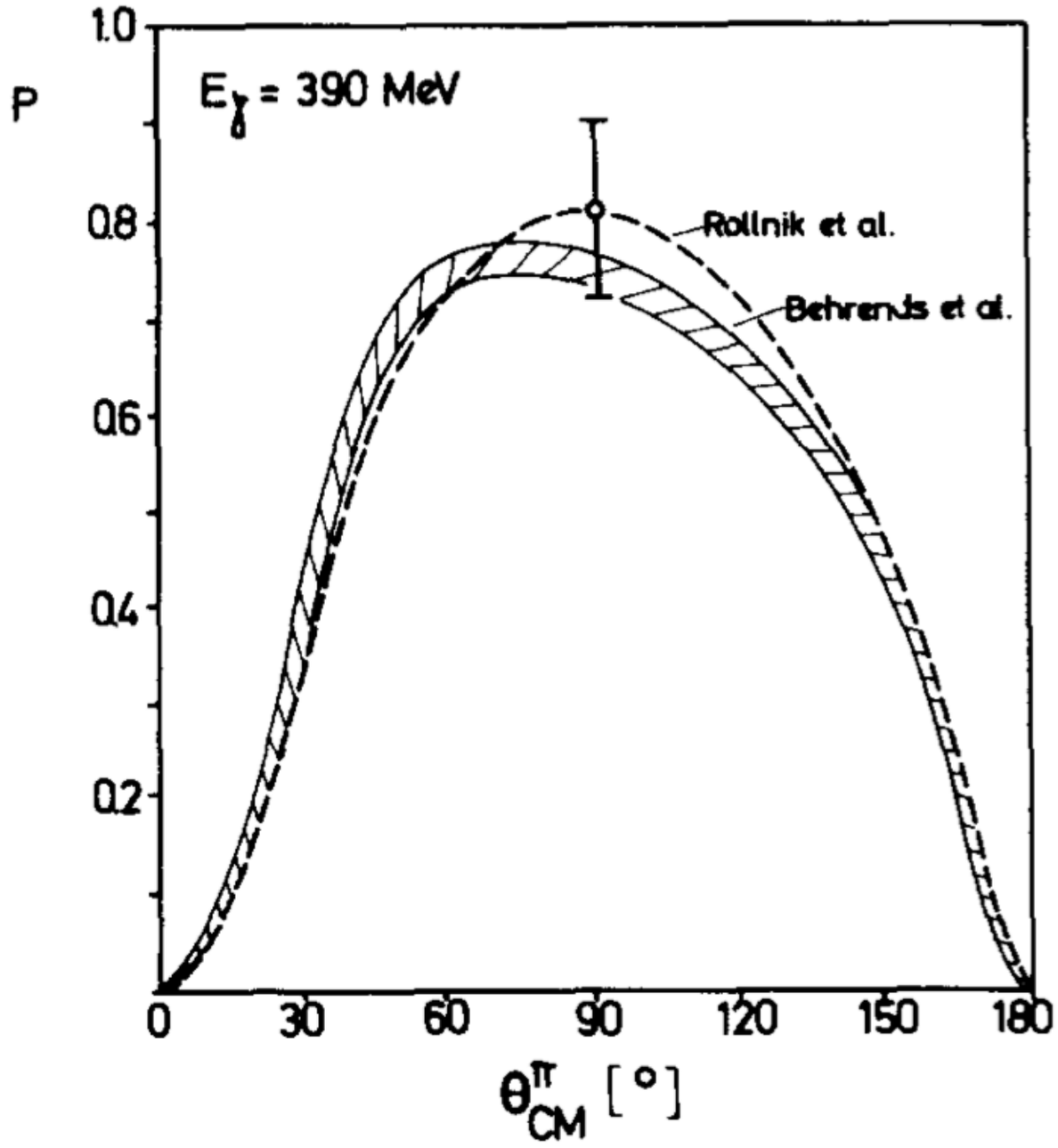

$$\gamma + p \rightarrow \pi^0 + p$$

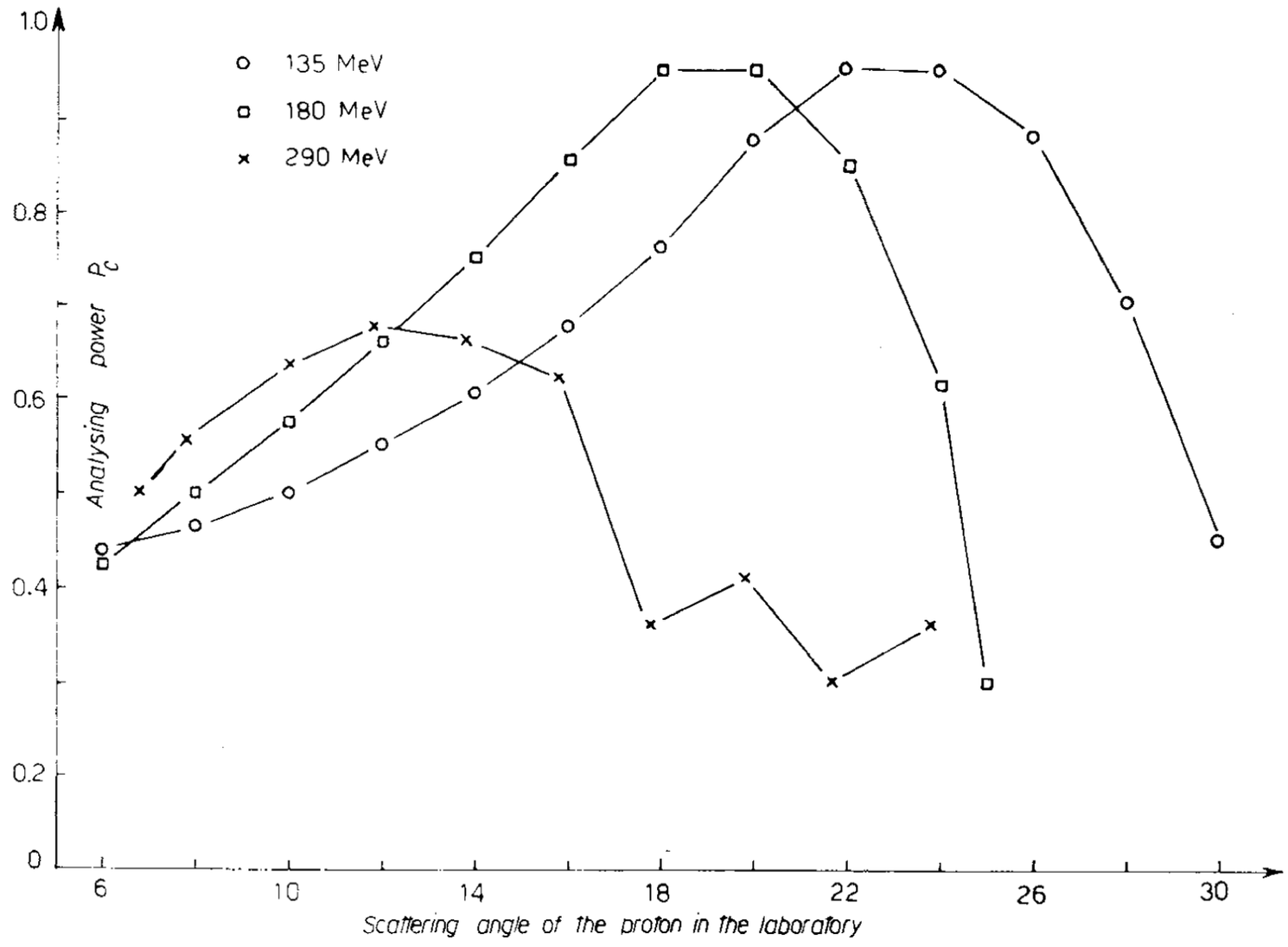

$$\gamma + n \rightarrow \pi^- + p\,,\ 90 \text{ degree}$$

Reaction	Polarization
$\gamma+n \rightarrow p+\pi^-$	-0.26 ± 0.06
$\gamma+p \rightarrow p+\pi^0$	-0.45 ± 0.06

Asymmetry for the linearly polarized photons

$$\Sigma = \frac{\sigma_{\perp} - \sigma_{\parallel}}{\sigma_{\perp} + \sigma_{\parallel}}$$

[18] F. F. Liu, D. J. Drickey, and R. F. Mozley, Phys. Rev. 136, B1183 (1964)

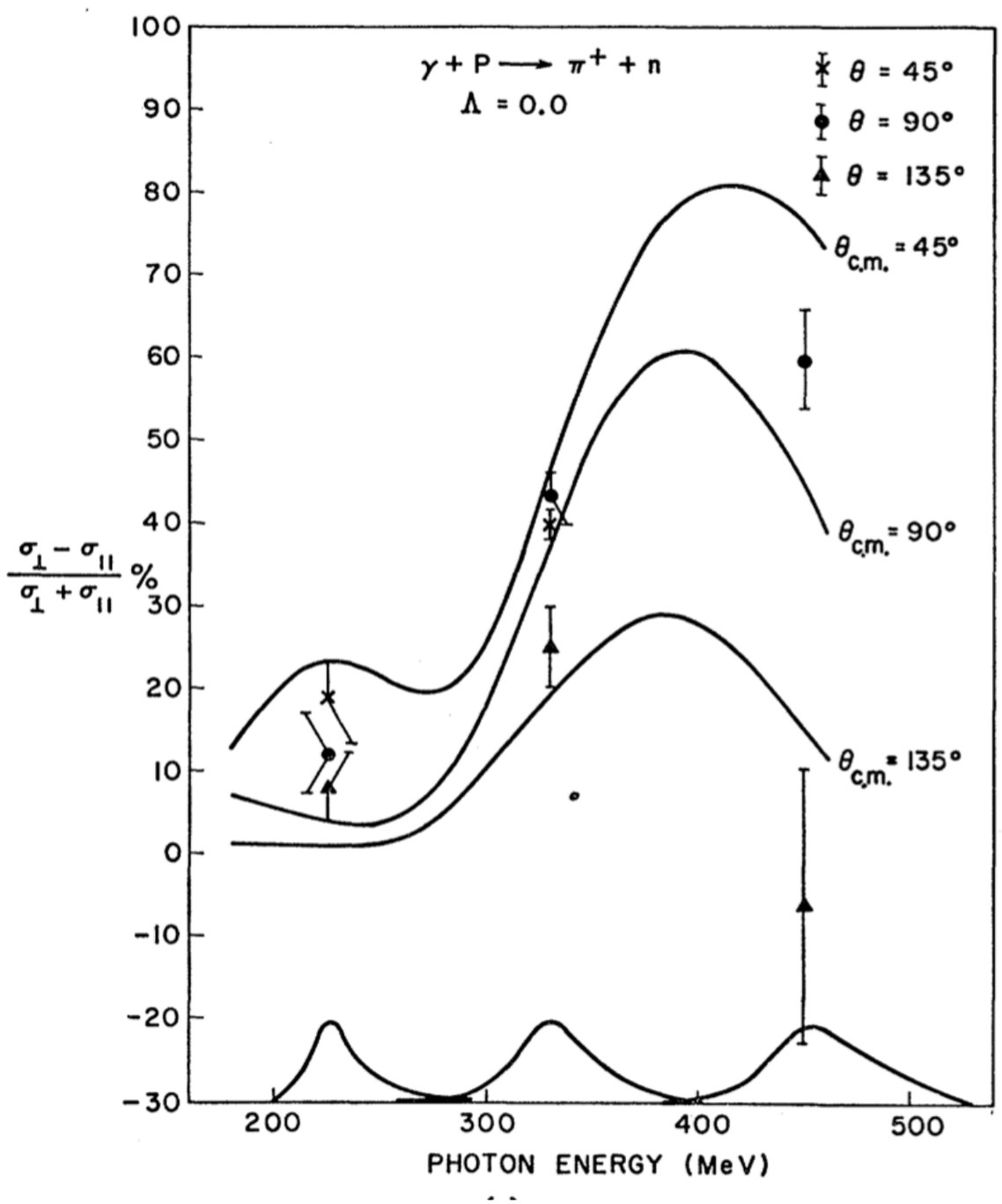

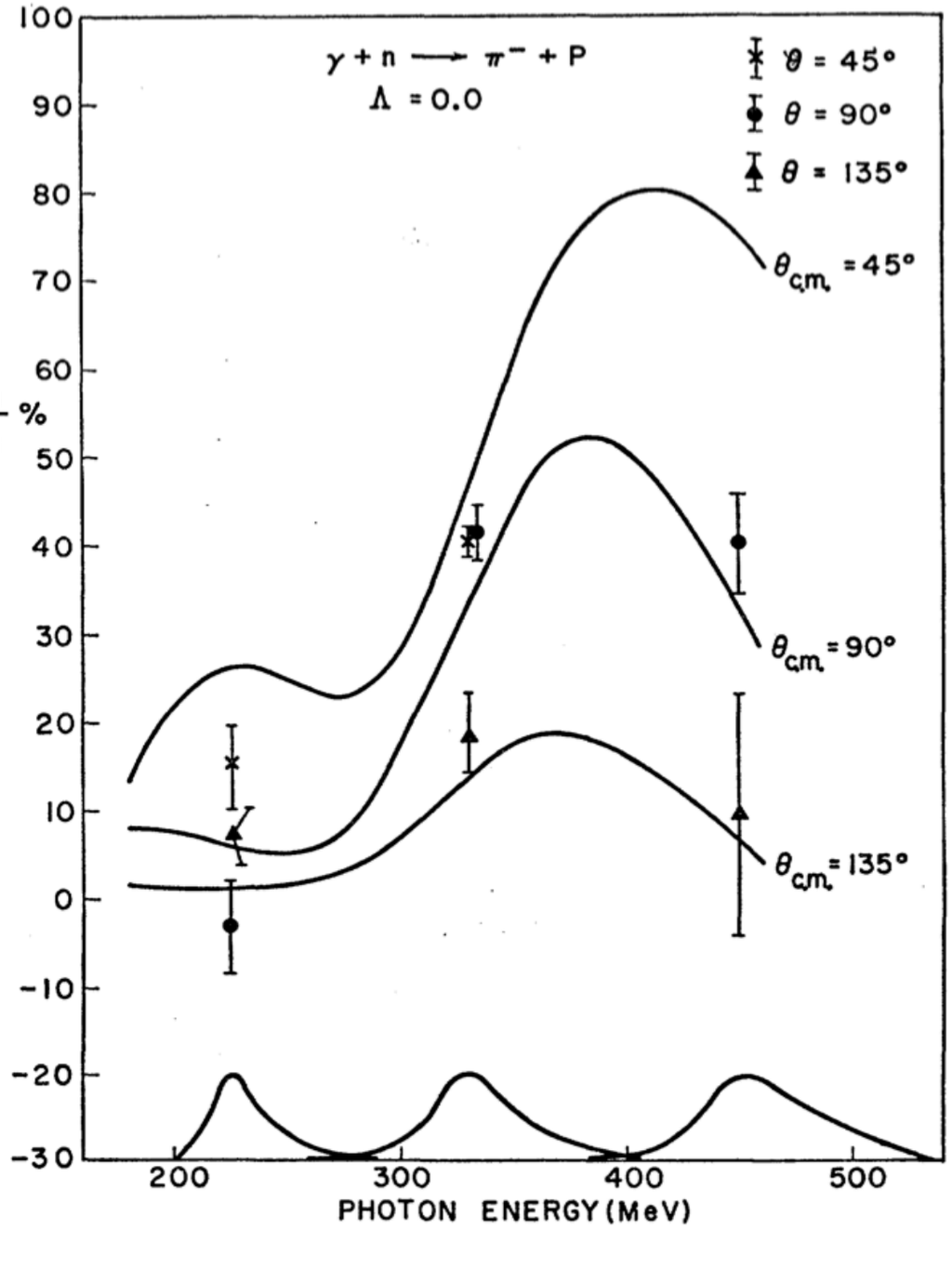

$$\gamma + p \rightarrow \pi^0 + p$$

[19] D. J. Drickey and R. F. Mozley, Phys. Rev. 136, B543 (1964)

E_γ MeV	θ	$(\sigma_\perp - \sigma_\parallel)/(\sigma_\perp + \sigma_\parallel)$
235	120°	0.289 ± 0.047
285	90°	0.462 ± 0.035
335	60°	0.462 ± 0.025
435	90°	0.529 ± 0.065

Asymmetry for the polarized target

[20] S. Arai, S. Fukui, et al., Phys. Lett. 40B, 426 (1972)

$$T = \frac{\sigma_+ - \sigma_-}{\sigma_+ + \sigma_-}$$

$$\gamma + p \rightarrow \pi^+ + n$$

Maximum energy of bremsstrahlung $E_{max.}$ (MeV)	Incident photon energy E_γ (MeV)	π^+ c. m. angle θ (deg.)	Asymmetry $T(\theta)$	Note
475	314 ± 16	91.4 ± 2.2	0.510 ± 0.071	
	340 ± 16	89.9 ± 2.5	0.598 ± 0.085	
	369 ± 17	88.6 ± 2.6	0.685 ± 0.094	
	398 ± 18	87.5 ± 2.9	0.678 ± 0.096	
	419 ± 13	86.9 ± 3.1	0.713 ± 0.137	
575	417 ± 22	89.7 ± 3.2	0.690 ± 0.085	
	449 ± 23	87.0 ± 3.3	0.603 ± 0.098	
	490 ± 24	86.7 ± 3.3	0.470 ± 0.089	
	534 ± 25	86.8 ± 3.4	0.156 ± 0.088	
750	513 ± 13	86.6 ± 3.4	0.346 ± 0.066	± 0.066
	537 ± 14	86.5 ± 3.4	0.181 ± 0.065	± 0.029
	561 ± 14	86.6 ± 3.4	0.136 ± 0.062	
	589 ± 15	86.6 ± 3.5	0.043 ± 0.060	
	616 ± 16	86.7 ± 3.5	0.083 ± 0.054	
	646 ± 16	87.1 ± 3.6	0.068 ± 0.053	
	675 ± 16	87.3 ± 3.6	0.171 ± 0.053	
1000	710 ± 23	87.6 ± 3.7	0.322 ± 0.092	± 0.026
	752 ± 24	88.0 ± 3.7	0.161 ± 0.115	± 0.012
	794 ± 25	88.4 ± 3.8	0.029 ± 0.150	~0
	840 ± 26	89.0 ± 3.8	−0.119 ± 0.207	
	883 ± 26	89.3 ± 3.9	0.064 ± 0.258	
	929 ± 27	89.8 ± 3.9	0.395 ± 0.267	

Neutral pion photoproduction from the proton near threshold

[21] M. Fuchs et al., Phys. Lett. B368, 20 (1996).

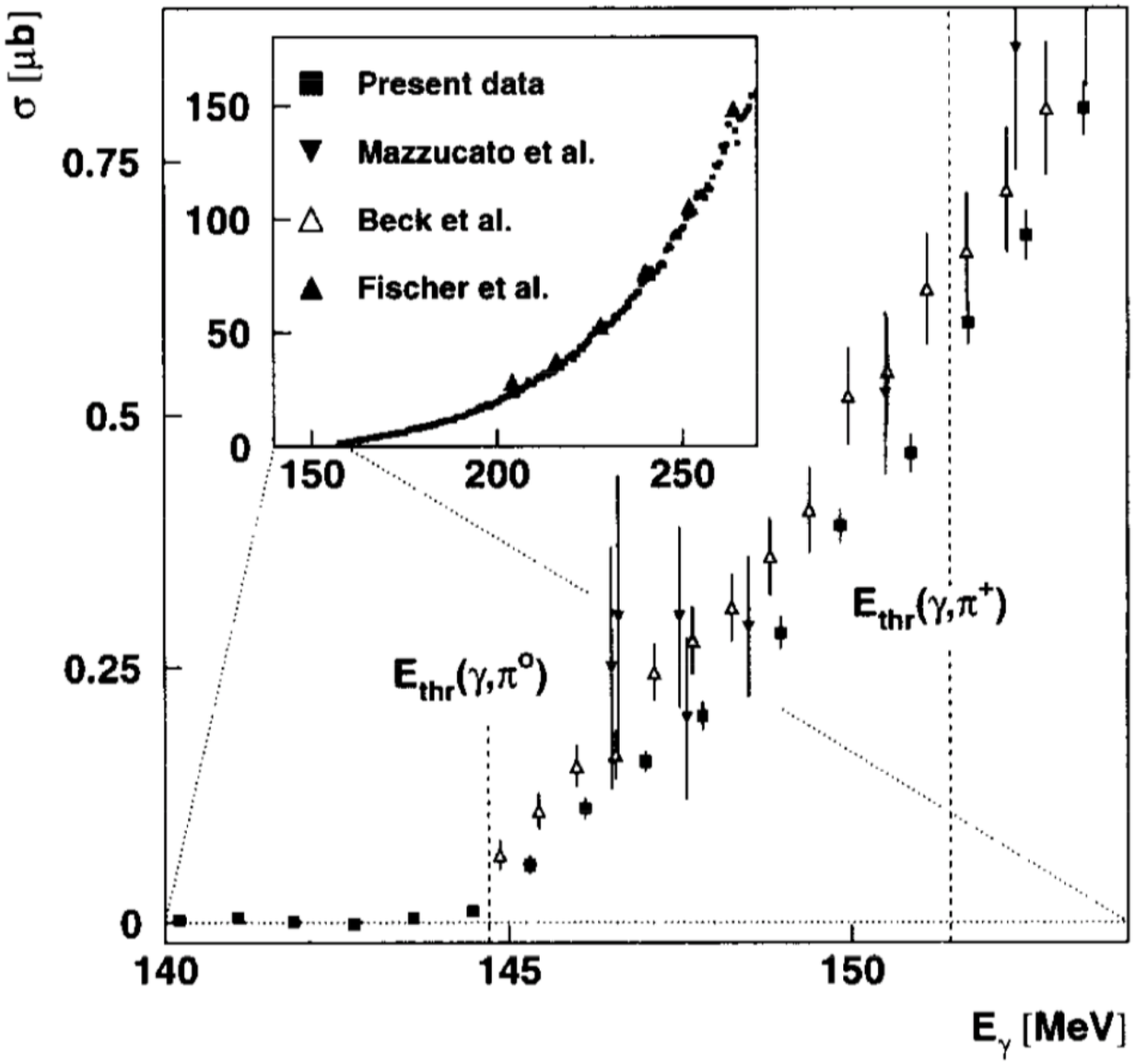

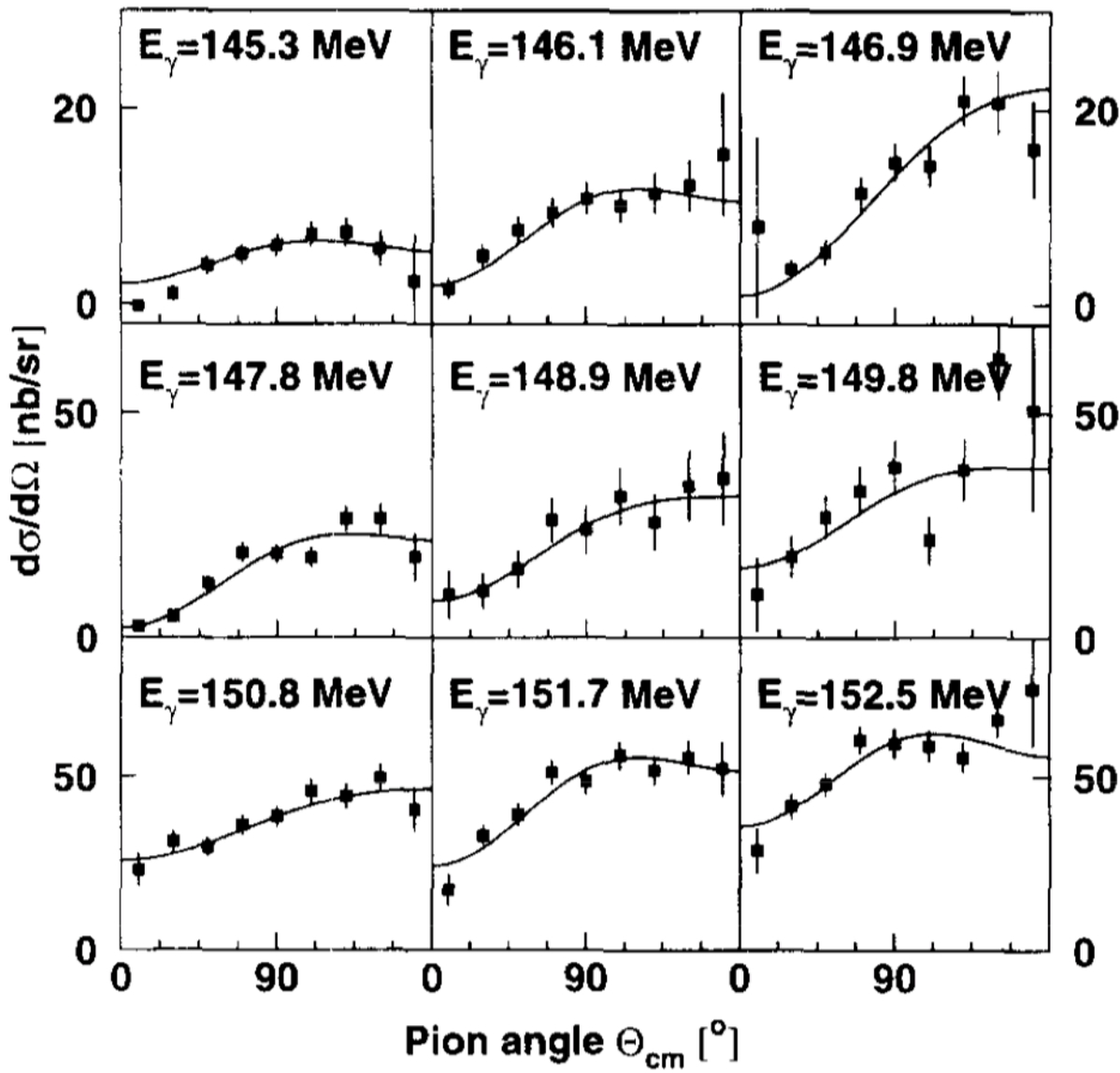

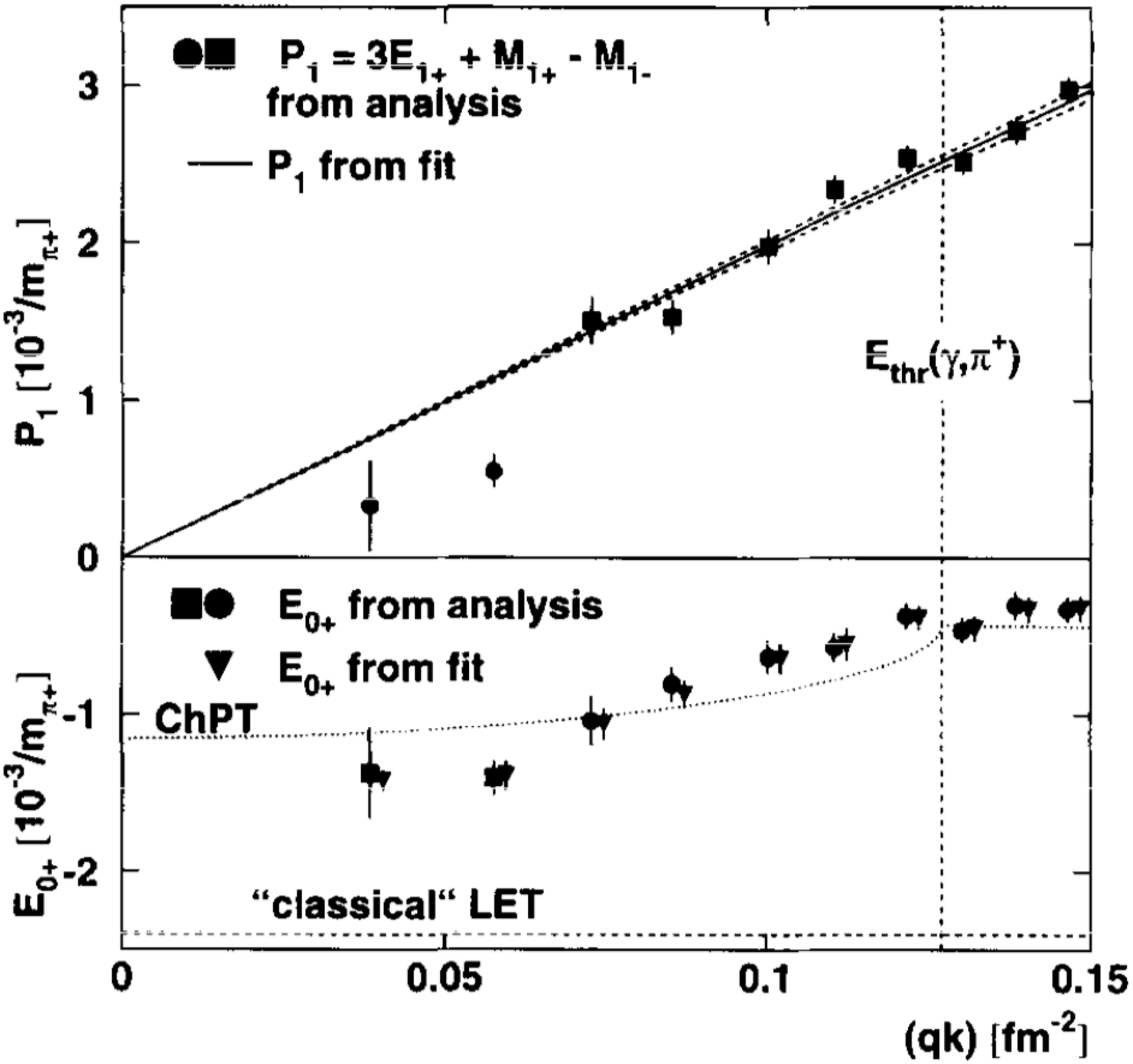
$P_1 = 3E_{1+} + M_{1+} - M_{1-}$
from analysis
P_1 from fit
$E_{thr}(\gamma,\pi^+)$
P_1 [$10^{-3}/m_{\pi+}$]
3
2
1
0
E_{0+} from analysis
E_{0+} from fit
ChPT
"classical" LET
E_{0+} [$10^{-3}/m_{\pi+}$]
-1
-2
0
0.05
0.1
0.15
(qk) [fm^{-2}]

Crystal Balls Holder

[22] A2 Collaboration • P. Adlarson et al., Phys.Rev.C 92 (2015).

$$\gamma + p \rightarrow \pi^0 + p$$

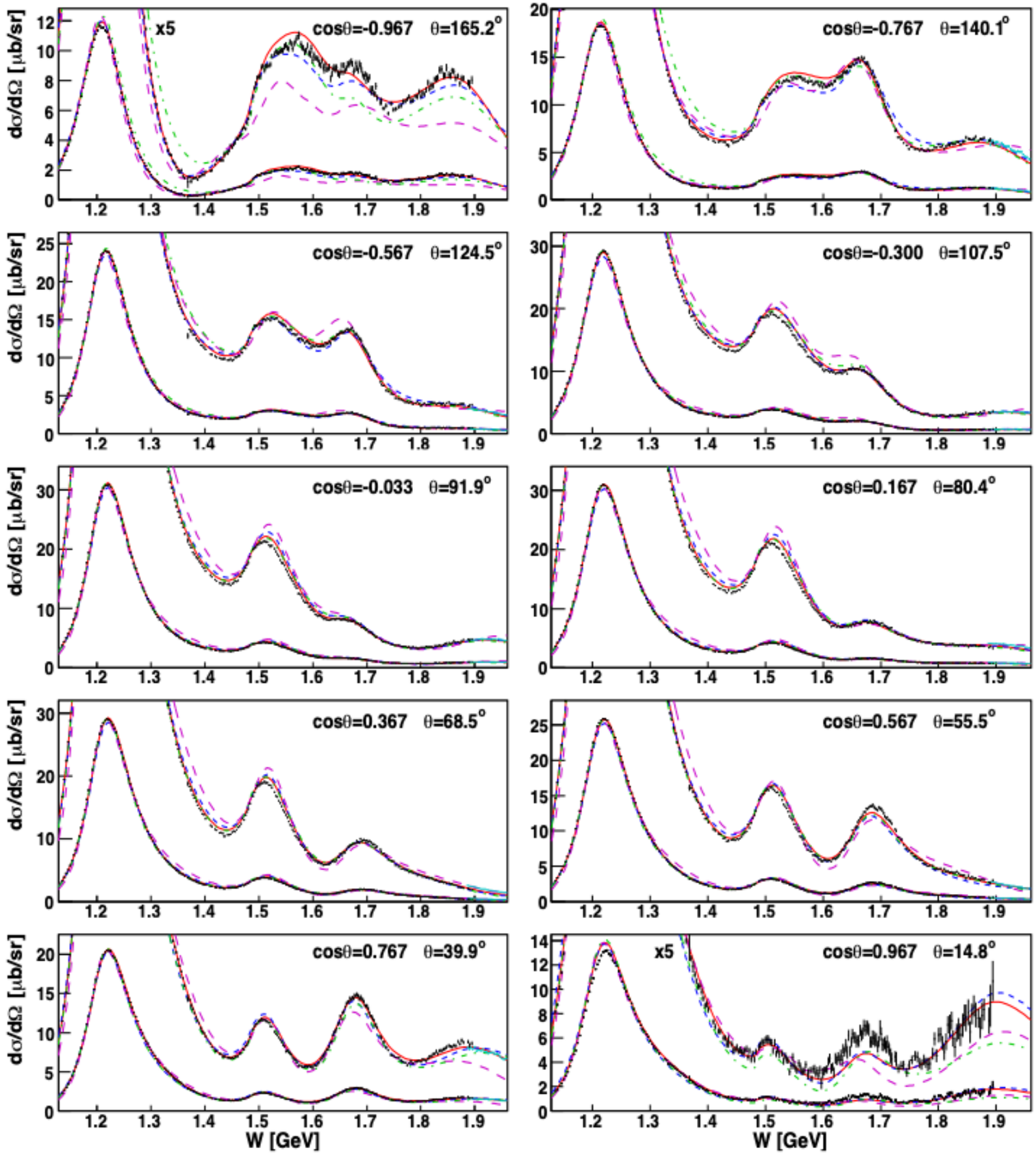

[23] A2 collaboration, Physics Letters B 750 (2015)

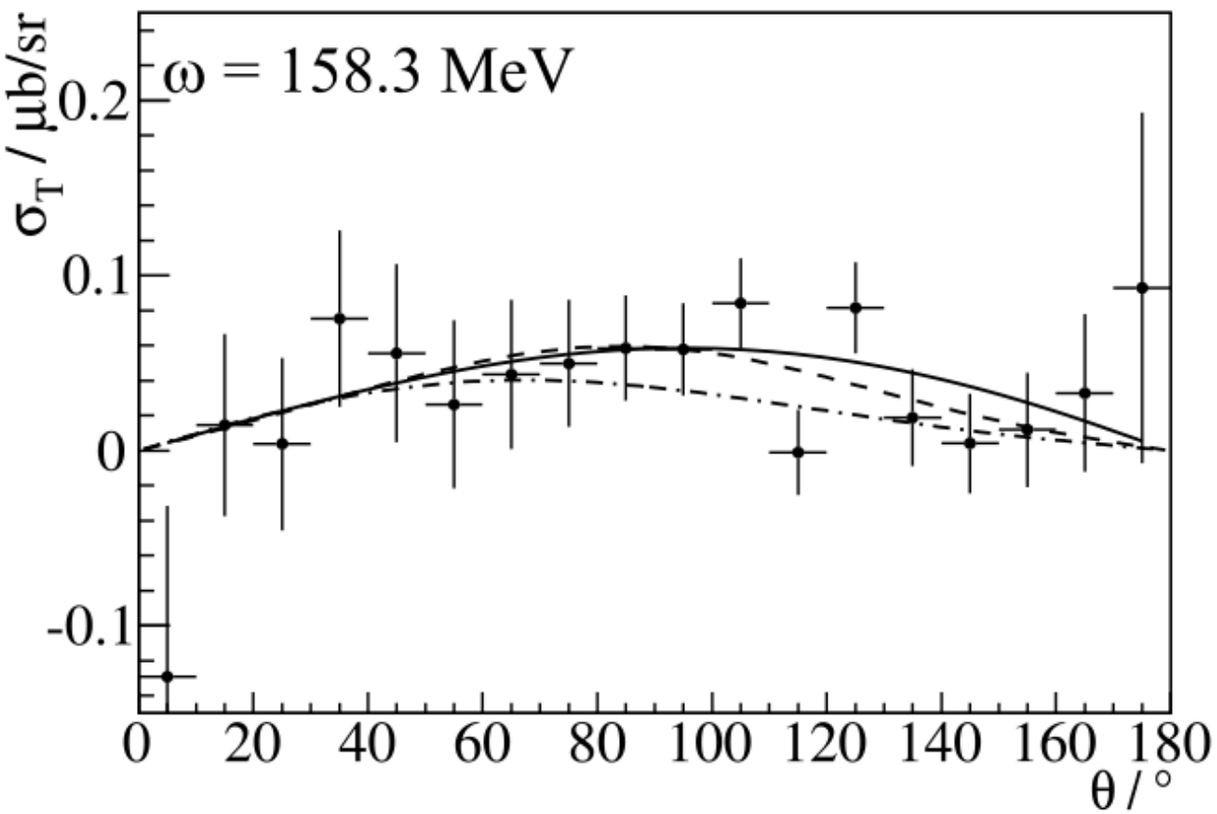

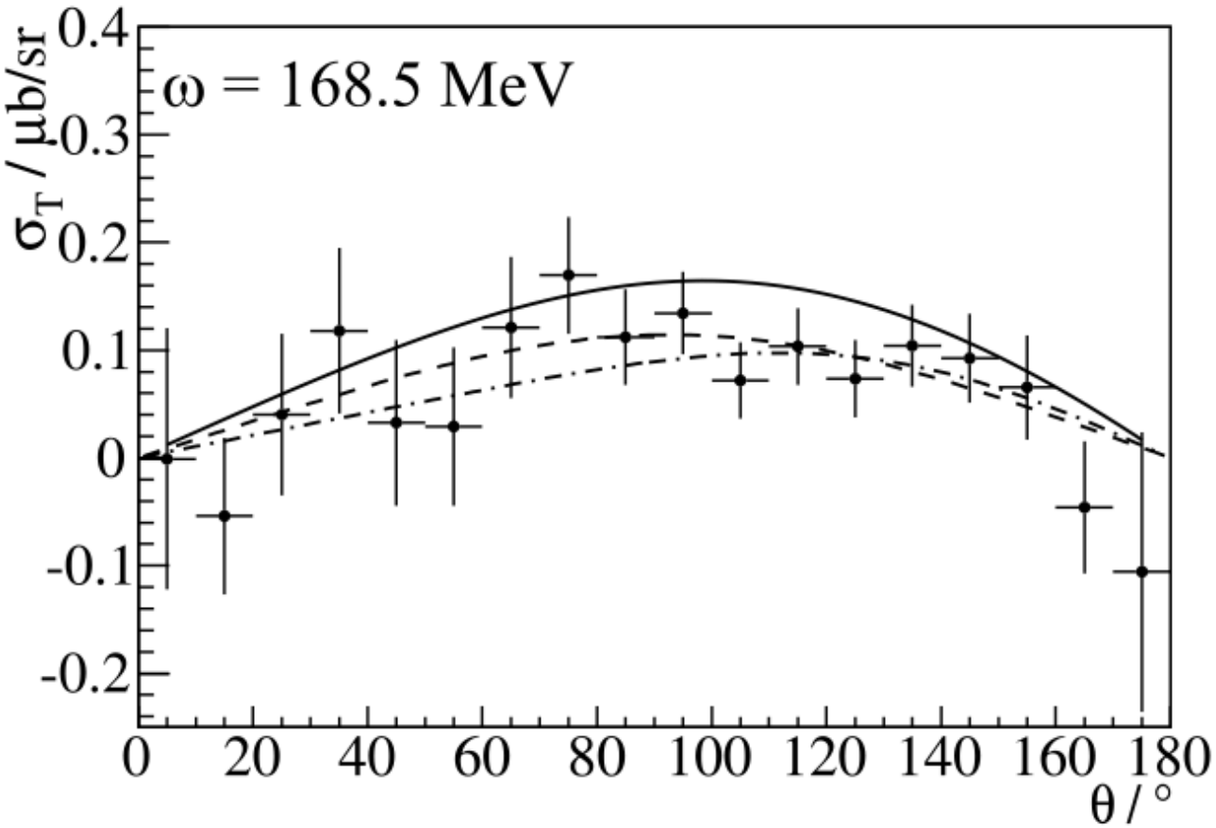

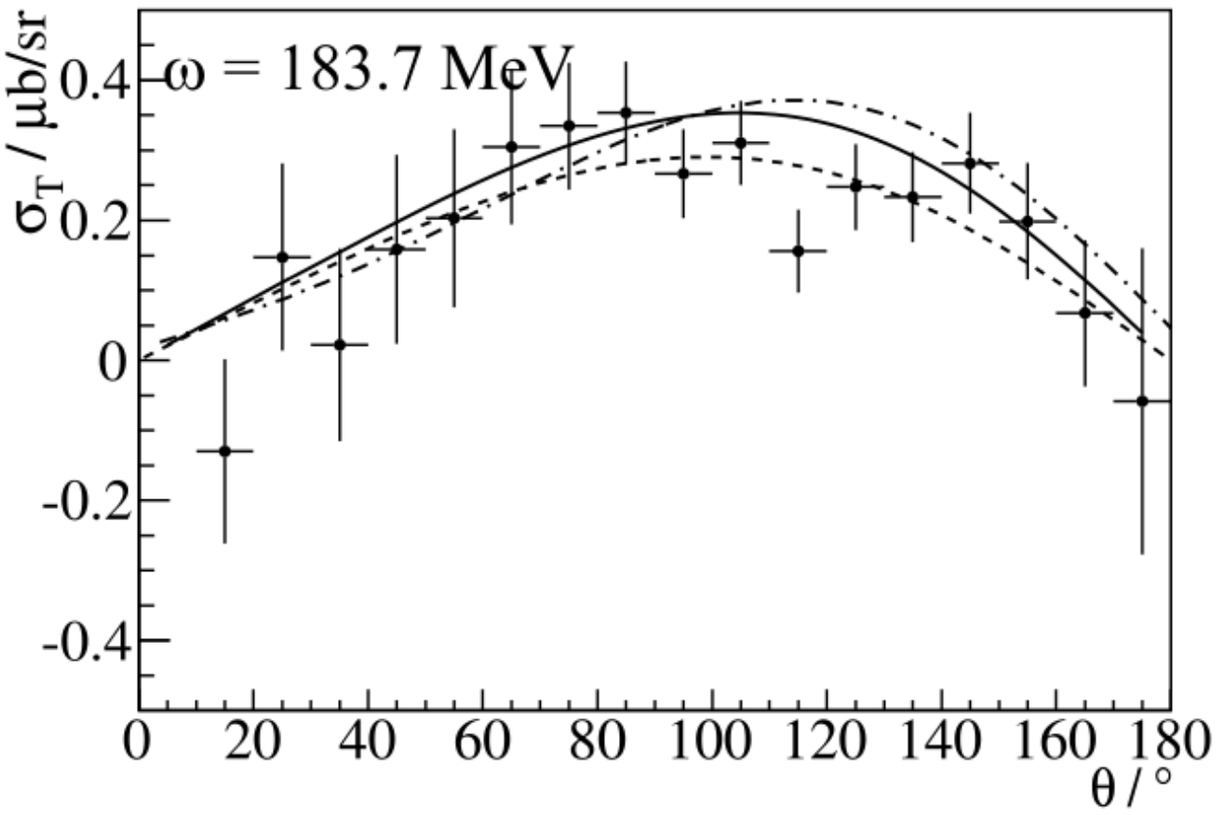

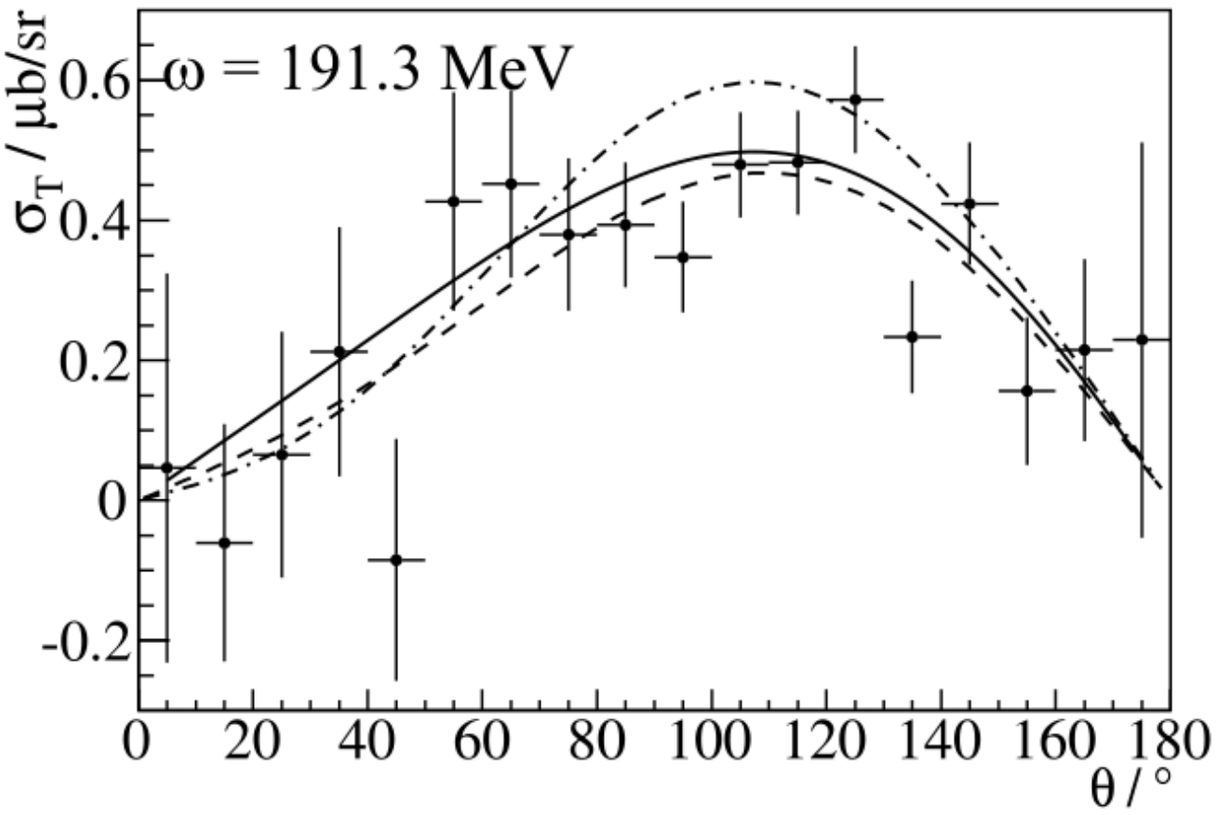

[24] A2 collaboration, Phys. Rev. C 100, 065205 (2019)

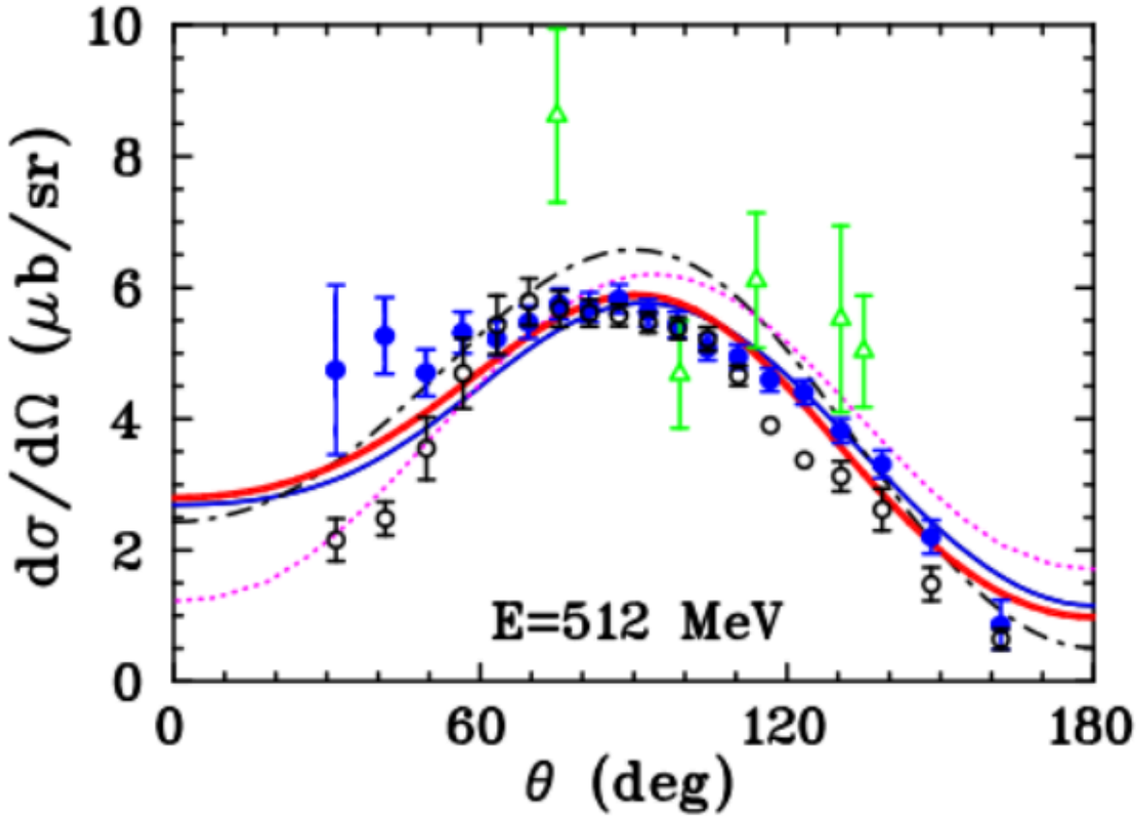

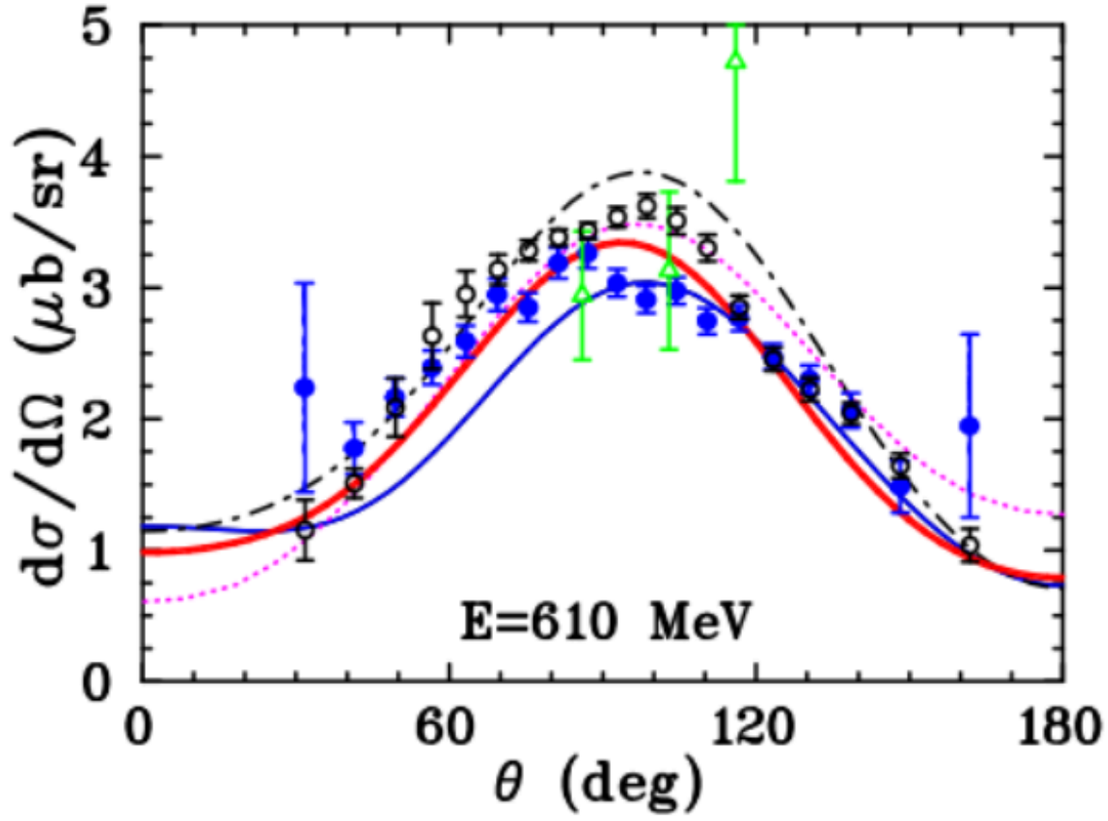

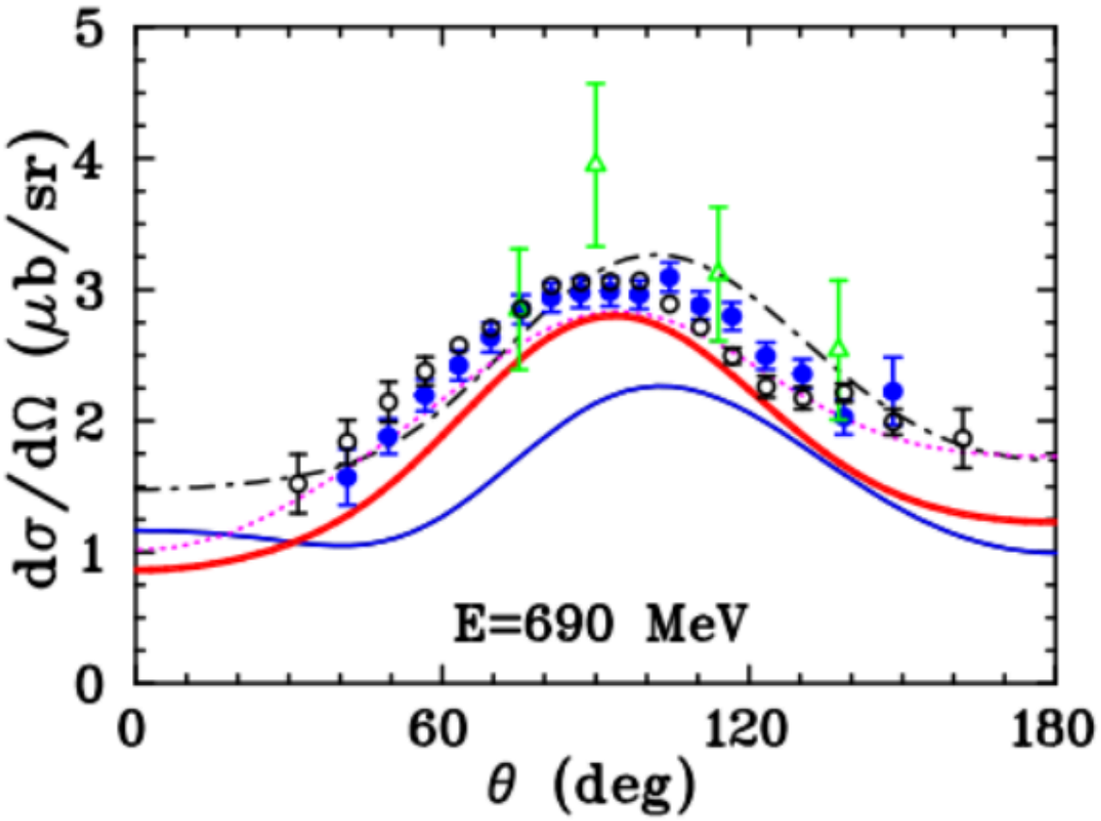

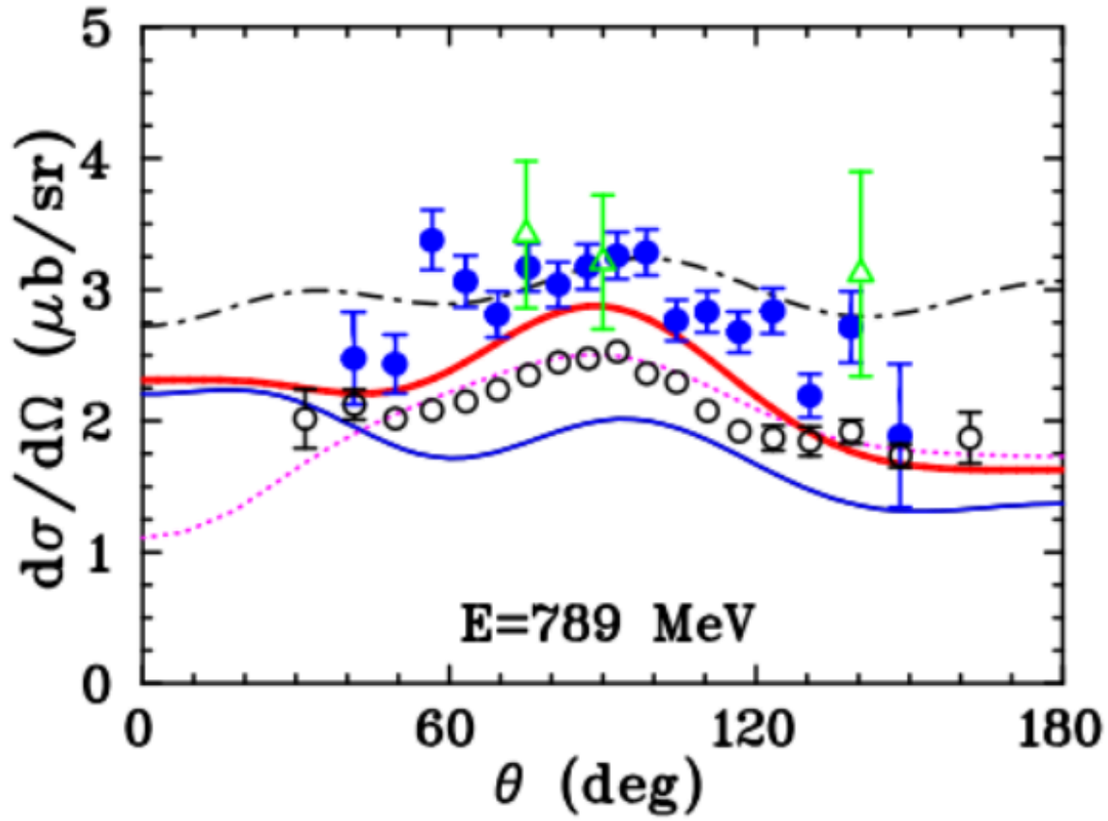

[25] A2 collaboration, EPJ Web of Conferences 199, 02010 (2019)

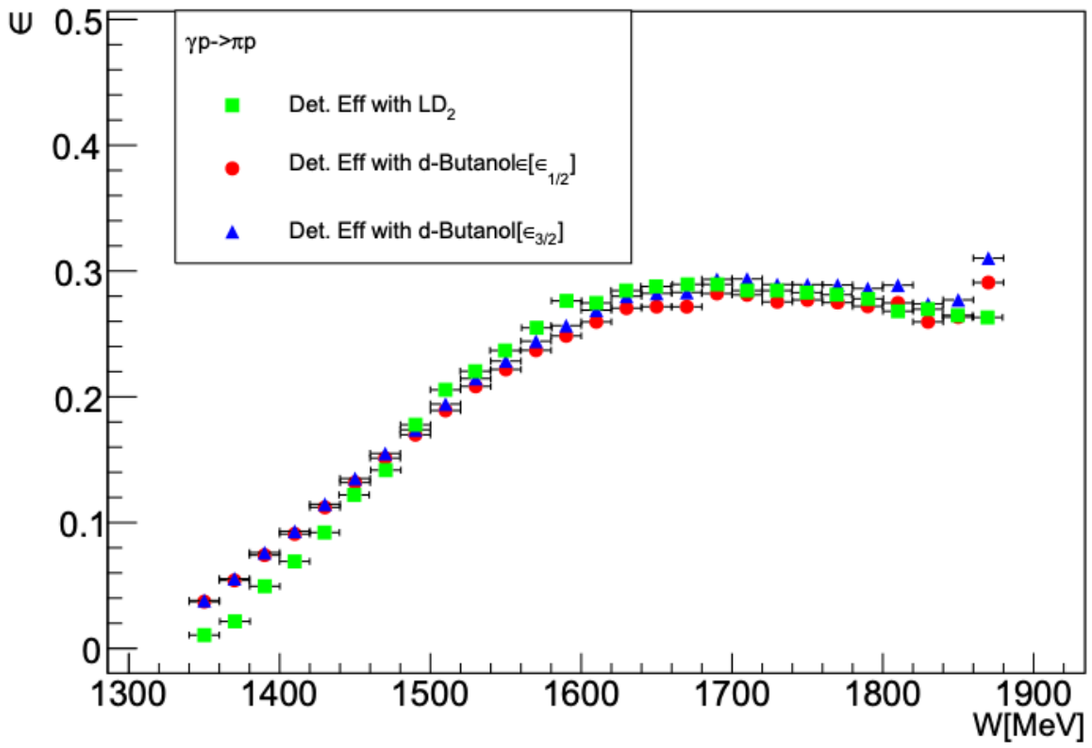

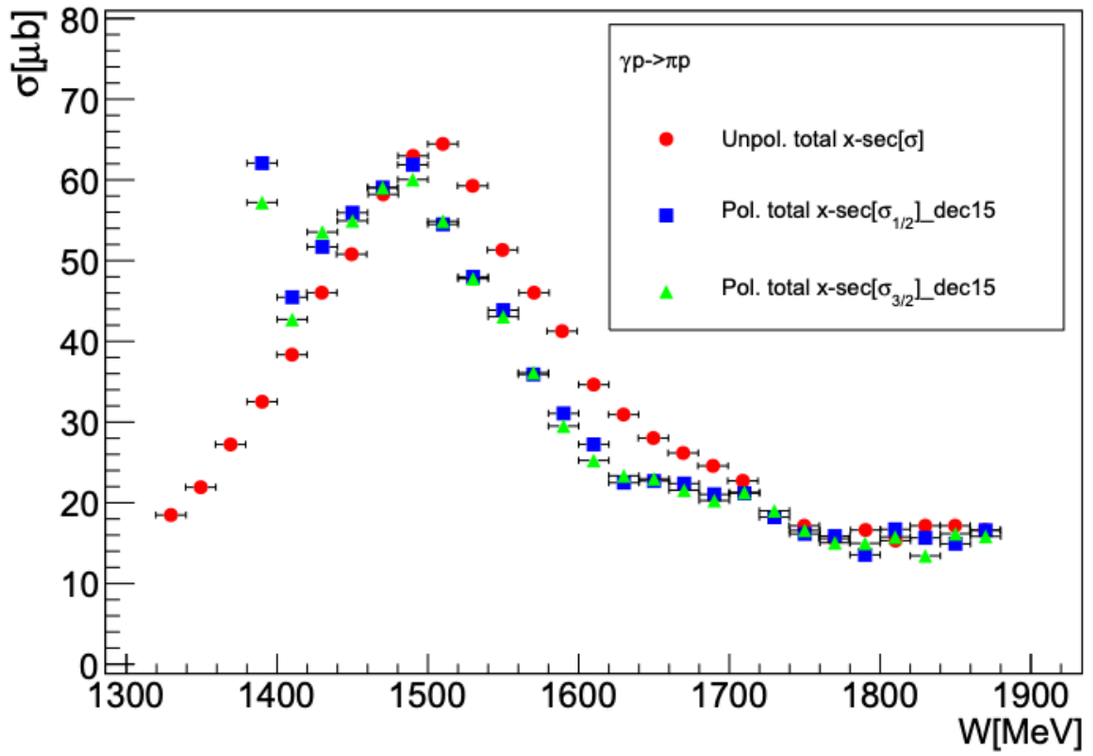

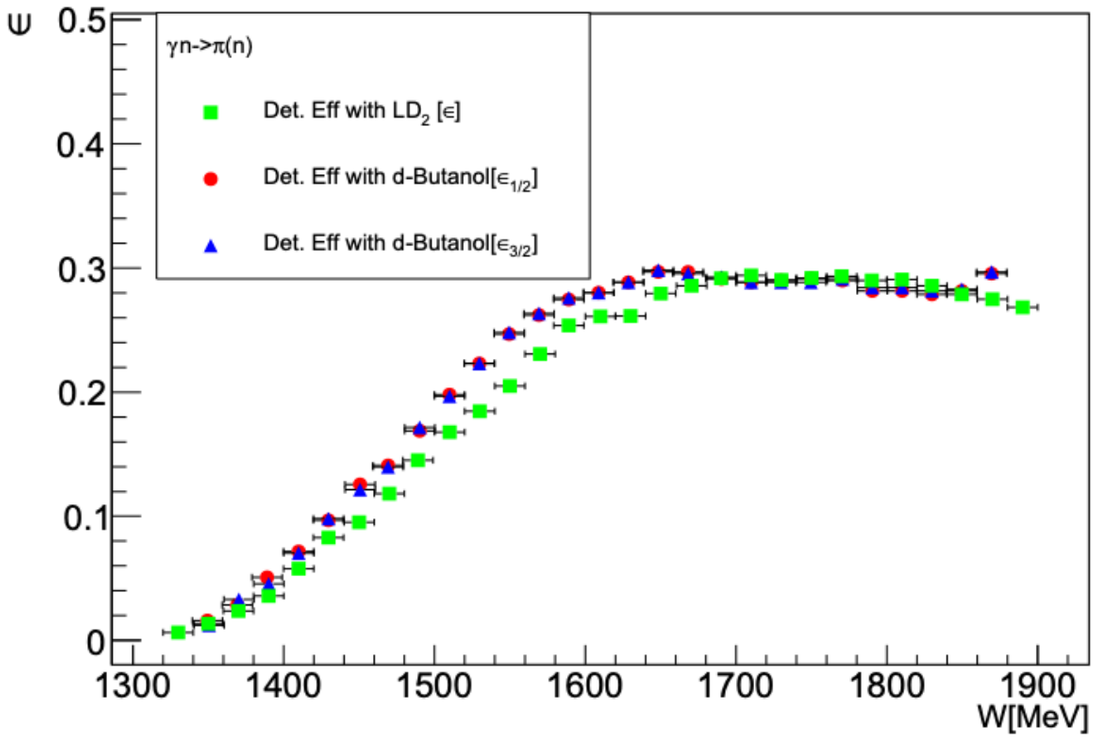

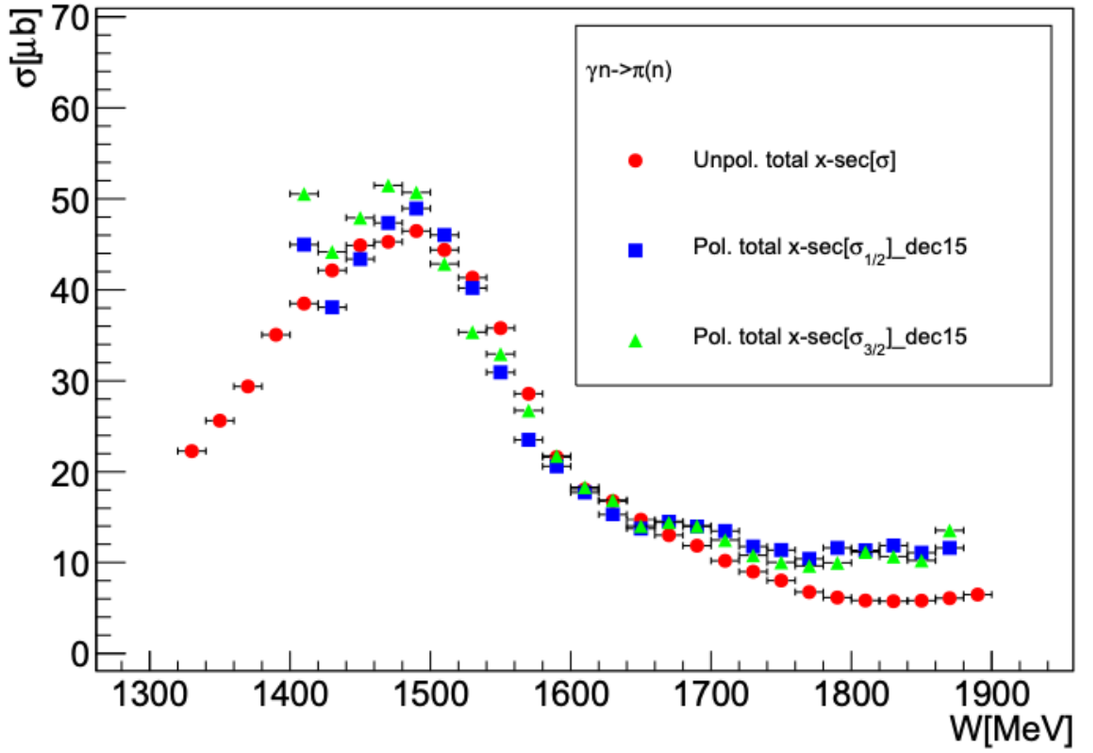

[26] A2 collaboration, Eur. Phys. J. A52 (2016)

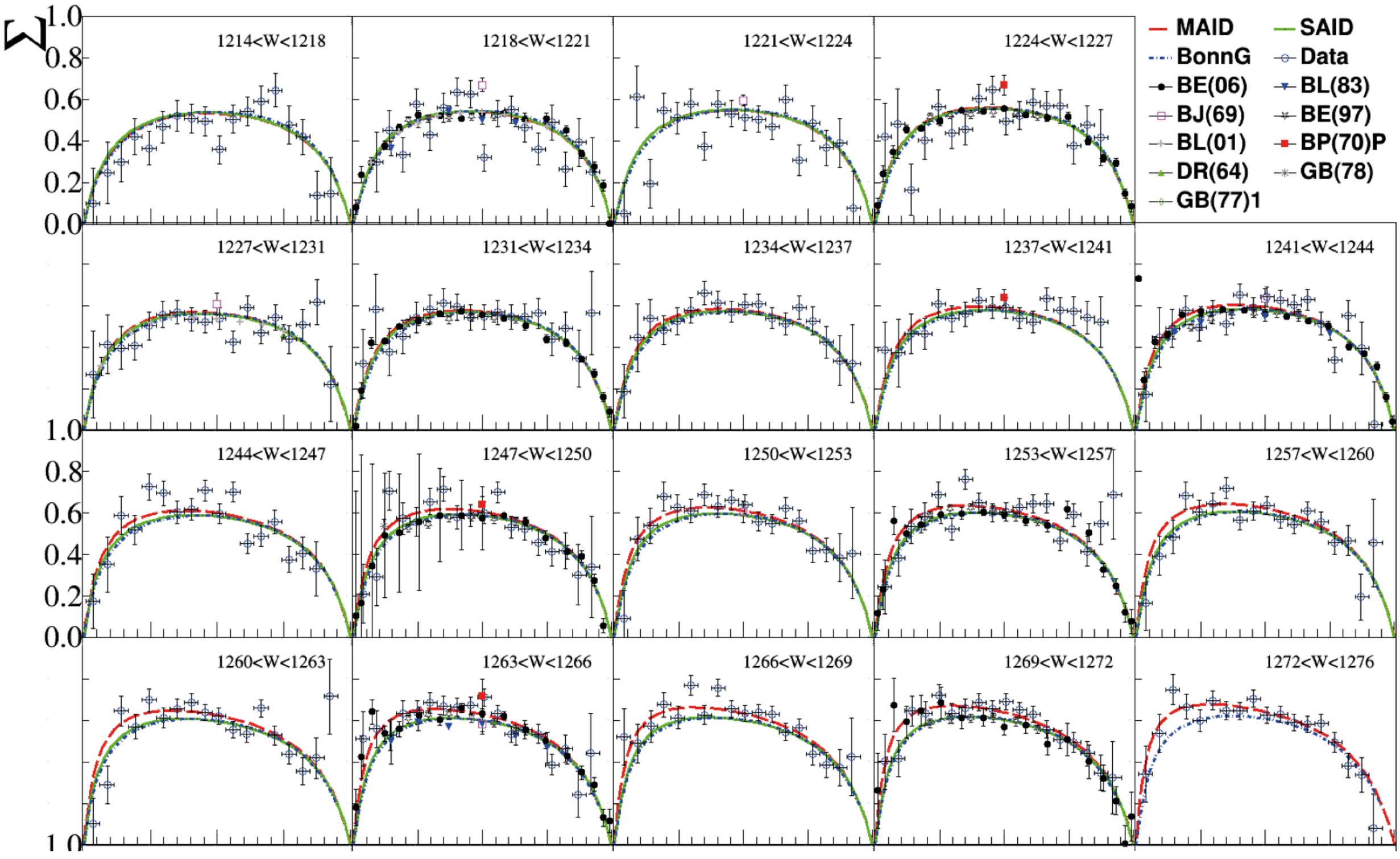

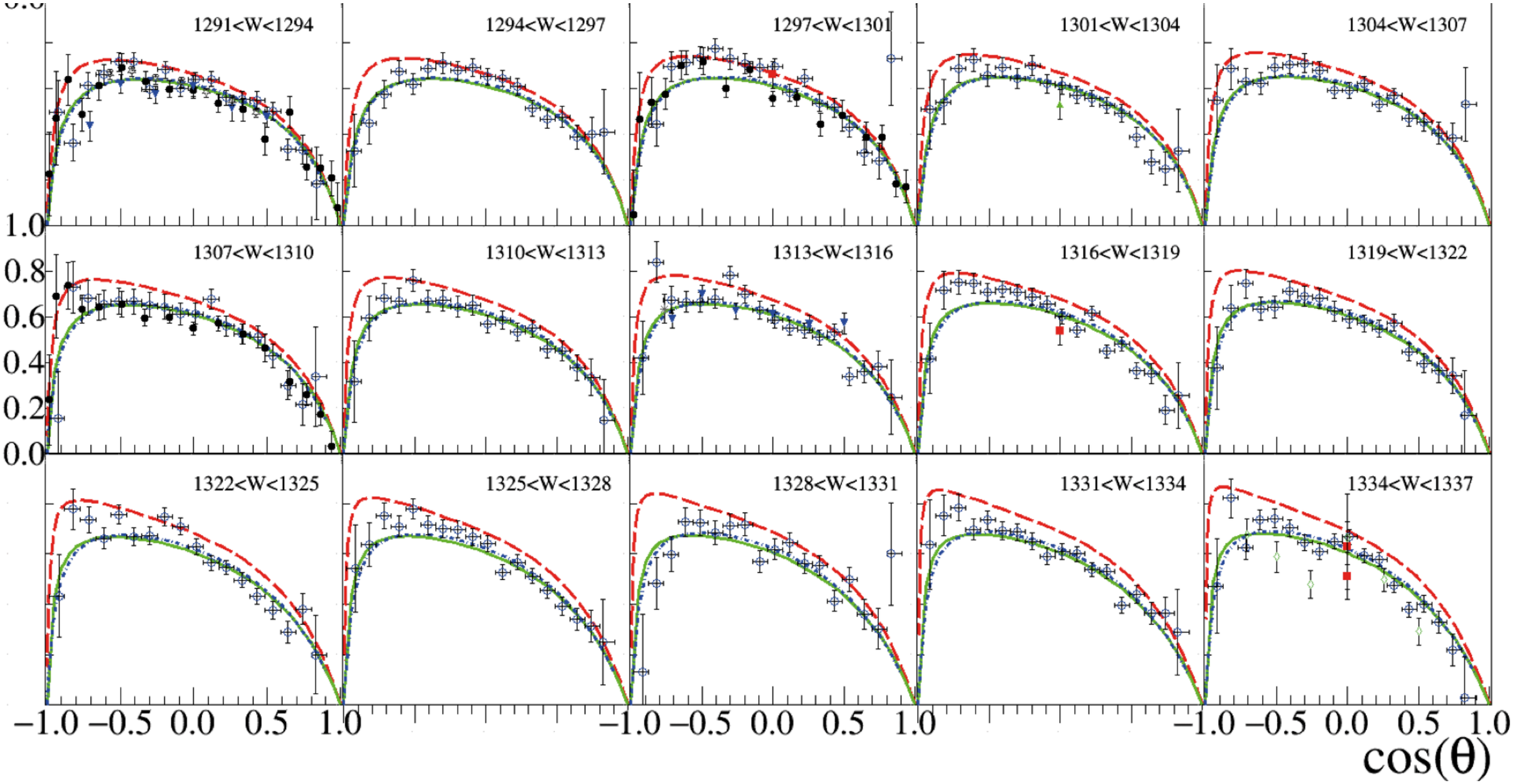
1291<W<1294
1294<W<1297
1297<W<1301
1301<W<1304
1304<W<1307
1307<W<1310
1310<W<1313
1313<W<1316
1316<W<1319
1319<W<1322
1322<W<1325
1325<W<1328
1328<W<1331
1331<W<1334
1334<W<1337
1.0
0.8
0.6
0.4
0.2
0.0
−1.0 −0.5 0.0 0.5 1.0
cos(θ)

[27] A2 collaboration, Phys. Rev. C 93, 055209 (2016)

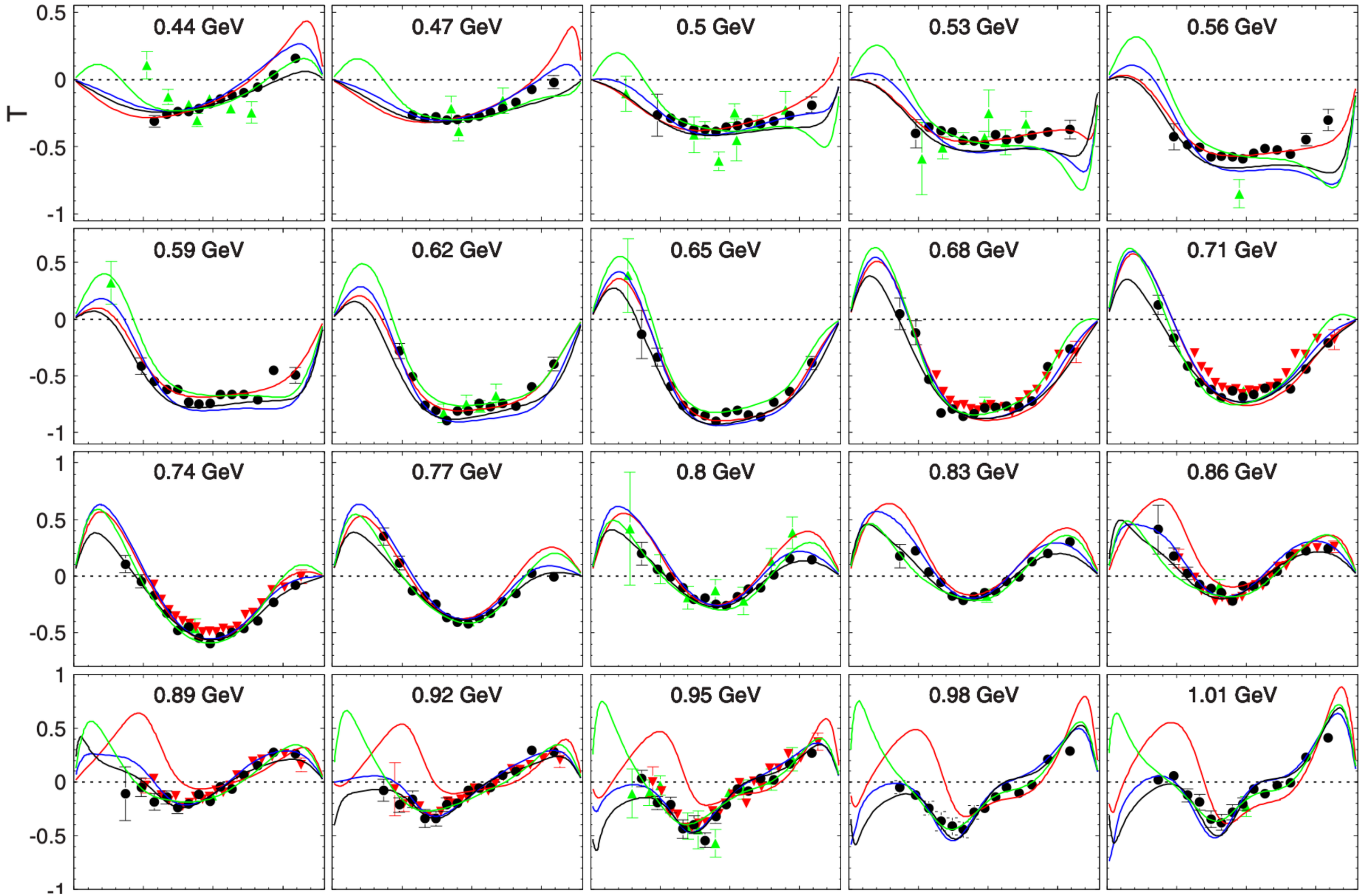

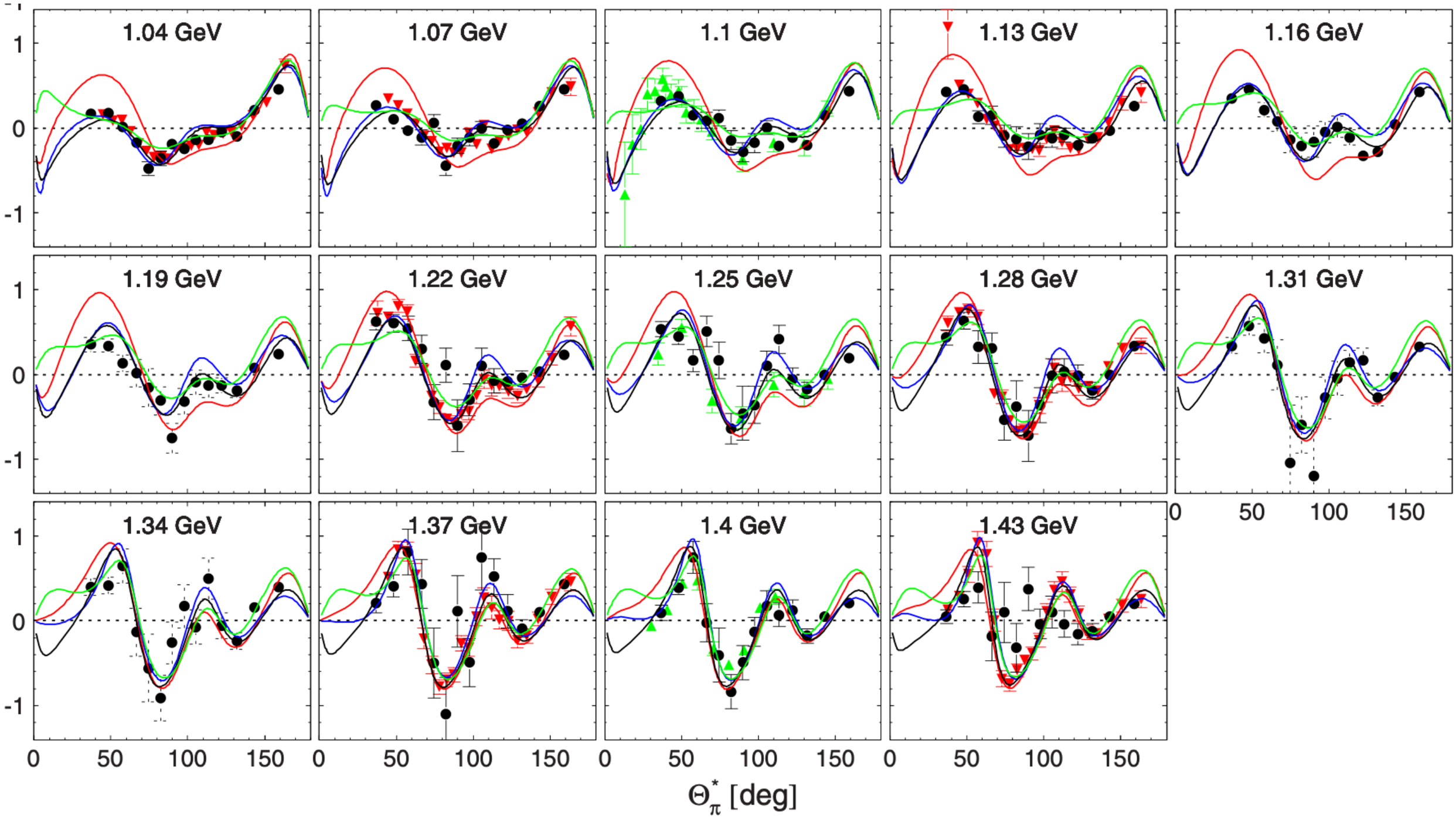
1.04 GeV
1.07 GeV
1.1 GeV
1.13 GeV
1.16 GeV
1.19 GeV
1.22 GeV
1.25 GeV
1.28 GeV
1.31 GeV
1.34 GeV
1.37 GeV
1.4 GeV
1.43 GeV
1
0
-1
0
50
100
150
Θ^*_π [deg]

In 1957 CGLN decomposition was developed.

[28] G.F. Chew, M.L. Goldberger, F.E. Low, Y. Nambu, Phys. Rev. 106, 1345 (1957)

PHYSICAL REVIEW VOLUME 106, NUMBER 6 JUNE 15, 1957

Relativistic Dispersion Relation Approach to Photomeson Production*†

G. F. CHEW,‡ *University of Illinois, Urbana, Illinois and Institute for Advanced Study, Princeton, New Jersey*
M. L. GOLDBERGER,§ *Fermi Institute for Nuclear Studies, University of Chicago, Chicago, Illinois*
F. E. LOW, *University of Illinois, Urbana, Illinois and Department of Physics and Laboratory for Nuclear Science, Massachusetts Institute of Technology, Cambridge, Massachusetts*

AND

Y. NAMBU, *Fermi Institute for Nuclear Studies, University of Chicago, Chicago, Illinois*

(Received February 21, 1957)

Relativistic dispersion relations for photomeson production, analogous to the pion-nucleon scattering dispersion relations, are formulated without proof. The assumption that the 33 resonance dominates the dispersion integrals then leads to detailed predictions about the photomeson amplitude. An attempt is made to keep first order (in v/c) nucleon recoil effects. Except for the latter, the predictions of the cutoff model are generally reproduced.

$$\frac{d\sigma}{d\Omega}=\frac{q}{k}|\langle 2|\mathcal{F}|1\rangle|^2$$

$$\mathcal{F}=i\boldsymbol{\sigma}\cdot\boldsymbol{\varepsilon}f_1+\frac{\boldsymbol{\sigma}\cdot\mathbf{q}\boldsymbol{\sigma}\cdot(\mathbf{k}\times\boldsymbol{\varepsilon})}{qk}\mathcal{F}_2+\frac{i\boldsymbol{\sigma}\cdot\mathbf{k}\mathbf{q}\cdot\boldsymbol{\varepsilon}}{qk}\mathcal{F}_3+\frac{i\boldsymbol{\sigma}\cdot\mathbf{q}\mathbf{q}\cdot\boldsymbol{\varepsilon}}{q^2}\mathcal{F}_4$$

$$\mathrm{Re}H_j(\nu,\nu_1)=R_j\left(\frac{1}{\nu_B-\nu}\pm\frac{1}{\nu_B+\nu}\right)+\frac{1}{\pi}\int_{\nu_0}^{\infty}d\nu'\,\mathrm{Im}H_j(\nu',\nu_1)\left[\frac{1}{\nu'-\nu}\pm\frac{1}{\nu'+\nu}\right],$$

$$\nu_B=-\nu_1=k\cdot q/2M,$$

$$\nu_0=1+\frac{1}{2M}(1+k\cdot q).$$

$$\mathcal{F}_1=\sum_{l=0}^{\infty}[lM_{l+}+E_{l+}]P_{l+1}'(x)+[(l+1)M_{l-}+E_{l-}]P_{l-1}'(x),$$

$$\mathcal{F}_2=\sum_{l=1}^{\infty}[(l+1)M_{l+}+lM_{l-}]P_l'(x),$$

$$\mathcal{F}_3=\sum_{l=1}^{\infty}[E_{l+}-M_{l+}]P_{l+1}''(x)+[E_{l-}+M_{l-}]P_{l-1}''(x),$$

$$\mathcal{F}_4=\sum_{l=1}^{\infty}[M_{l+}-E_{l+}-M_{l-}-E_{l-}]P_l''(x).$$

Breit-Wigner form

[29] R.L. Walker, Phys. Rev. 182 (1969) 1729.

$$H_1(\theta,\phi) = -(1/\sqrt{2})e^{i\phi}\sin\theta\cos\tfrac{1}{2}\theta\,(\mathcal{F}_3+\mathcal{F}_4)\,,$$
$$H_2(\theta,\phi) = \sqrt{2}\cos\tfrac{1}{2}\theta\,[(\mathcal{F}_2-\mathcal{F}_1) + \tfrac{1}{2}(1-\cos\theta)(\mathcal{F}_3-\mathcal{F}_4)]\,,$$
$$H_3(\theta,\phi) = (1/\sqrt{2})e^{2i\phi}\sin\theta\sin\tfrac{1}{2}\theta\,(\mathcal{F}_3-\mathcal{F}_4)\,,$$
$$H_4(\theta,\phi) = \sqrt{2}e^{i\phi}\sin\tfrac{1}{2}\theta\,[(\mathcal{F}_1+\mathcal{F}_2)+\tfrac{1}{2}(1+\cos\theta)(\mathcal{F}_3+\mathcal{F}_4)]\,.$$

$$A(W) = A(W_0)\left(\frac{k_0 q_0}{kq}\right)^{1/2}\frac{W_0\Gamma^{1/2}\Gamma_\gamma{}^{1/2}}{s_0 - s - iW_0\Gamma}$$

$$P(\theta) = -\frac{q}{k}\frac{1}{\sigma(\theta)}\,\mathrm{Im}(H_1H_3^* + H_2H_4^*)$$

$$\Sigma(\theta) = \frac{q}{k}\frac{1}{\sigma(\theta)}\,\mathrm{Re}(H_1H_4^* - H_2H_3^*)$$

$$T(\theta) = \frac{q}{k}\frac{1}{\sigma(\theta)}\,\mathrm{Im}(H_1H_2^* + H_3H_4^*)$$

The effective Lagrangian description [30] R.D. Peccei, Phys. Rev. 181 (1969)

$$\mathfrak{L}_{\mathrm{el}} = eA^\alpha\{\epsilon_{ij3}\partial_\alpha\pi_i\pi_j + \bar{N}[\tfrac{1}{2}(1+\tau_3)]\gamma_\alpha N + (f\sqrt{2}/m)\bar{N}\gamma_\alpha\gamma_5(\tau_+\pi^- - \tau_-\pi^+)N\}$$
$$+ eF^{\alpha\beta}\{(\kappa_p/4M)\bar{N}\sigma_{\alpha\beta}[\tfrac{1}{2}(1+\tau_3)]N + (\kappa_n/4M)\bar{N}\sigma_{\alpha\beta}[\tfrac{1}{2}(1-\tau_3)]N + (\kappa^*/4M)[\bar{N}_3{}^{*\lambda}(i\gamma_\alpha g_{\lambda\beta} - i\gamma_\beta g_{\lambda\alpha} - \tfrac{1}{2}\gamma_\lambda\sigma_{\alpha\beta})\gamma_5 N + \bar{N}(i\gamma_\alpha g_{\lambda\beta} - i\gamma_\beta g_{\lambda\alpha} + \tfrac{1}{2}\sigma_{\alpha\beta}\gamma_\lambda)\gamma_5 N_3{}^{*\lambda}]\}$$
$$\mathfrak{L}_{\pi NN} = (f/m)\bar{N}i\gamma_\alpha\gamma_5\tau_i N\partial^\alpha\pi_i\,,$$
$$\mathfrak{L}_{\pi NN^*} = (ih/m)[\bar{N}_{\alpha i}{}^*(4g^{\alpha\beta}+\gamma^\alpha\gamma^\beta)N - \bar{N}(4g^{\beta\alpha}+\gamma^\beta\gamma^\alpha)N_{\alpha i}{}^*]\partial_\beta\pi_i\,,$$

Methods developed later:

Parametrization based on K-matrix

[31] R.A. Arndt, R.L. Workman, Zh. Li, L.D. Roper, Phys. Rev. C 42 (1990).

$$(1-iK_{\gamma\gamma})T_{\gamma\pi}=(1+iT_{\pi\pi})\left[K_{\gamma\pi}-\frac{K_{\gamma\Delta}K_{\pi\pi}}{K_{\pi\Delta}}\right]+\frac{K_{\gamma\Delta}}{K_{\pi\Delta}}T_{\pi\pi}$$

$$\equiv A_I(1+iT_\pi)+A_R T_\pi$$

Combination of Breit-Wigner form and the effective Lagrangian

[32] R.M. Davidson, N.C. Mukhopadhyay, R. Wittman, Phys. Rev. D 43 (1991).

$$L=L_{\pi N\Delta}+L^1_{\gamma N\Delta}+L^2_{\gamma N\Delta} \qquad qf^{\Delta}_{1+}=\frac{M_\Delta\Gamma_\Delta(s)}{M_\Delta^2-s}\equiv\frac{1}{\epsilon} \qquad T_{\gamma\pi}=K_{\gamma\pi}(1+iT_{\pi\pi})$$

Unitarity Isobar Model [33] D. Drechsel, O. Hanstein, S. Kamalov, L. Tiator, Nuclear Phys. A 645 (1999).

$$A_{l\pm}(W)=\bar{A}_{l\pm}f_{\gamma N}(W)\frac{\Gamma_{\text{tot}}W_R e^{i\phi}}{W_R^2-W^2-iW_R\Gamma_{\text{tot}}}f_{\pi N}(W)C_{\pi N}$$

Beter-Salpeter Equation [34]T. Sato, T.-S.H. Lee, Phys. Rev. C 54, 2660 (1996).

$$T_{\gamma\pi}(E) = t_{\gamma\pi}(E) + \bar{\Gamma}_{\Delta\to\pi N}(E) G_{\Delta}(E) \bar{\Gamma}_{\gamma N\to\Delta}(E)$$

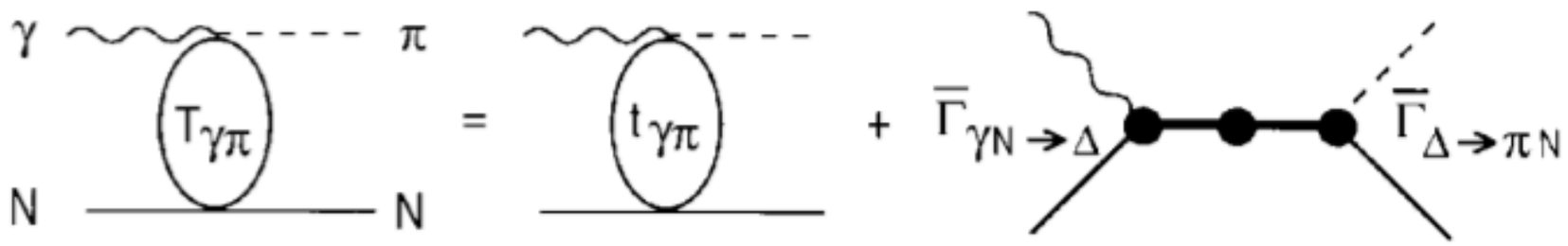

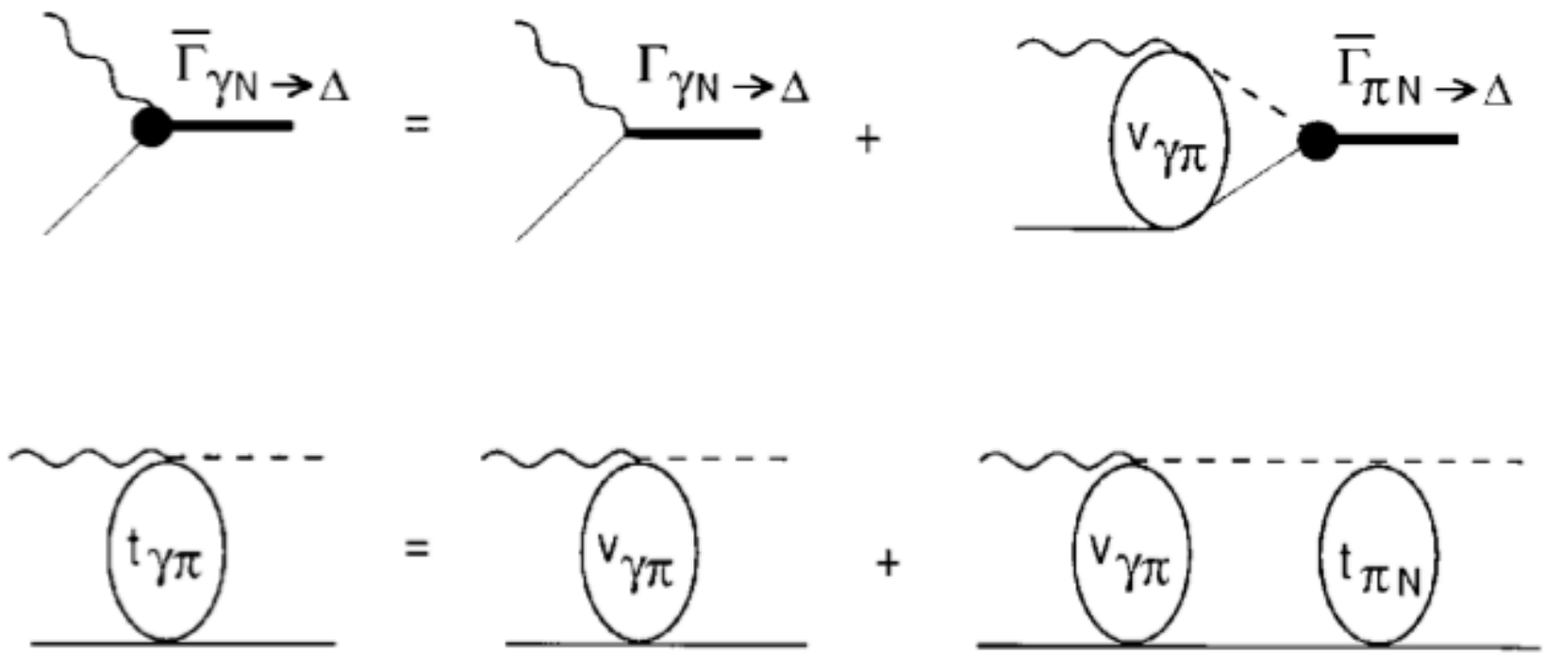

N/D Method

[9] A. Gasparyan and M. Lutz, Nucl. Phys. A848, 126 (2010).

$$T_{ab}(\sqrt{s}) = \sum_c D^{-1}_{ac}(\sqrt{s}) N_{cb}(\sqrt{s})$$

$$N_{ab}(\sqrt{s}) = U_{ab}(\sqrt{s}) + \sum_{c,d} \int_{\mu_{\rm thr}}^{\infty} \frac{dw}{\pi} \frac{\sqrt{s}-\mu_M}{w-\mu_M} \frac{N_{ac}(w)\rho_{cd}(w)[U_{db}(w)-U_{db}(\sqrt{s})]}{w-\sqrt{s}}$$

$$D_{ab}(\sqrt{s}) = \delta_{ab} - \sum_c \int_{\mu_{\rm thr}}^{\infty} \frac{dw}{\pi} \frac{\sqrt{s}-\mu_M}{w-\mu_M} \frac{N_{ac}(w)\rho_{cb}(w)}{w-\sqrt{s}}$$

Laurent-Pietarinen expansion [35] A. Svarc et al., Phys. Rev. C89, 065208 (2014).

$$T(W) = \sum_{i=1}^{k} \frac{a_{-1}^{(i)}}{W - W_i} + B^L(W),$$

$$B^L(W) = \sum_{n=0}^{M} c_n \, X(W)^n + \sum_{n=0}^{N} d_n \, Y(W)^n + \sum_{n=0}^{L} e_n \, Z(W)^n + \cdots,$$

$$X(W) = \frac{\alpha - \sqrt{x_P - W}}{\alpha + \sqrt{x_P - W}},$$

$$Y(W) = \frac{\beta - \sqrt{x_Q - W}}{\beta + \sqrt{x_Q - W}},$$

$$Z(W) = \frac{\gamma - \sqrt{x_R - W}}{\gamma + \sqrt{x_R - W}} + \cdots,$$

$$a_{-1}^{(i)}, W_i, W \in \mathbb{C},$$

$$c_n, d_n, e_n, \alpha, \beta, \gamma, \ldots \in \mathbb{R},$$

$$x_P, x_Q, x_R \in \mathbb{R} \text{ or } \mathbb{C},$$

$$k, M, N, L \ldots \in \mathbb{N}.$$

Research on low energy photoproduciton based on chiral perturbation theory

[36] G. H. Guerrero Navarro, M. J. Vicente Vacas, A. N. Hiller Blin, and D. L. Yao, Phys. Rev. D100, 094021 (2019).

$$\mathcal{L}_{\text{eff}} = \sum_{i=1}^{2} \mathcal{L}_{\pi\pi}^{(2i)} + \sum_{j=1}^{3} \mathcal{L}_{N}^{(j)} + \mathcal{L}_{\pi N\Delta}^{(1)} + \mathcal{L}_{\gamma N\Delta}^{(2)}$$

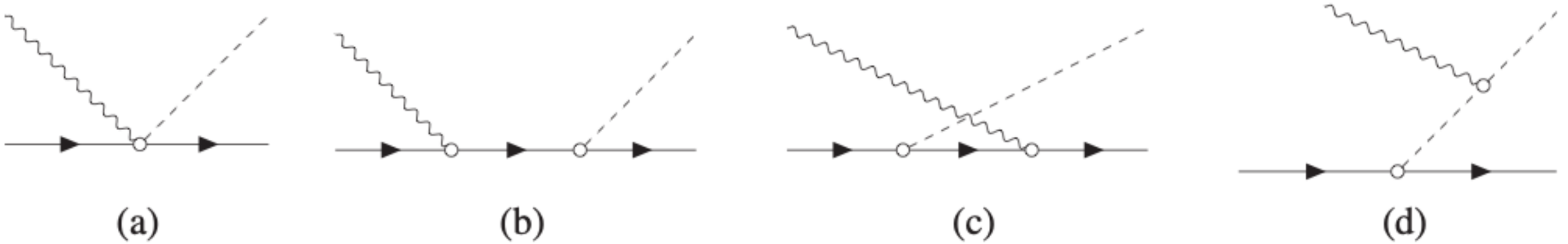

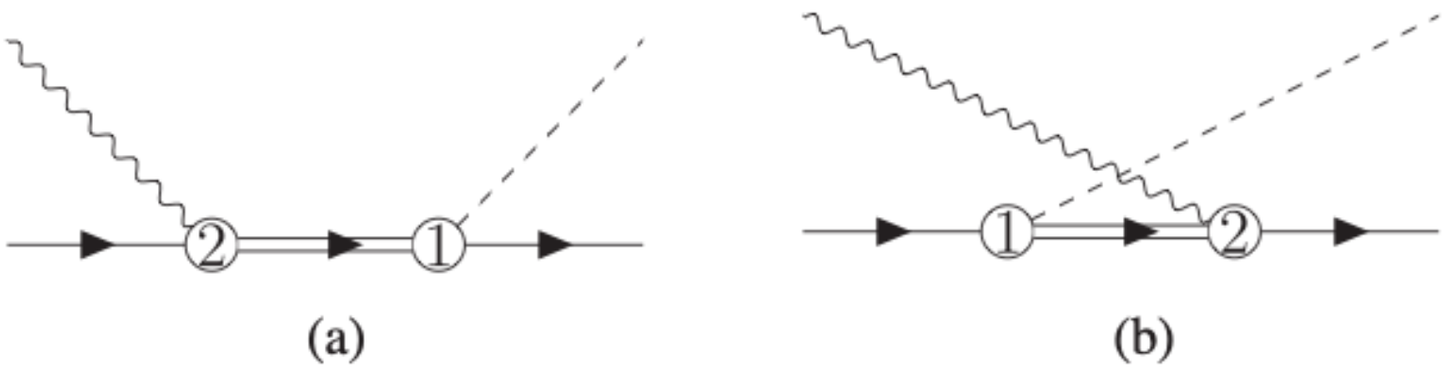

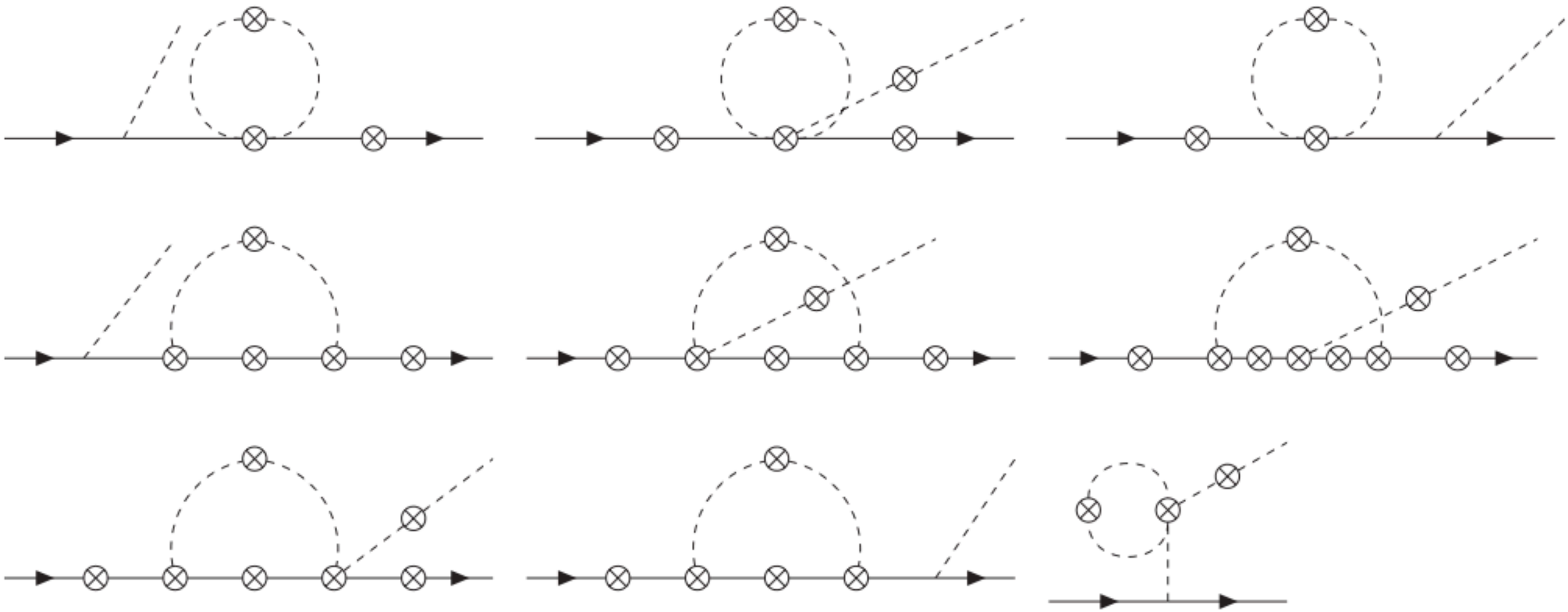

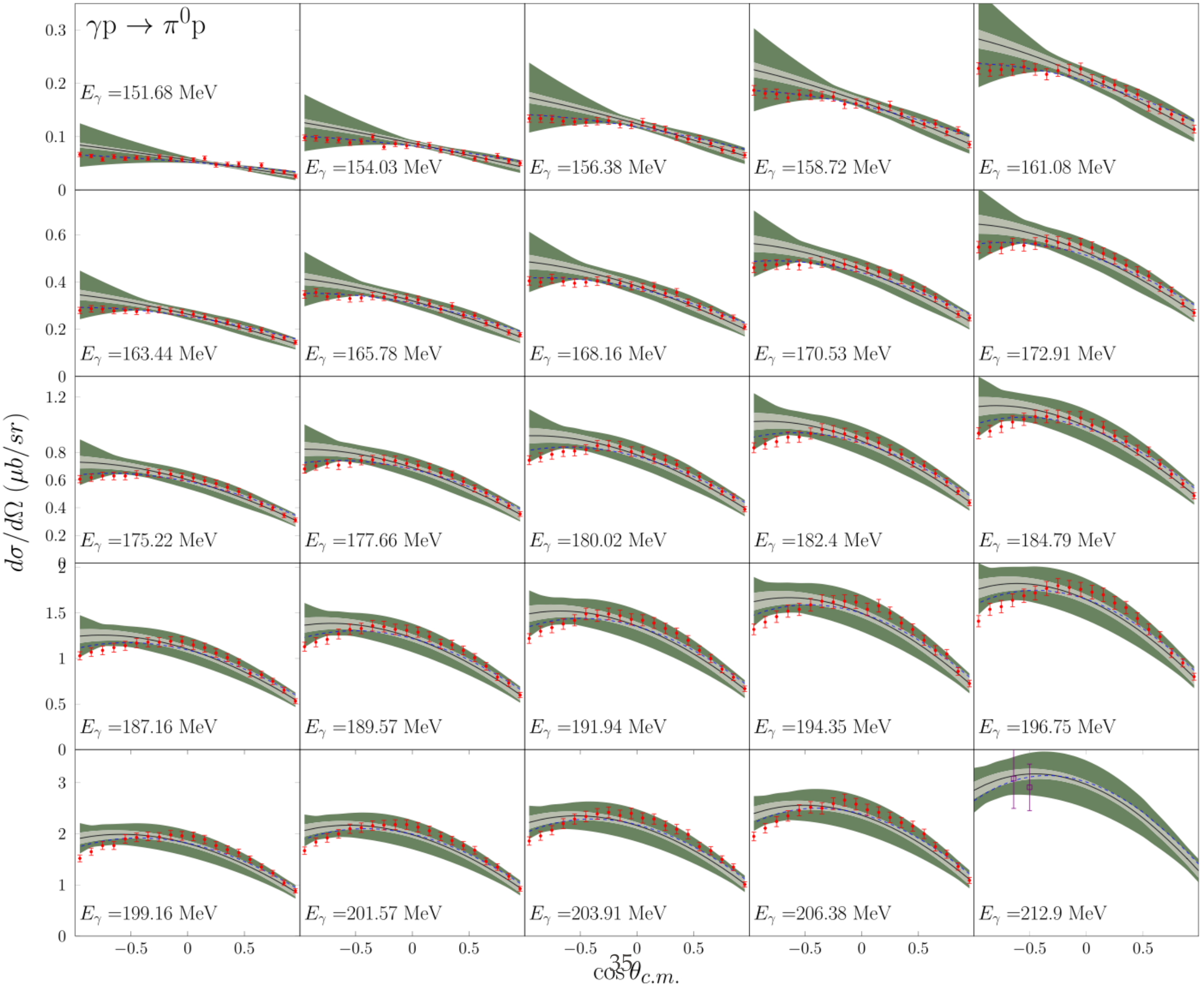
$\gamma p \to \pi^0 p$
E_γ =151.68 MeV
E_γ =154.03 MeV
E_γ =156.38 MeV
E_γ =158.72 MeV
E_γ =161.08 MeV
E_γ =163.44 MeV
E_γ =165.78 MeV
E_γ =168.16 MeV
E_γ =170.53 MeV
E_γ =172.91 MeV
E_γ =175.22 MeV
E_γ =177.66 MeV
E_γ =180.02 MeV
E_γ =182.4 MeV
E_γ =184.79 MeV
E_γ =187.16 MeV
E_γ =189.57 MeV
E_γ =191.94 MeV
E_γ =194.35 MeV
E_γ =196.75 MeV
E_γ =199.16 MeV
E_γ =201.57 MeV
E_γ =203.91 MeV
E_γ =206.38 MeV
E_γ =212.9 MeV
$d\sigma/d\Omega$ $(\mu b/sr)$
$\cos\theta_{c.m.}$

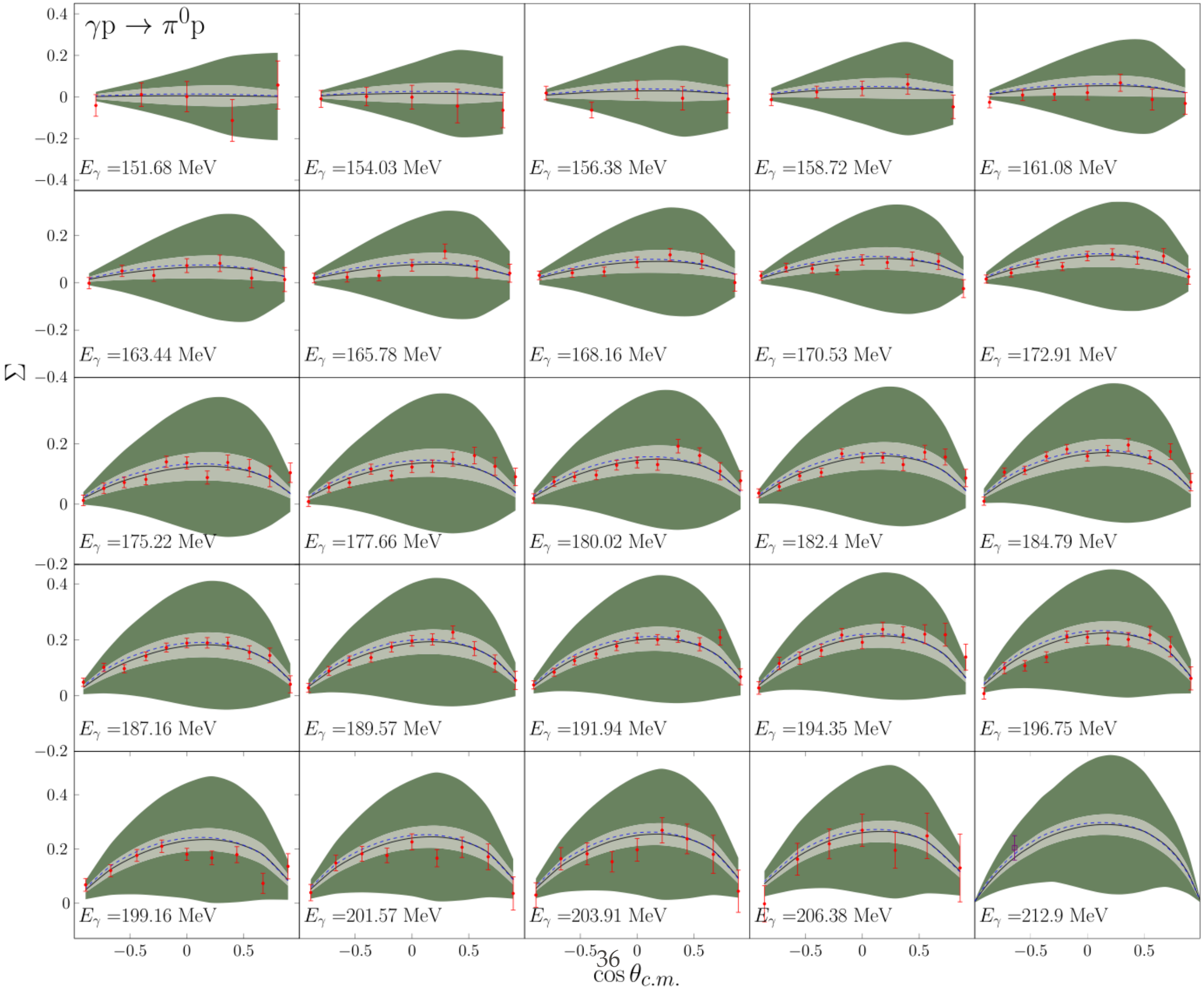
$\gamma p \to \pi^0 p$
Σ
E_γ =151.68 MeV
E_γ =154.03 MeV
E_γ =156.38 MeV
E_γ =158.72 MeV
E_γ =161.08 MeV
E_γ =163.44 MeV
E_γ =165.78 MeV
E_γ =168.16 MeV
E_γ =170.53 MeV
E_γ =172.91 MeV
E_γ =175.22 MeV
E_γ =177.66 MeV
E_γ =180.02 MeV
E_γ =182.4 MeV
E_γ =184.79 MeV
E_γ =187.16 MeV
E_γ =189.57 MeV
E_γ =191.94 MeV
E_γ =194.35 MeV
E_γ =196.75 MeV
E_γ =199.16 MeV
E_γ =201.57 MeV
E_γ =203.91 MeV
E_γ =206.38 MeV
E_γ =212.9 MeV
0.4
0.2
0
−0.2
−0.4
−0.5
0
0.5
$\cos\theta_{c.m.}$

2. Dispersion Relation

$$\mathscr{M}(s) = \mathscr{M}_L + \mathscr{D}\left(-\frac{s^n}{\pi}\int_{s_R}^{\infty} \frac{\left(\mathrm{Im}\mathscr{D}^{-1}\right)\mathscr{M}_L}{s'^n(s'-s)}\mathrm{d}s' + \mathscr{P} \right)$$

2.1 Amplitude [37] G. F. Chew, M. L. Goldberger, F. E. Low, and Y. Nambu, Phys. Rev. 106, 1345 (1957).

Lorentz structure

$$L_\mu^1 = i\gamma_5\gamma_\mu\gamma\cdot q$$

$$L_\mu^2 = 2i\gamma_5\left(P_\mu q\cdot q' - q'_\mu P\cdot q\right)$$

$$L_\mu^2 = \gamma_5\left(\gamma_\mu q'\cdot q - q'_\mu\gamma\cdot q\right)$$

$$L_\mu^4 = 2\gamma_5\left(\gamma_\mu P\cdot q - P_\mu\gamma\cdot q\right)$$

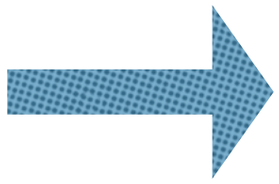

$$\mathscr{M}^I(s,t) \equiv \bar{u}(p')\mathscr{T}^I u(p) = \bar{u}(p')\left[\sum_{i=1}^{4}\mathscr{A}_i^I(s,t)\,L_\mu^i\epsilon^\mu\right]u(p)$$

Partial wave decomposition

$$\mathscr{M}^{IJ}_{H_s}(s) = \frac{1}{32\pi}\int d\cos\theta\,\mathscr{M}^I_{H_s}(s,t)d^J_{\lambda,\lambda'}(\theta) \qquad \mathscr{M}(S_{11}) = \left(\mathscr{M}^{I=\frac{1}{2}J=\frac{1}{2}}_{+++} + \mathscr{M}^{I=\frac{1}{2}J=\frac{1}{2}}_{++-}\right)$$

Isospin structure

$$\mathscr{M}(\gamma + N \to \pi^a + N') = \chi'_N \left\{ \delta_{a3}\, \mathscr{M}^+ + \frac{1}{2}[\tau_a, \tau_3]\, \mathscr{M}^- + \tau_3\, \mathscr{M}^0 \right\} \chi_N$$

$$\mathscr{M}^{I=\frac{3}{2}} = \sqrt{\frac{2}{3}} \left(\mathscr{M}^+ - \mathscr{M}^- \right)$$

$$\mathscr{M}^{I=\frac{1}{2}} = -\frac{1}{\sqrt{3}} \left(\mathscr{M}^+ + 2\mathscr{M}^- + 3\mathscr{M}^0 \right) \qquad \text{(p target)}$$

$$\mathscr{M}^{I=\frac{1}{2}} = \frac{1}{\sqrt{3}} \left(\mathscr{M}^+ + 2\mathscr{M}^- - 3\mathscr{M}^0 \right) \qquad \text{(n target)}$$

Target asymmetry due to electromagnetic interaction

2.2 Dispersion Relation

Unitarity

[38] O. Babelon, J.-L. Basdevant, D. Caillerie, and G. Mennessier, Nucl. Phys. B113, 445 (1976).
[39] O. Babelon, J.-L. Basdevant, D. Caillerie, M. Gourdin, and G. Mennessier, Nucl. Phys.B114, 252 (1976).
[40] Y. Mao, X. G. Wang, O. Zhang, H. Q. Zheng, and Z. Y. Zhou, Phys. Rev. D79, 116008 (2009).
[41] L. Y. Dai and M. R. Pennington, Phys. Rev. D94, 116021 (2016).

$$\frac{\mathscr{M}(s+i\epsilon)-\mathscr{M}(s-i\epsilon)}{2i}=\mathrm{Im}\mathscr{M}(s+i\epsilon)=\mathscr{T}^{*}(s+i\epsilon)\rho(s+i\epsilon)\mathscr{M}(s+i\epsilon)$$

Analyticity and Dispersion Relation

$$\mathscr{M}=\mathscr{M}_R+\mathscr{M}_L$$

$$\mathscr{M}(s+i\epsilon)=\mathcal{S}(s+i\epsilon)\mathscr{M}(s-i\epsilon)\longrightarrow\mathscr{M}_R^{+}=\mathcal{S}\mathscr{M}_R^{-}+(\mathcal{S}-1)\mathscr{M}_L$$

$$\frac{\mathscr{D}^{+}}{\mathscr{D}^{-}}=\frac{\mathscr{M}^{+}}{\mathscr{M}^{-}}=\mathcal{S}\longrightarrow\mathscr{D}(s)=\tilde{\mathscr{P}}(s)\exp\left[\frac{s}{\pi}\int_{s_R}^{\infty}\frac{\delta(s')}{s'(s'-s)}\mathrm{d}s'\right]$$

[41] R. Omnès, Nuovo Cim. 8, 316 (1958).

$$\mathrm{Im}\left(\mathscr{D}^{-1}\mathscr{M}_R\right)=-\left(\mathrm{Im}\mathscr{D}^{-1}\right)\mathscr{M}_L$$

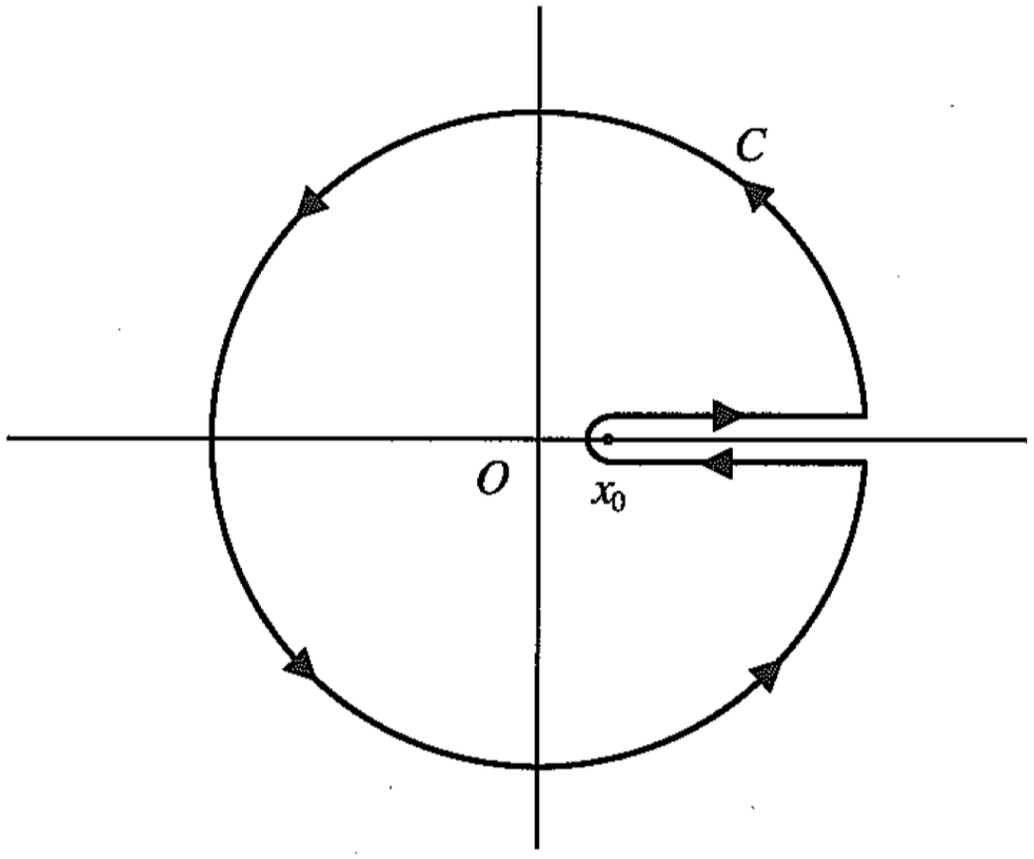

$$f(z) = \frac{1}{2\pi i}\left[\int_{x_0+i\epsilon}^{\infty+i\epsilon} \frac{f(\xi)}{\xi - z}\,d\xi - \int_{x_0-i\epsilon}^{\infty-i\epsilon} \frac{f(\xi)}{\xi - z}\,d\xi\right]$$
$$= \frac{1}{2\pi i}\left[\int_{x_0}^{\infty} \frac{f(x+i\epsilon)}{x - z + i\epsilon}\,dx - \int_{x_0}^{\infty} \frac{f(x-i\epsilon)}{x - z - i\epsilon}\,dx\right]$$

$$f(z) = \frac{1}{\pi}\int_{x_0}^{\infty} \frac{\mathrm{Im}[f(x+i\epsilon)]}{x - z}\,dx$$

$$\mathrm{Im}\left(\mathscr{D}^{-1}\mathscr{M}_R\right) = -\left(\mathrm{Im}\mathscr{D}^{-1}\right)\mathscr{M}_L$$

$$\mathscr{M}(s) = \mathscr{M}_L + \mathscr{D}\left(-\frac{s^n}{\pi}\int_{s_R}^{\infty} \frac{\left(\mathrm{Im}\mathscr{D}^{-1}\right)\mathscr{M}_L}{s'^n(s'-s)}\mathrm{d}s' + \mathscr{P}\right)$$

3. Chiral Perturbation Calculation

3.1 Lagrangian Analysis

Lagrangian up to $\mathcal{O}(q^2)$ [42] S. Scherer and M. R. Schindler, Lect. Notes Phys. 830, 1 (2012).

$$\mathscr{L}_{\pi N}^{(1)} = \bar{\Psi}\left(i\gamma^{\mu}D_{\mu} - m + \frac{g}{2}\gamma^{\mu}\gamma_5 u_{\mu}\right)\Psi$$

$$\mathscr{L}_{\pi N}^{(2)} = \bar{\Psi}\sigma^{\mu\nu}\left[\frac{c_6}{2}f_{\mu\nu}^{+} + \frac{c_7}{2}v_{s,\mu\nu}\right]\Psi$$

$$\mathscr{L}_{\pi\pi}^{(2)} = \frac{F^2}{4}Tr\left[D_{\mu}U(D^{\mu}U)^{\dagger}\right] + \frac{F^2}{4}Tr\left(\chi U^{\dagger} + U\chi^{\dagger}\right)$$

Figure 4. Feynman diagram.

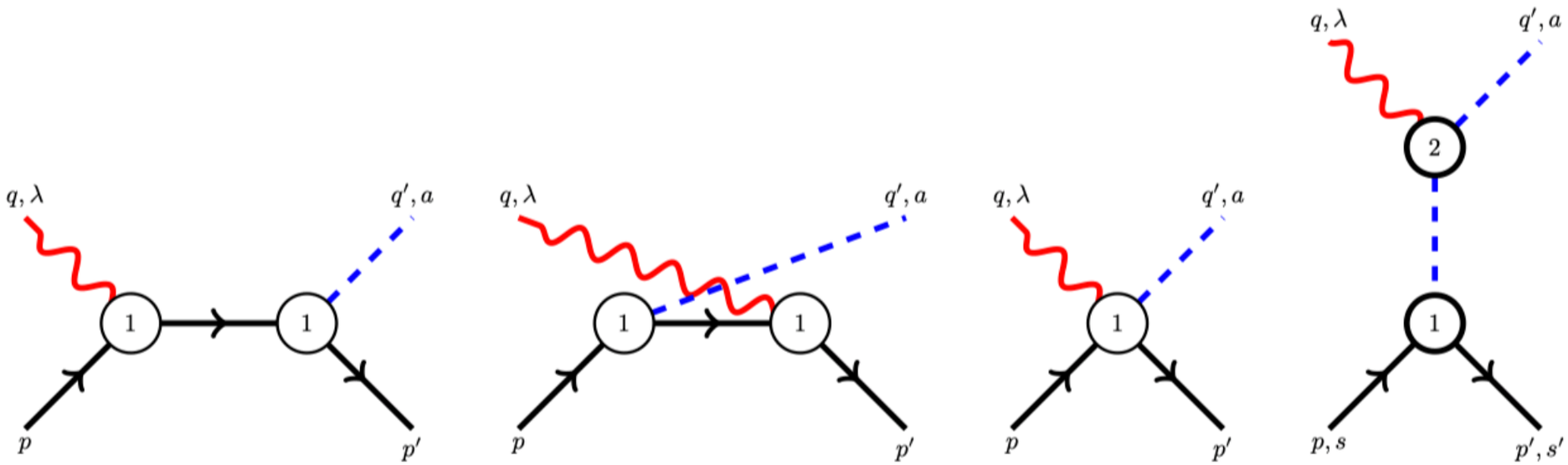

(a) s channel (b) u channel (c) contact diagram (d) t channel

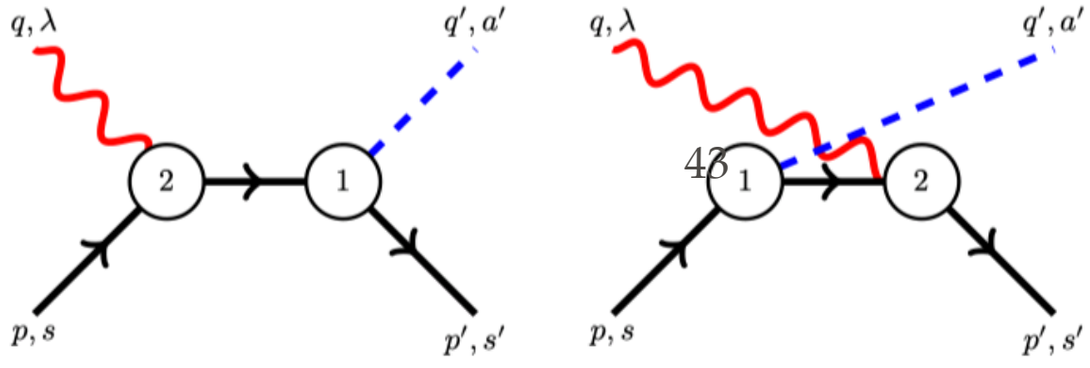

(a) s channel (b) u channel

Invariant amplitude

$$\mathscr{A}_1^+ = -\frac{ieg_A m_N}{2F_\pi}\left(\frac{1}{u-m_N^2}+\frac{1}{s-m_N^2}\right)-\frac{ieg_A c_6}{F}\left(\frac{2m_N^2}{u-m_N^2}+\frac{2m_N^2}{s-m_N^2}+1\right)$$

$$\mathscr{A}_1^0 = -\frac{ieg_A m_N}{2F_\pi}\left(\frac{1}{u-m_N^2}+\frac{1}{s-m_N^2}\right)-\frac{ieg_A c_7}{2F}\left(\frac{2m_N^2}{u-m_N^2}+\frac{2m_N^2}{s-m_N^2}+1\right)$$

$$\mathscr{A}_1^- = -\frac{ieg_A m_N}{2F_\pi}\left(-\frac{1}{u-m_N^2}+\frac{1}{s-m_N^2}\right)-\frac{ieg_A c_6}{F}\left(-\frac{2m_N^2}{u-m_N^2}+\frac{2m_N^2}{s-m_N^2}\right)$$

$$\mathscr{A}_2^+ = \frac{ieg_A m_N}{4F_\pi P\cdot q}\left(\frac{1}{u-m_N^2}-\frac{1}{s-m_N^2}\right)$$

$$\mathscr{A}_2^0 = \frac{ieg_A m_N}{4F_\pi P\cdot q}\left(\frac{1}{u-m_N^2}-\frac{1}{s-m_N^2}\right)$$

$$\mathscr{A}_2^- = -\frac{ieg_A m_N}{4F_\pi P\cdot q}\left(\frac{1}{u-m_N^2}+\frac{1}{s-m_N^2}+\frac{4}{t-m_\pi^2}\right)$$

$$\mathscr{A}_3^+ = \frac{eg_A c_6 m_N}{F_\pi}\left(\frac{1}{u-m_N^2}-\frac{1}{s-m_N^2}\right)$$

$$\mathscr{A}_3^0 = \frac{eg_A c_7 m_N}{2F_\pi}\left(\frac{1}{u-m_N^2}-\frac{1}{s-m_N^2}\right)$$

$$\mathscr{A}_3^- = \frac{eg_A c_6 m_N}{F_\pi}\left(-\frac{1}{u-m_N^2}-\frac{1}{s-m_N^2}\right)$$

$$\mathscr{A}_4^+ = -\frac{eg_A c_6 m_N}{F_\pi}\left(\frac{1}{u-m_N^2}+\frac{1}{s-m_N^2}\right)$$

$$\mathscr{A}_4^0 = -\frac{eg_A c_7 m_N}{2F_\pi}\left(\frac{1}{u-m_N^2}+\frac{1}{s-m_N^2}\right)$$

$$\mathscr{A}_4^- = -\frac{eg_A c_6 m_N}{F_\pi}\left(-\frac{1}{u-m_N^2}+\frac{1}{s-m_N^2}\right)$$

$$\mathscr{D}_1 = \ln\left(-\sqrt{s-s_L}\sqrt{s-s_R}+m_N^2-m_\pi^2+s\right)$$
$$-\ln\left(\sqrt{s-s_L}\sqrt{s-s_R}+m_N^2-m_\pi^2+s\right)$$

$$\mathscr{D}_2 = \ln\left(-\sqrt{s-s_L}\sqrt{s-s_R}-m_N^2+m_\pi^2+s\right)$$
$$-\ln\left(\sqrt{s-s_L}\sqrt{s-s_R}-m_N^2+m_\pi^2+s\right)$$

$$\mathscr{D}_3 = \ln\left(\sqrt{s-s_L}\sqrt{s-s_R}+m_N^2-m_\pi^2+3s\right)$$
$$-\ln\left(-\sqrt{s-s_L}\sqrt{s-s_R}+m_N^2-m_\pi^2+3s\right)$$

3.2 Singularities

Figure 5. Singularities

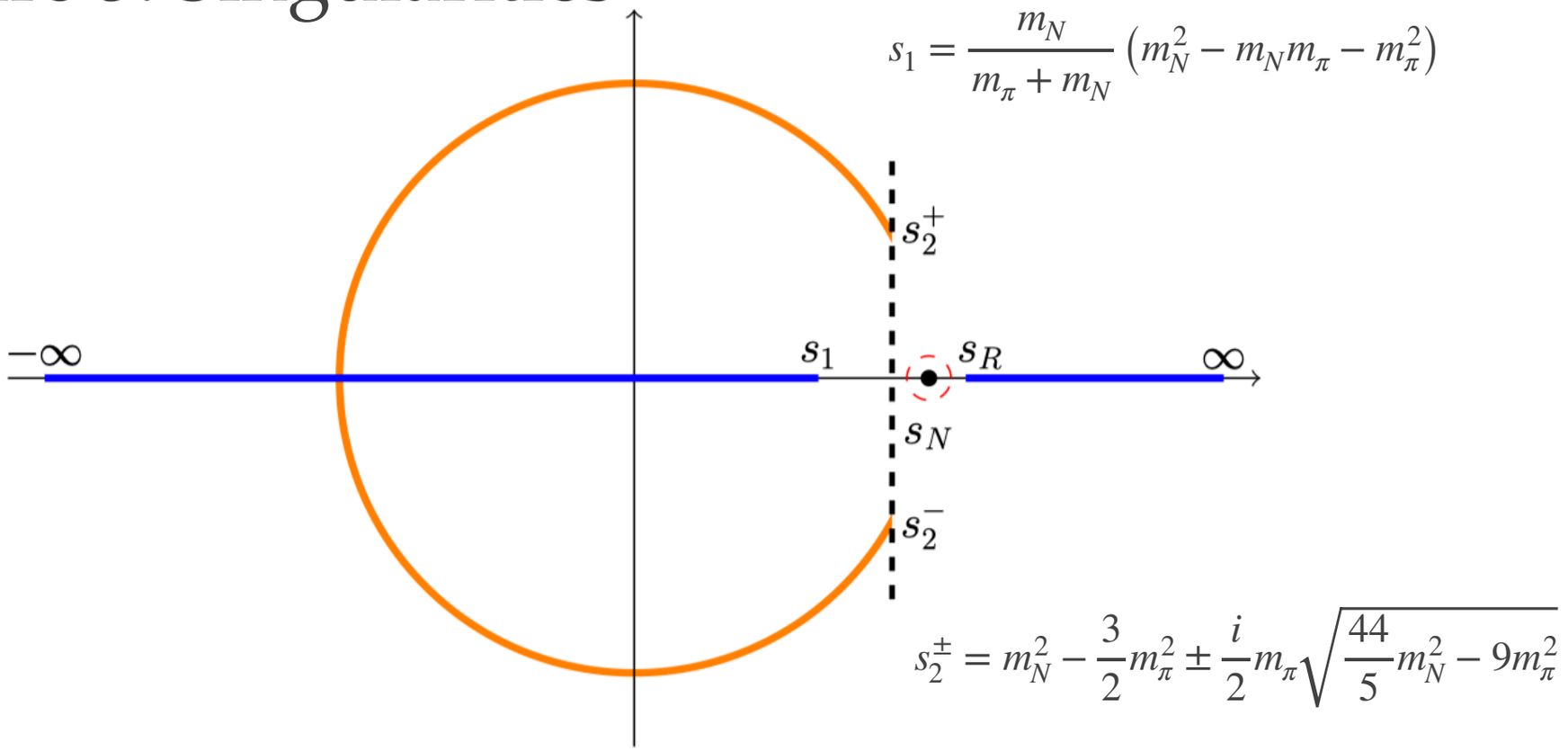

Dynamical structure: $\dfrac{1}{\sqrt{\rho_{\gamma N}\rho_{\pi N}}}\ln\dfrac{\alpha(s)-\beta(s)}{\alpha(s)+\beta(s)}$

[43] J. Kennedy and T. D. Spearman, Phys. Rev. 126, 1596 (1962).

Unitarity cut: $s \in [s_R, \infty)$

u-channel crossed cut: $s \in (-\infty, s_1]$ $(u \geq (m_N + m_\pi)^2)$

t-channel crossed cut: the arc $(4m_\pi^2 \leq t \leq 4m_N^2)$

$s \in (-\infty, 0]$ $(4m_N^2 \leq t)$

Trivial cut: $s \in (-\infty, 0]$ generated by logarithms

$s_N = m_N^2$ pole: t-channel pion pole exchange and
u-channel nucleon pole exchange

Kinematical structure: Square root

Difference of cuts: $\dfrac{\sqrt{s-s_L}\sqrt{s-s_R}}{\sqrt{(s-s_L)(s-s_R)}}$

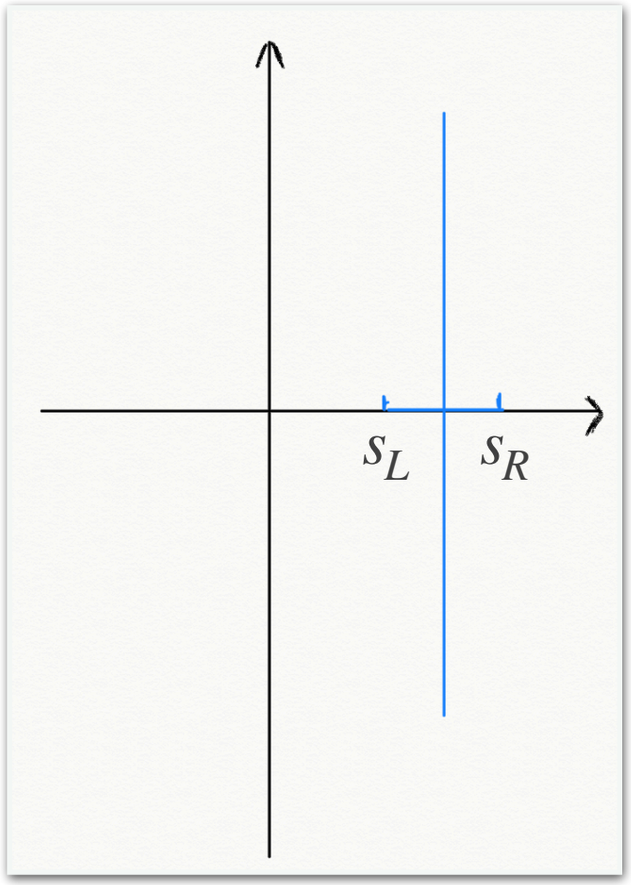

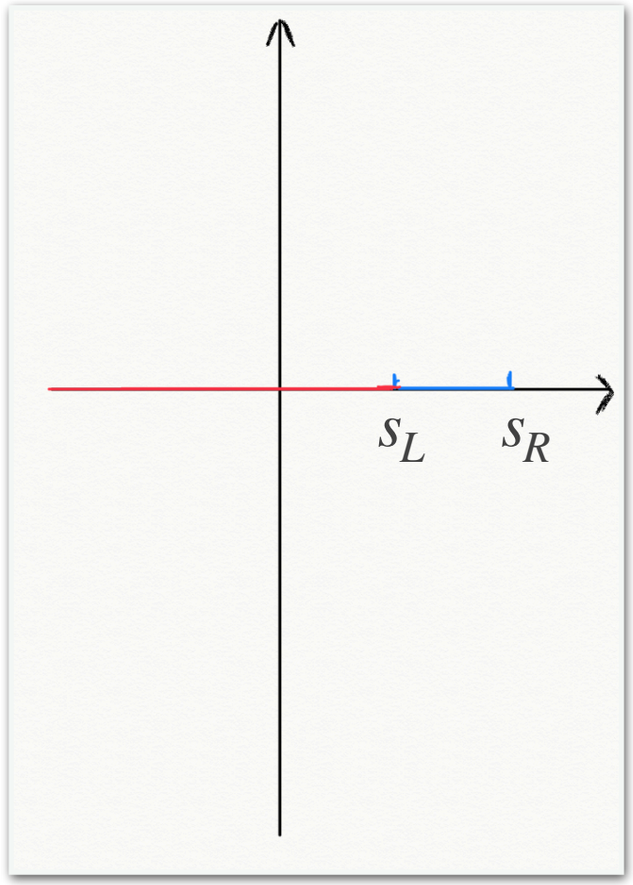

$$\mathscr{M}_L = \mathscr{M}^{(2)}_{tree}$$

Table 3. Analysis of arguments causing singularities

Arguments	Negative Region
$s - s_R$	$(-\infty, s_R)$
$s - s_L$	$(-\infty, s_L)$
s	$(-\infty,0)$
$s + m_N^2 - m_\pi^2 + \sqrt{s - s_R}\sqrt{s - s_L}$	-
$s + m_N^2 - m_\pi^2 - \sqrt{s - s_R}\sqrt{s - s_L}$	$(-\infty,0)$
$3s + m_N^2 - m_\pi^2 + \sqrt{s - s_R}\sqrt{s - s_L}$	$\left(-\infty, \frac{1}{2}\left(m_\pi^2 - 2m_N^2\right)\right)$
$3s + m_N^2 - m_\pi^2 - \sqrt{s - s_R}\sqrt{s - s_L}$	$(-\infty,0)$
$s - m_N^2 + m_\pi^2 + \sqrt{s - s_R}\sqrt{s - s_L}$	$(0,s_L)$
$s - m_N^2 + m_\pi^2 - \sqrt{s - s_R}\sqrt{s - s_L}$	$(-\infty, s_L)$

4. Numerical Analysis

4.1 Fit [44] R. L. Workman, M. W. Paris, W. J. Briscoe, and I. I. Strakovsky, Phys. Rev. C86, 015202 (2012).

Figure 6. S_{11} channel fit results

$$\mathscr{P} = a + b \times s$$

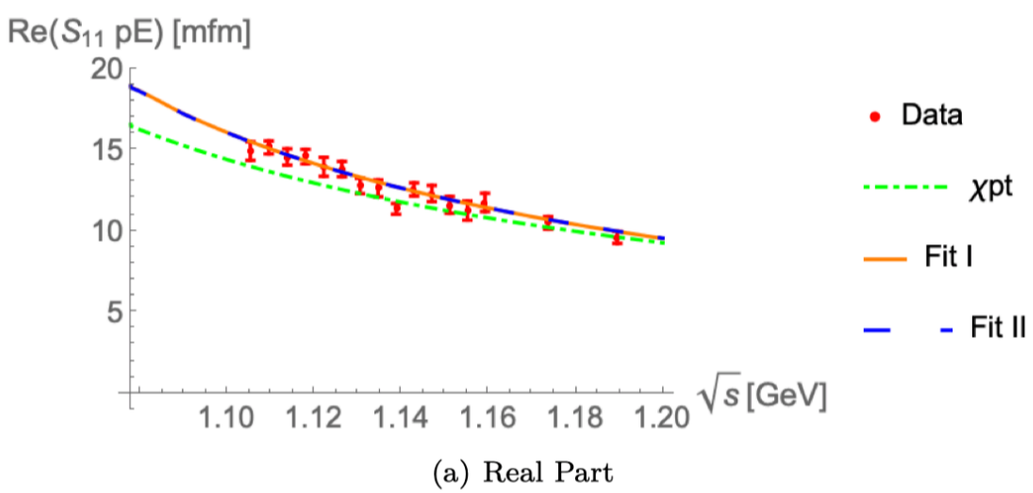

(a) Real Part

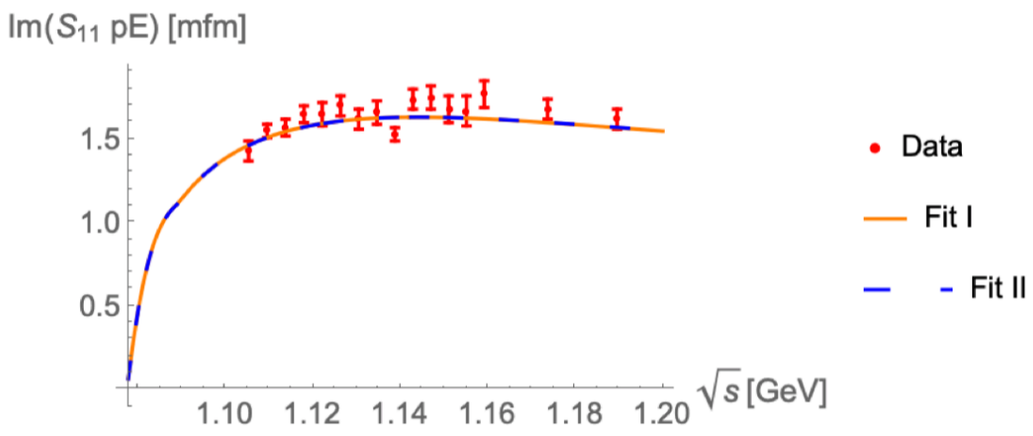

(b) Imaginary Part

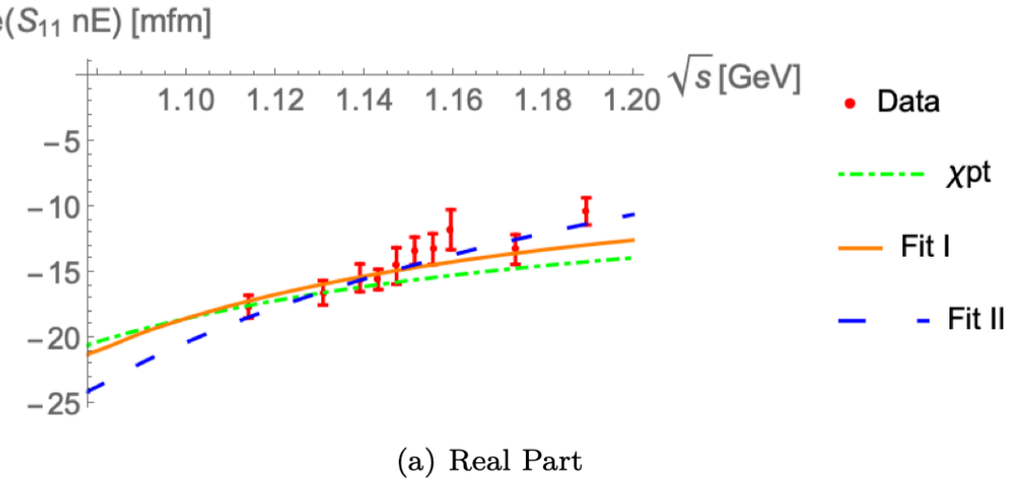

(a) Real Part

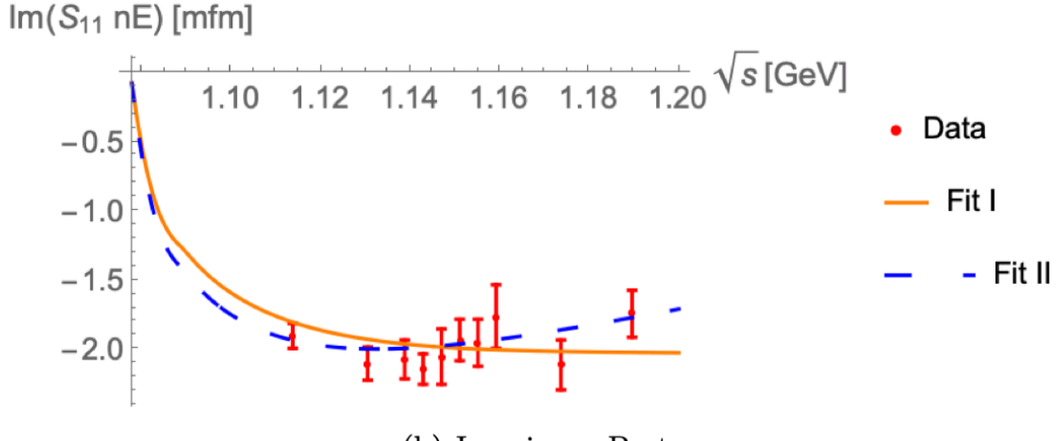

(b) Imaginary Part

Table 2. Fit results. a is dimensionless ， the unit of b is GeV^{-1}.

Target	Case	Parameter	Value	$\chi^2/d.o.f$
p	Fit I	$10^4 \times a$	-7.12 ± 13.34	1.58
	Fit II	$10^4 \times a$	2.87 ± 325.25	1.63
		$10^4 \times b$	-21.0 ± 250.4	
n	Fit I	$10^2 \times a$	-1.43 ± 0.35	1.22
	Fit II	$10^2 \times a$	12.50 ± 6.90	0.643
		$10^2 \times b$	-10.4 ± 5.2	

Parameters of Fit II are high correlated.

4.2 About $N^*(890)$

Analytic Continuation

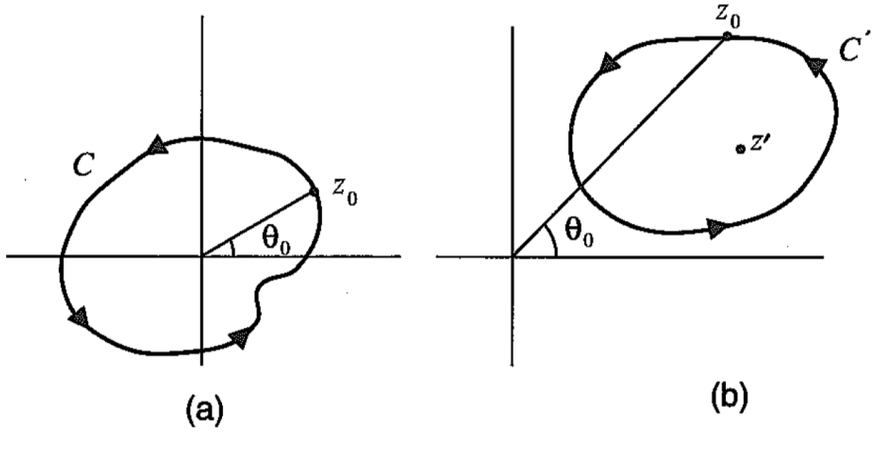

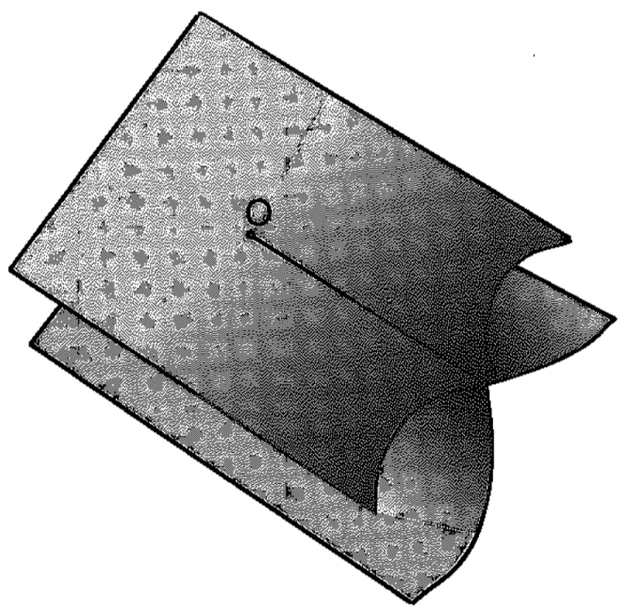

$$T(s) = \left[T(s^*)\right]^*$$

$$S(s) = \left[S(s^*)\right]^*$$

$$T(s - \mathrm{i}\epsilon) = T^{\mathrm{II}}(s + \mathrm{i}\epsilon)$$

$$T(s + \mathrm{i}\epsilon) - T^{\mathrm{II}}(s + \mathrm{i}\epsilon) = 2\mathrm{i}\rho(s + \mathrm{i}\epsilon)T(s + \mathrm{i}\epsilon)T^{\mathrm{II}}(s + \mathrm{i}\epsilon)$$

$$T^{\mathrm{II}} = \frac{T}{1 + 2\mathrm{i}\rho T} = \frac{T}{S}$$

$$S^{\mathrm{II}} = 1 + 2\mathrm{i}\rho^{\mathrm{II}}T^{\mathrm{II}} = 1 - 2\mathrm{i}\rho\frac{T}{S} = \frac{1}{S}$$

Couplings Extraction

$$\mathscr{M}^{\mathrm{II}}(s) = \frac{\mathscr{M}(s)}{\mathscr{S}(s)} \qquad \mathscr{S}(s) \approx \mathscr{S}'(z_{\mathrm{R}})\left(s - z_{\mathrm{R}}\right) \qquad \mathscr{M}^{\mathrm{II}}(s) = \frac{\mathscr{M}(s)}{\mathscr{S}'(z_{\mathrm{R}})\left(s - z_{\mathrm{R}}\right)}$$

$$g_\gamma g_\pi = \frac{\mathscr{M}(z_{\mathrm{R}})}{\mathscr{S}'(z_{\mathrm{R}})}$$

$$g_\pi^2 = \frac{\mathscr{T}(z_{\mathrm{R}})}{\mathscr{S}'(z_{\mathrm{R}})}$$

$$\mathscr{A}^{\frac{1}{2}} = g_\gamma \sqrt{\frac{\pi}{q_r^2 m_N}} \rho_{\gamma N}$$

$$\Gamma_{\gamma N} = \left| \rho_{\gamma N} \frac{g_\gamma^2}{\sqrt{z_R}} \right|$$

Table 3. Residues. The unit of residue is $10^{-2} \times \mathrm{GeV}^2$, the unit of pole position is GeV.

		$g_\gamma g_\pi$				g_π^2	
		Fit I		Fit II			
Target	Pole Position	Moduli	Phase	Moduli	Phase	Moduli	Phase
p	0.882-0.190i	$1.212^{+0.014}_{-0.013}$	$-79.2^{+1.3}_{-1.2}$	$1.203^{+0.302}_{-0.277}$	$-78.9^{+11.4}_{-6.9}$	19.7	32.6
	0.960-0.192i	1.467 ± 0.016	-71.3 ± 0.9	$1.459^{+0.279}_{-0.274}$	$-71.2^{+3.5}_{-2.4}$	21.4	33.6
n	0.882-0.190i	$0.6416^{+0.0265}_{-0.0164}$	111 ± 7	$2.025^{+0.731}_{-0.706}$	$81.4^{+6.9}_{-3.4}$		
	0.960-0.192i	$1.111^{+0.050}_{-0.043}$	-103 ± 3	$2.342^{+0.603}_{-0.605}$	98^{+2}_{-1}		

$N^*(890)$ vs $N^*(1535)$: $0.2\mathrm{GeV}^2$ vs $0.08\mathrm{GeV}^2$ ($|g_\pi^2|$);
$0.032\mathrm{GeV}$ vs $0.024\mathrm{GeV}^2$ ($|g_\gamma|$).

[45] R. L. Workman, L. Tiator, and A. Sarantsev, Phys. Rev. C87, 3 (2013).

[46] A. Švarc et al., Phys. Rev. C89, 065208 (2014).

Table 4. Decay amplitude at pole position and decay width. The unit of $\mathscr{A}^{\frac{1}{2}}$ is $\mathrm{GeV}^{-\frac{1}{2}}$, and the unit of $\Gamma_{\gamma N}$ is MeV.

Target	$\mathscr{A}^{\frac{1}{2}}$				$\Gamma_{\gamma N}$	
	Fit I		Fit II		Fit I	Fit II
	Moduli	Phase	Moduli	Phase		
p	0.165 ± 0.002	-129 ± 2	$0.165^{+0.042}_{-0.038}$	-129^{+12}_{-7}	$0.369^{+0.009}_{-0.008}$	$0.363^{+0.204}_{-0.149}$
	$0.191^{+0.003}_{-0.002}$	-43 ± 1	$0.191^{+0.037}_{-0.036}$	-43^{+4}_{-3}	0.396 ± 0.009	$0.391^{+0.164}_{-0.134}$
n	$0.0878^{+0.0413}_{-0.0380}$	31 ± 7	$0.277^{+0.101}_{-0.097}$	$10.7^{+6.9}_{-3.4}$	$0.103^{+0.009}_{-0.006}$	1.03 ± 0.60
	$0.144^{+0.007}_{-0.006}$	130 ± 3	0.305 ± 0.079	125^{+2}_{-1}	$0.227^{+0.021}_{-0.018}$	1.01 ± 0.46

$$N^*(1535): \ |\mathscr{A}^{\frac{1}{2}}| = 0.074\mathrm{GeV}^{-\frac{1}{2}}, \ \Gamma_{\gamma N} \approx 0.3\mathrm{MeV}$$

[47] R. A. Arndt, W. J. Briscoe, I. I. Strakovsky, and R. L. Workman, Phys. Rev. C74, 1 (2006).

5. Summary and Outlook

1. Use a dispersion relation about single pion photoproduction ;
2. Extract couplings of $N^*(890)$;
3. The couple channel analysis and research on single pion eletroproduction are ongoing.

Thank you !

6.Backup

Relevant interaction vertex

$$\mathscr{L}^{(1)}_{\pi N} \supset +\frac{g_A}{2F_\pi}\partial_\mu\phi\bar{\Psi}\gamma_5\gamma^\mu\Psi - \frac{e}{2}A_\mu\bar{\Psi}\left[\gamma^\mu\left(\tau_3+1\right)\right]\Psi - i\frac{eg_A}{4F_\pi}A_\mu\bar{\Psi}\left(\gamma_5\gamma^\mu\left[\phi,\tau_3\right]\right)\Psi$$

$$\mathscr{L}^{(2)}_{\pi N} \supset -e\bar{\Psi}\sigma^{\mu\nu}\left[\frac{c_6}{2}\left(\partial_\mu A_\nu - \partial_\nu A_\mu\right)\tau_3 + \frac{c_7}{4}\left(\partial_\mu A_\nu - \partial_\nu A_\mu\right)\right]\Psi$$

$$\mathscr{L}^{(2)}_{\pi\pi} \supset -\frac{ie}{8}A^\mu Tr\left(\left\{\partial_\mu\phi,\left[\phi,\tau_3\right]\right\}\right)$$

Normalization about multipole amplitude

$$E^{I=\frac{1}{2}\ \mathrm{II}}_{0+}(s\to z_R) = -\sqrt{\frac{2}{3s}}\frac{g_\gamma g_\pi}{s-z_R} = -\sqrt{\frac{2}{3s}}\frac{g_\gamma g_\pi}{2\sqrt{z_R}(\sqrt{s}-\sqrt{z_R})}$$

$\pi\pi$ 散射相移拟合

$$M_\rho = 757.0 \pm 0.4\,\mathrm{MeV}\,, \qquad \Gamma_\rho = 152.2 \pm 0.6\,\mathrm{MeV}$$
$$M_{f^0} = 984.5 \pm 2.3\,\mathrm{MeV}\,, \qquad \Gamma_{f^0} = 34.4 \pm 6.8\,\mathrm{MeV}$$
$$M_\sigma = 457 \pm 15\,\mathrm{MeV}\,, \qquad \Gamma_\sigma = 551 \pm 28\,\mathrm{MeV}\,.$$

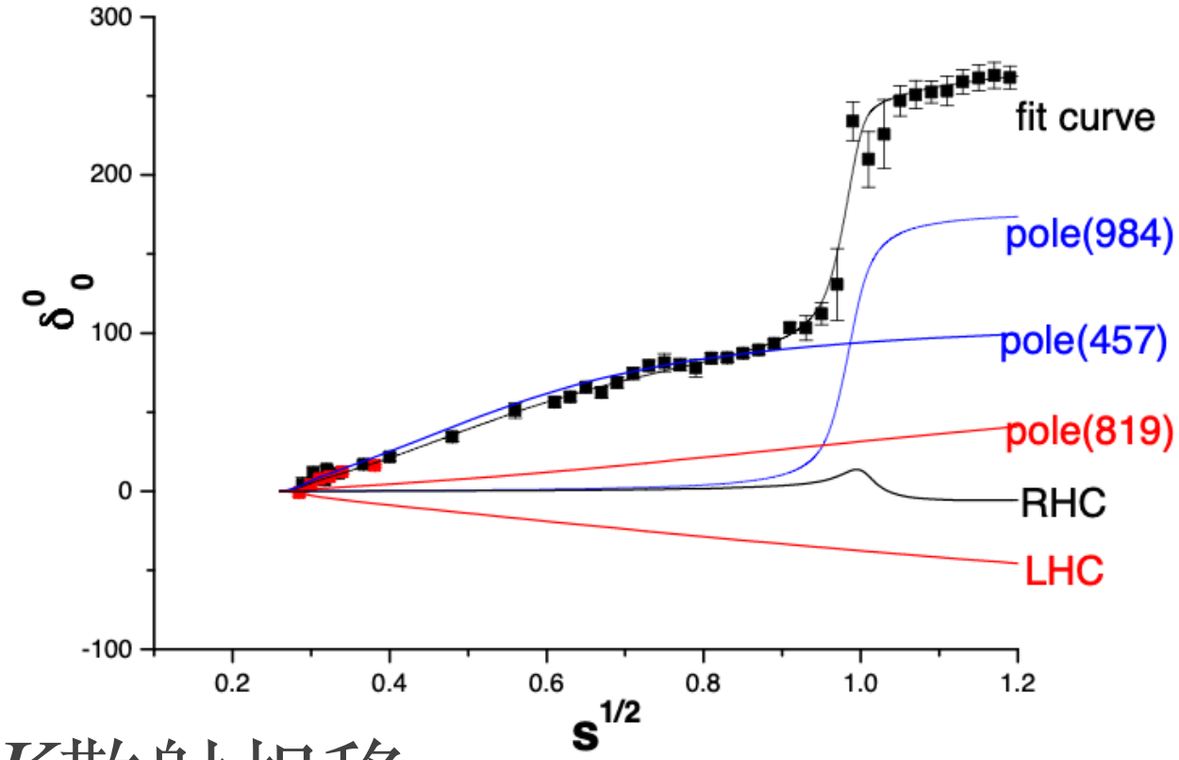

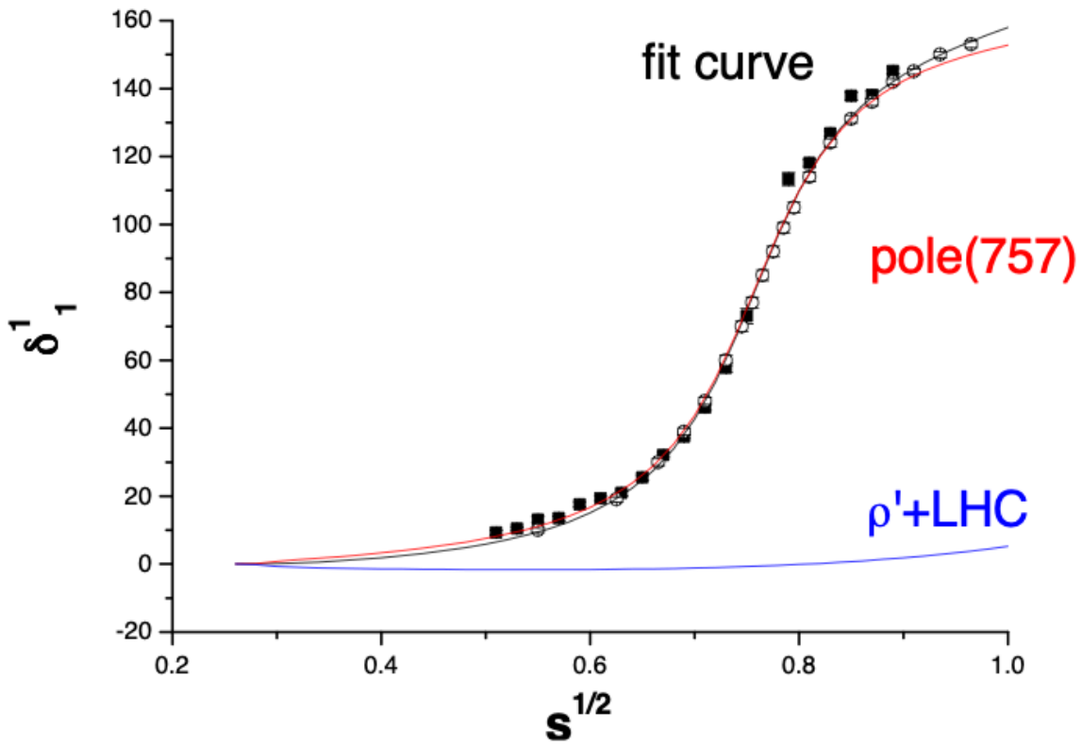

πK散射相移

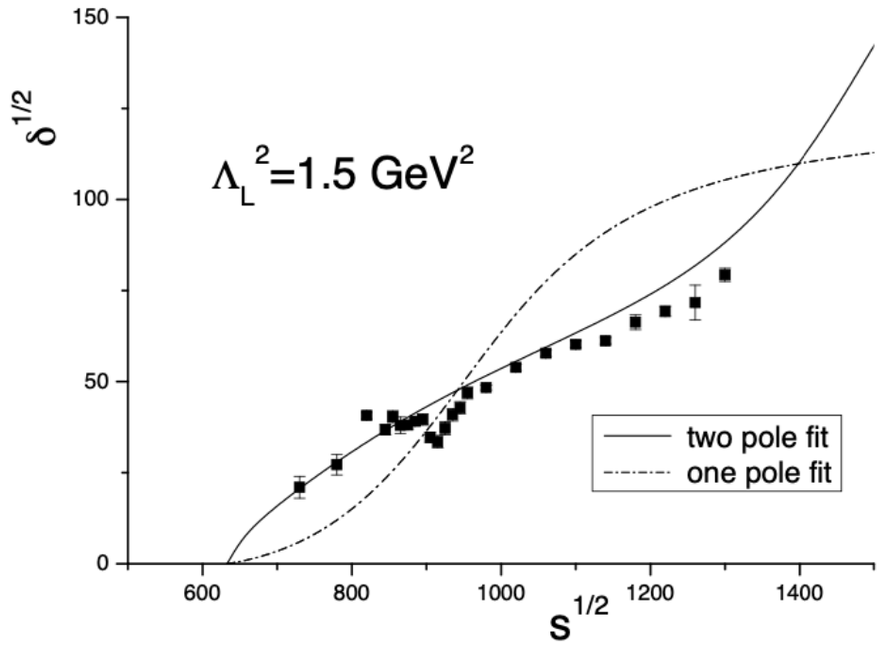

$\chi^2_{d.o.f.} = 623.6/(68-4)$;
$M_\kappa = 651 \pm 20 MeV$, $\Gamma_\kappa = 685 \pm 13 MeV$;
$M_{K_0^{II}(1430)} = 1491 \pm 7 MeV$, $\Gamma_{K_0^{II}(1430)} = 346 \pm 14 MeV$

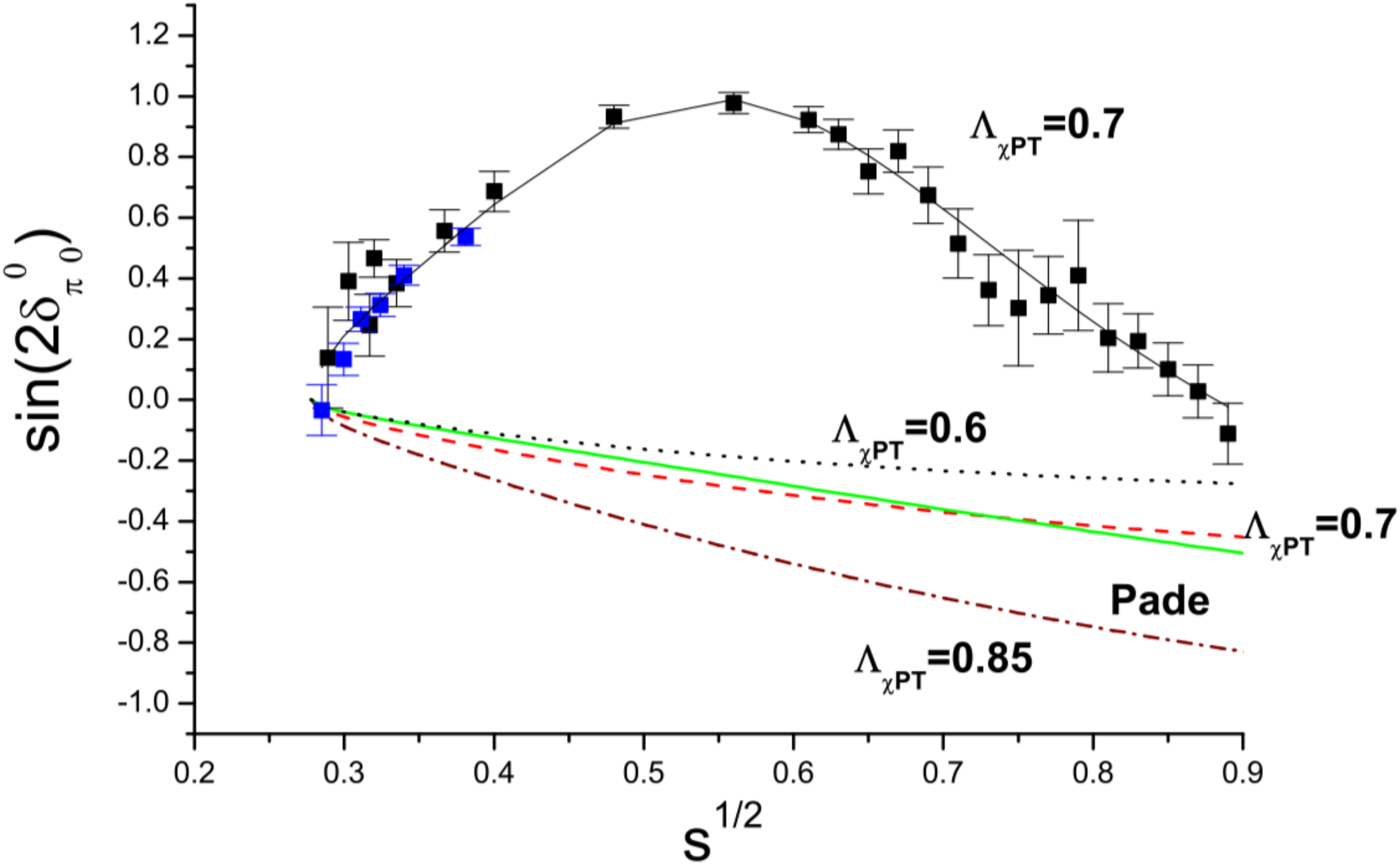
$\sin(2\delta^0_{\pi^0})$
$s^{1/2}$
$\Lambda_{\chi PT}$=0.7
$\Lambda_{\chi PT}$=0.6
$\Lambda_{\chi PT}$=0.7
Pade
$\Lambda_{\chi PT}$=0.85
1.2
1.0
0.8
0.6
0.4
0.2
0.0
-0.2
-0.4
-0.6
-0.8
-1.0
0.2
0.3
0.4
0.5
0.6
0.7
0.8
0.9

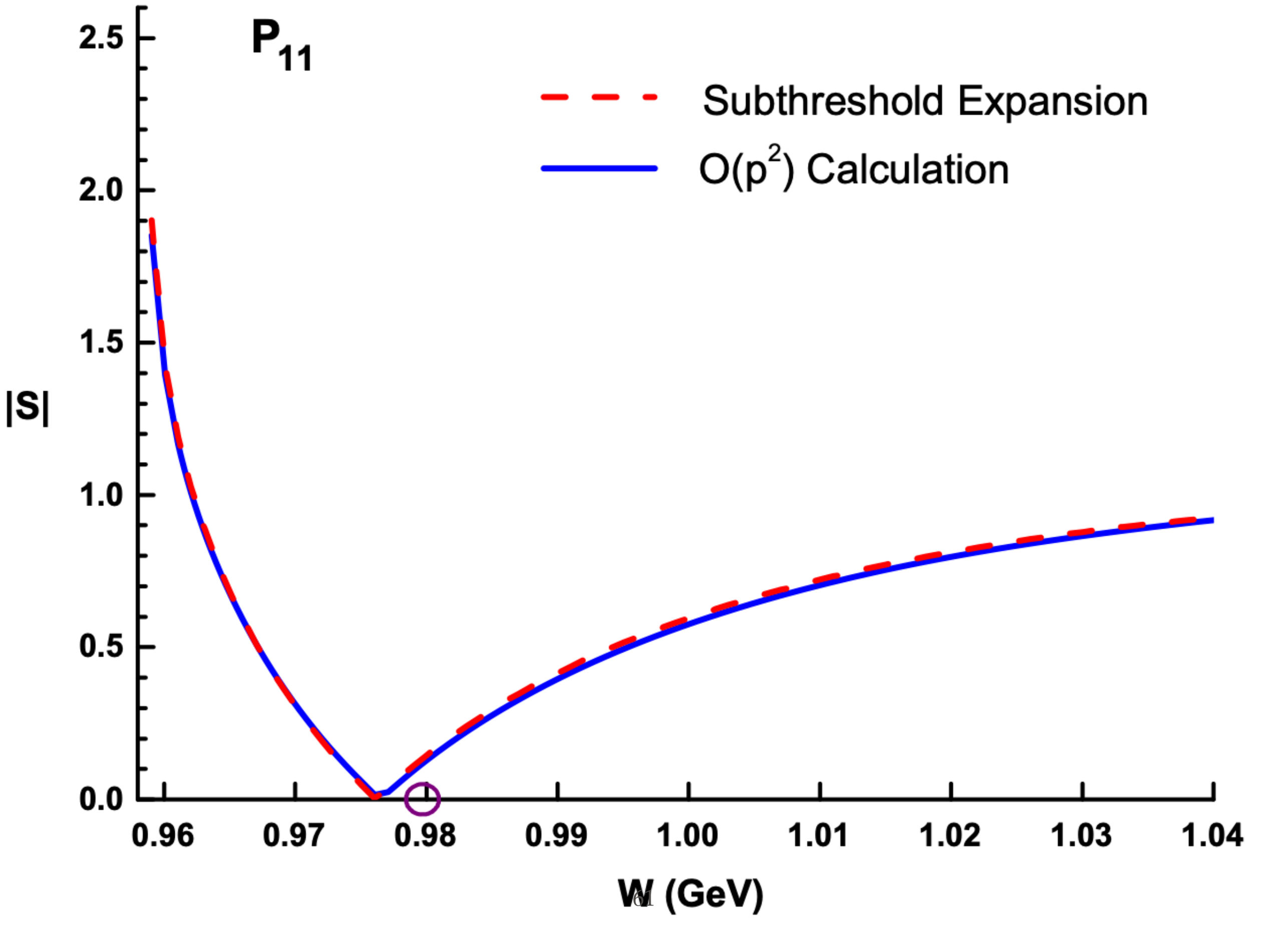
P11
Subthreshold Expansion
O(p2) Calculation
|S|
2.5
2.0
1.5
1.0
0.5
0.0
0.96
0.97
0.98
0.99
1.00
1.01
1.02
1.03
1.04
W (GeV)

Photoprodcution of mesons in Hydrogen

[D. C. Oakley and R. L. Walker, Phys. Rev., 1283 (1955).

$$\gamma + p \rightarrow p + \pi^0 \qquad \pi^0 \rightarrow 2\gamma$$

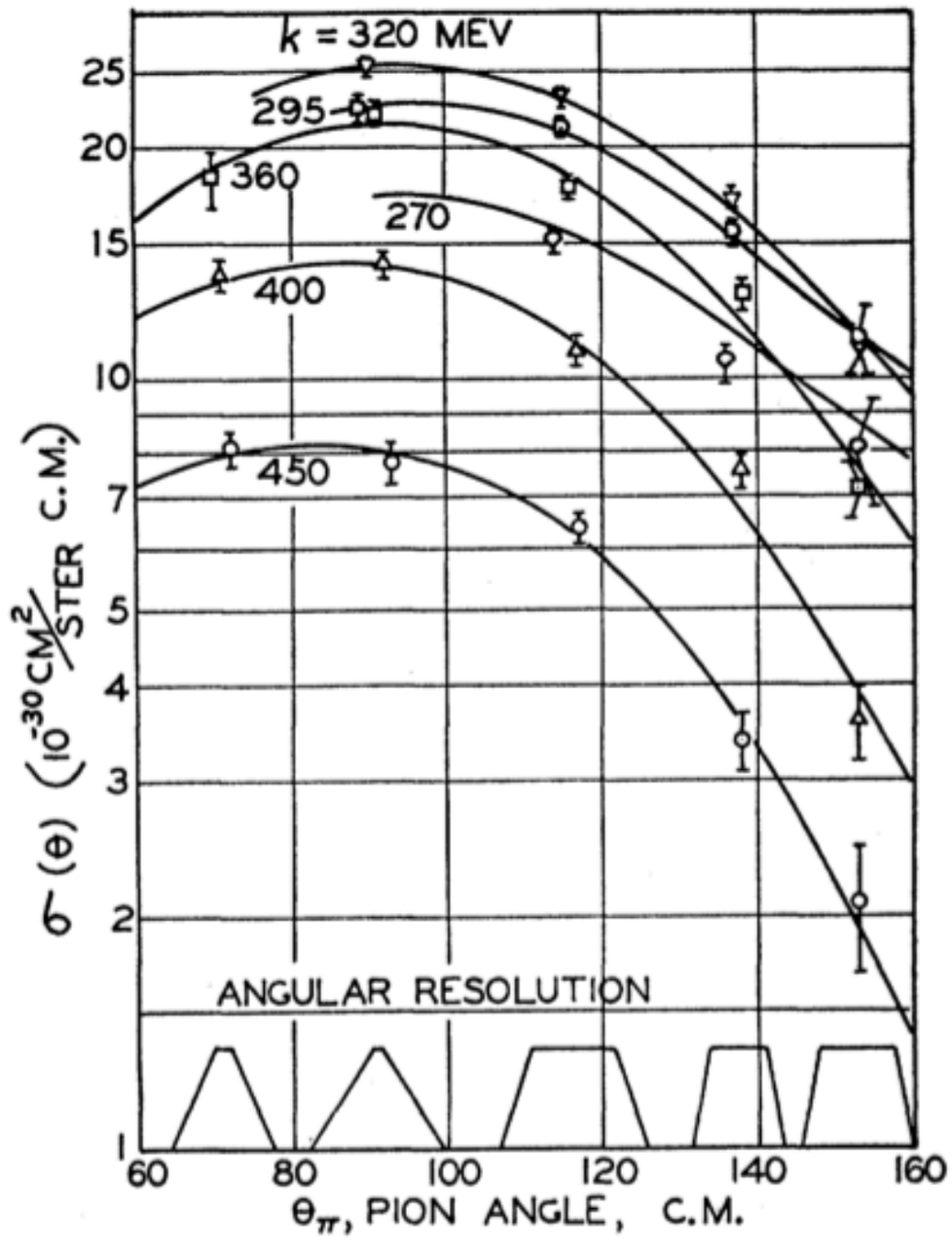

$$\gamma + p \rightarrow n + \pi^+$$ R. L. Walker et al, Phys. Rev., 210 (1955)

$$\pi - \mu - e$$

decay

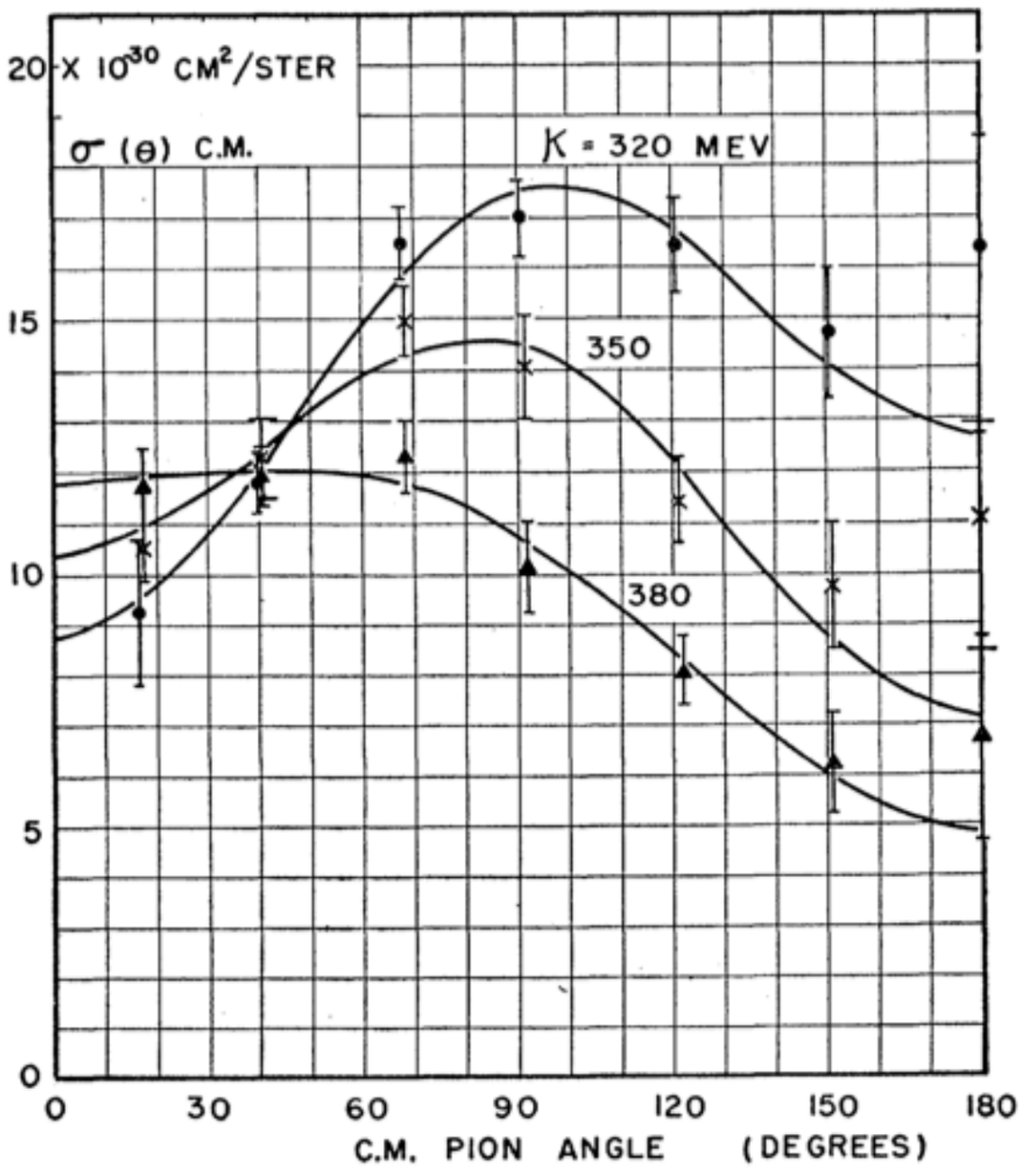

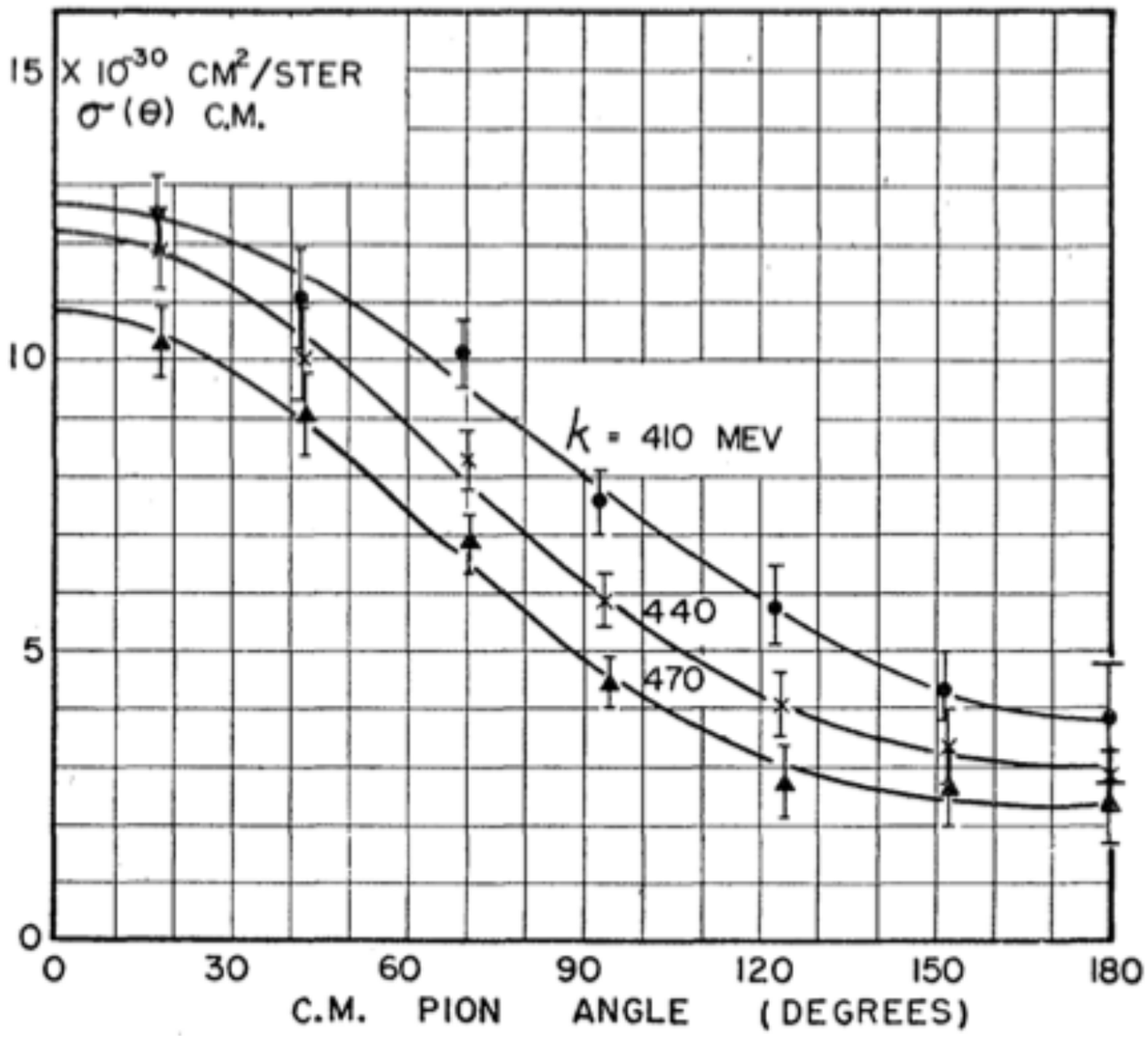

Photoproduction of negative and positive Pions from Deuterium

G. Neugebauer, W. Wales and R. L. Walker, Phys. Rev., 1726 (1960)

$$\gamma + d \rightarrow \pi^+ + p + p$$
$$\gamma + d \rightarrow \pi^- + n + n$$

$$\gamma + p \rightarrow \pi^+ + n$$
$$\gamma + n \rightarrow \pi^- + p$$

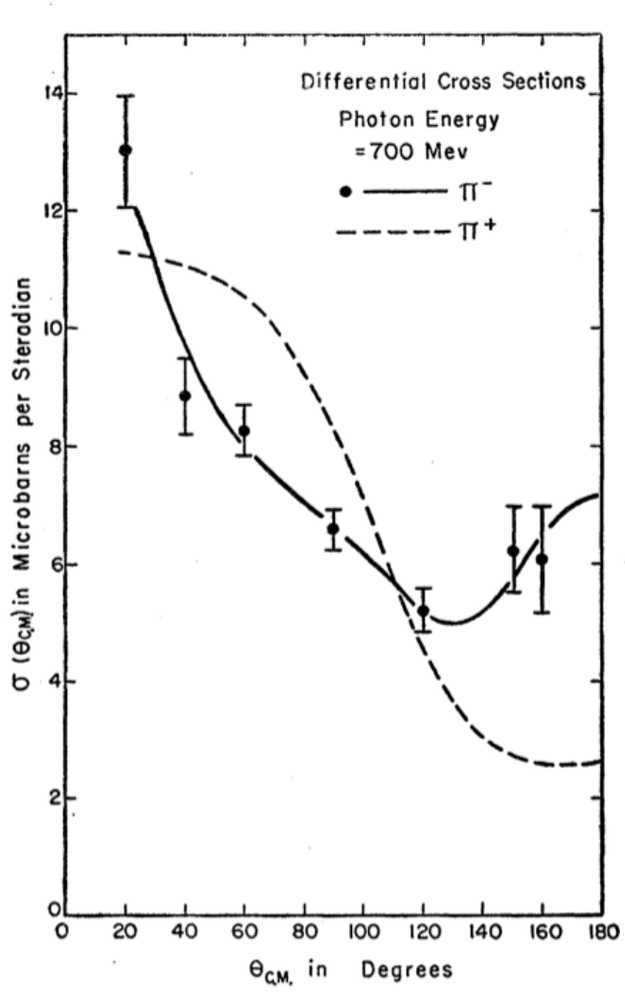

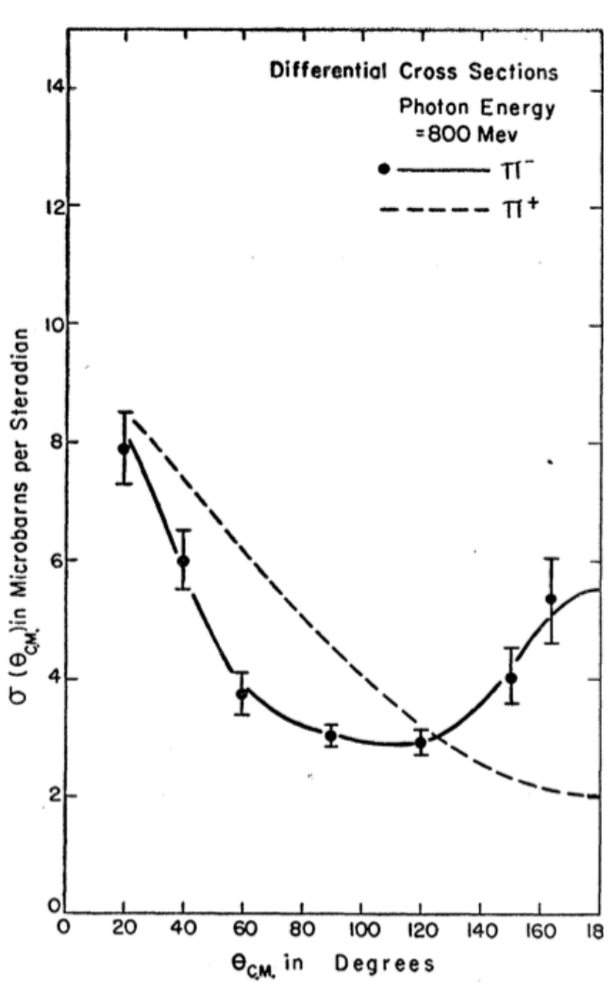

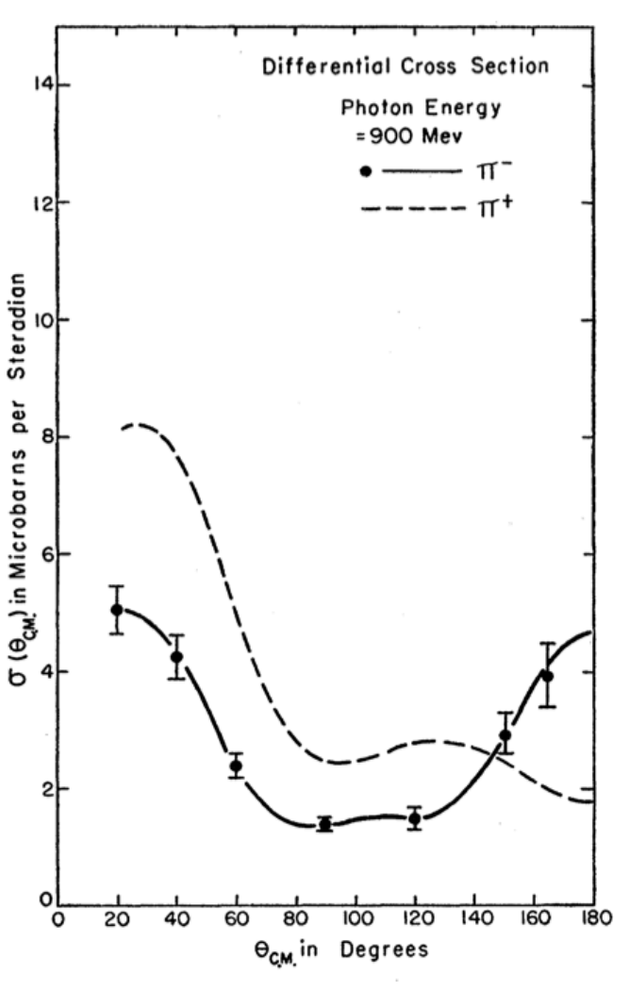

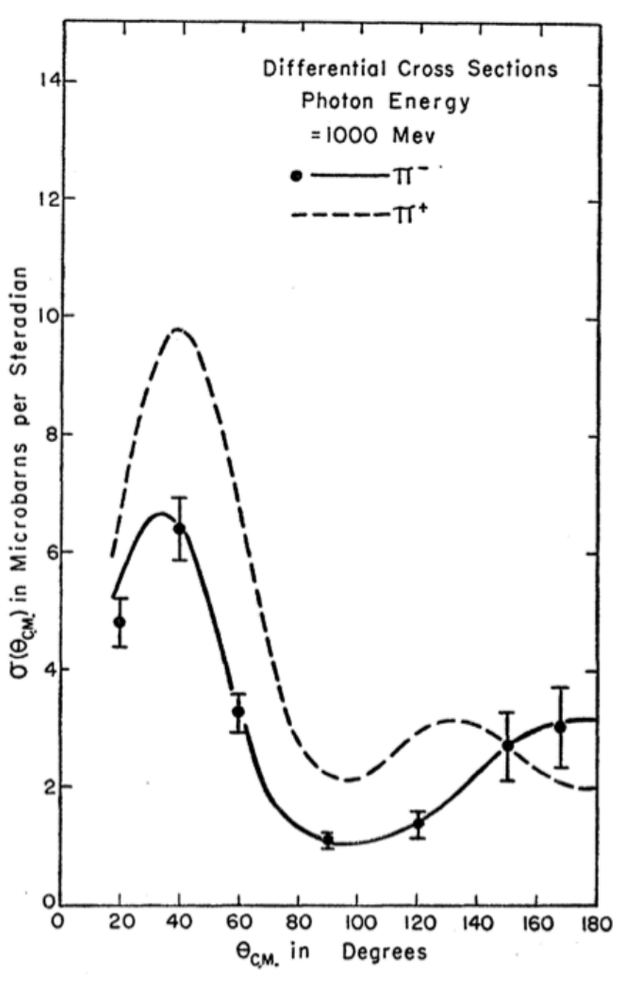

More detailed experimental datas and multipole amplitudes analysis

J. Ahrens et al., GDH, A2, Eur. Phys. J. A21, 323 (2004).

Target: C_4H_9OH

$p\pi^0$

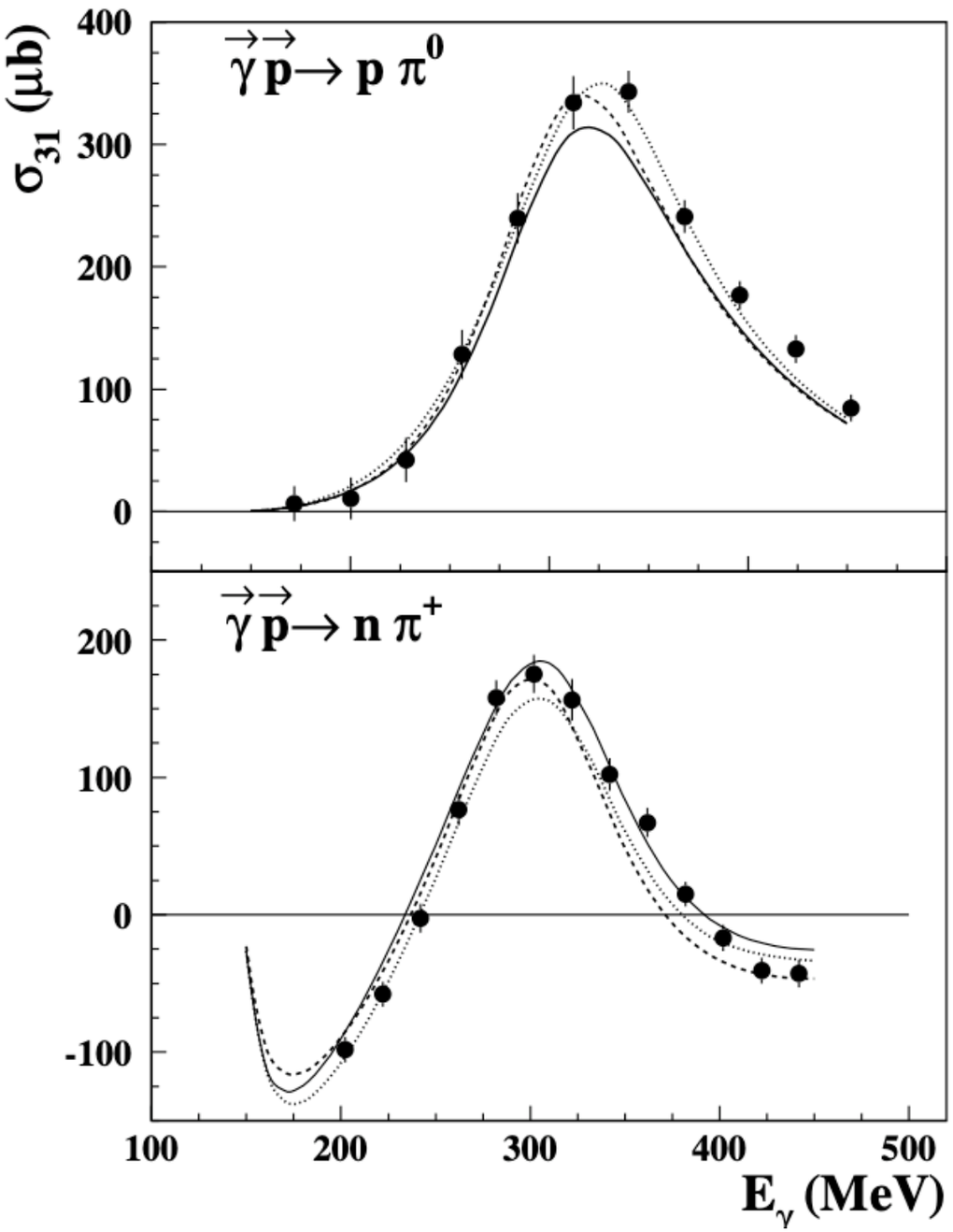

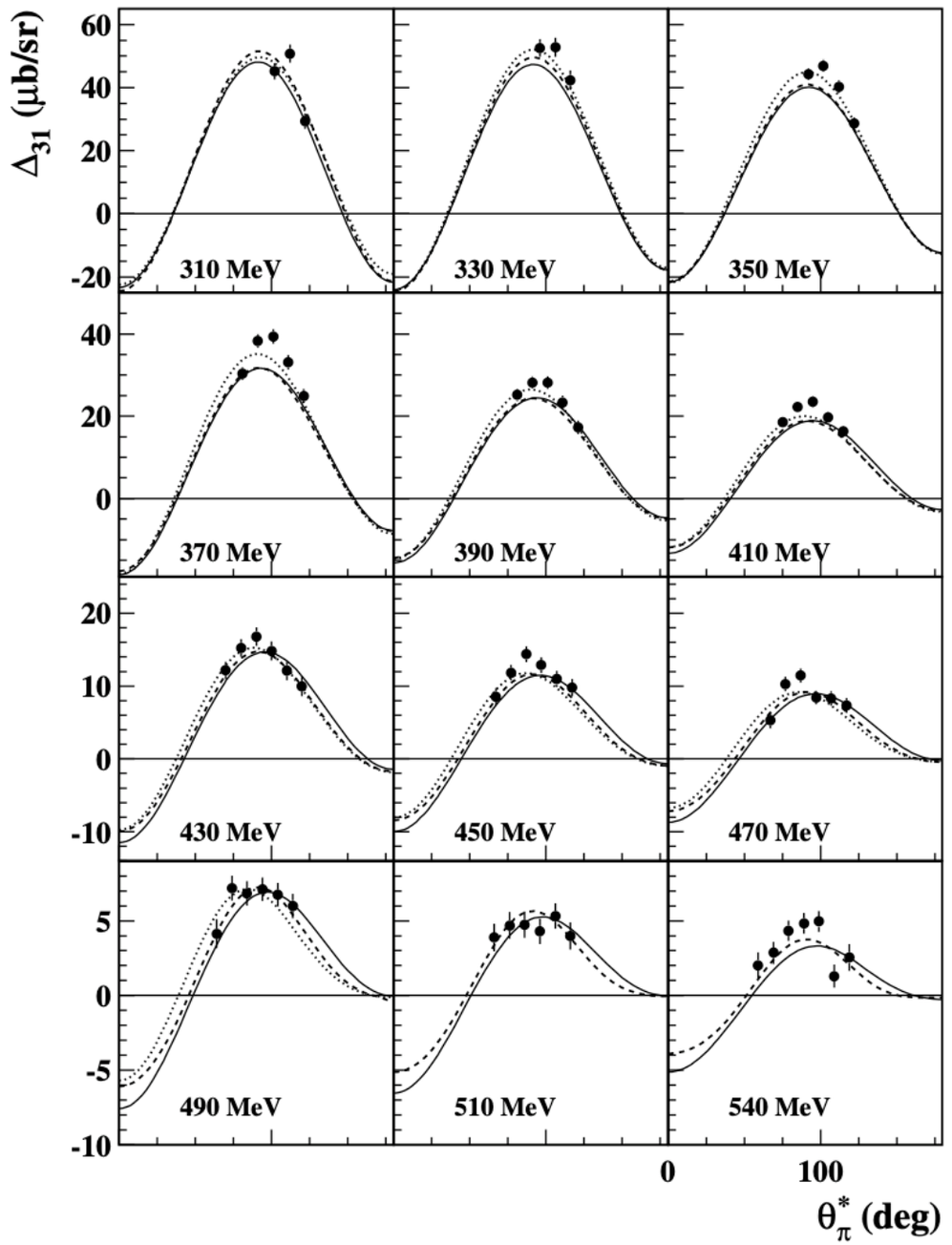

$n\pi^+$

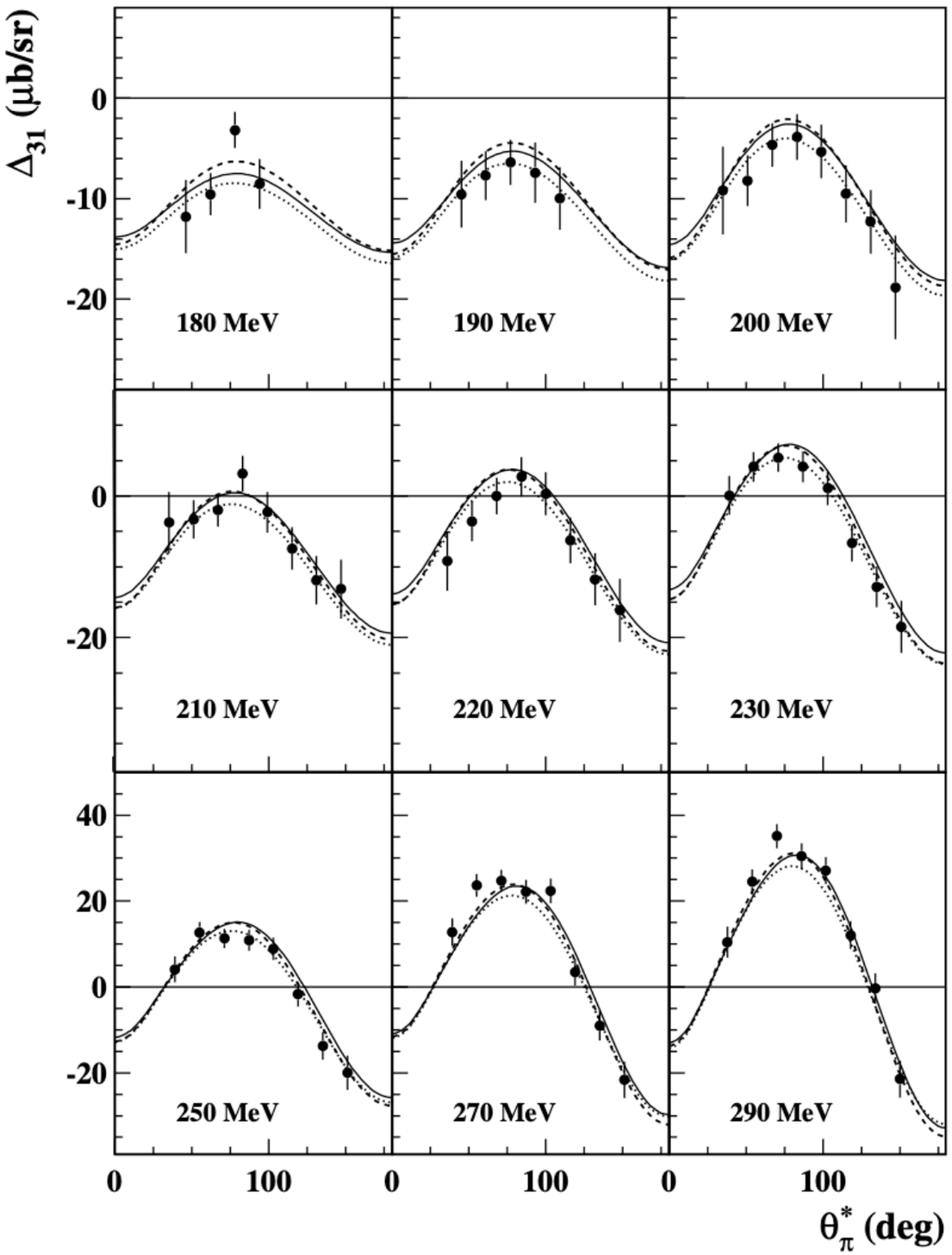
Δ_{31} (μb/sr)
0
-10
-20
180 MeV
190 MeV
200 MeV
0
-20
210 MeV
220 MeV
230 MeV
40
20
0
-20
250 MeV
270 MeV
290 MeV
0
100
0
100
0
100
θ^*_π (deg)

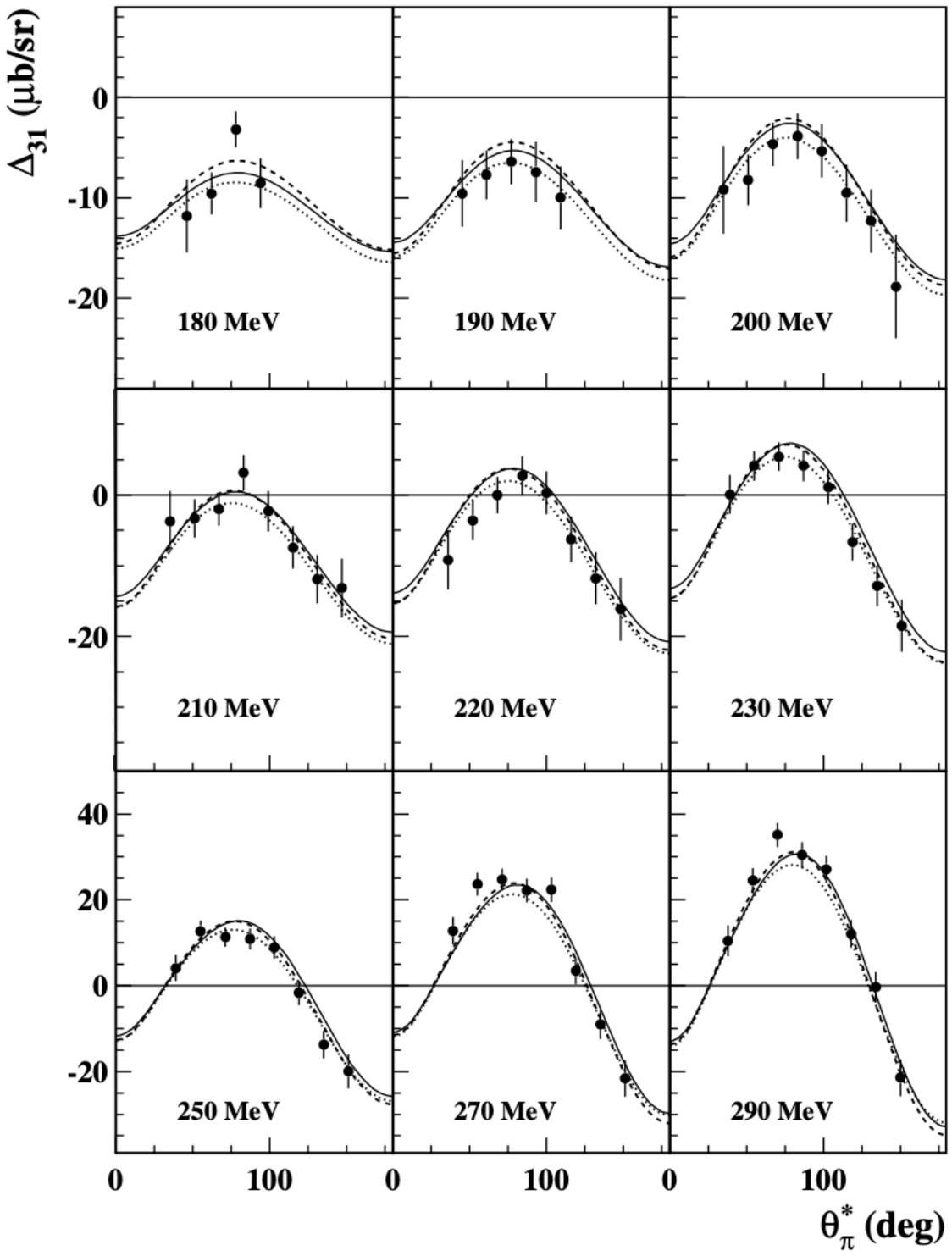
Δ_{31} (μb/sr)
0
-10
-20
180 MeV
190 MeV
200 MeV
0
-20
210 MeV
220 MeV
230 MeV
40
20
0
-20
250 MeV
270 MeV
290 MeV
0
100
0
100
0
100
θ^*_π (deg)

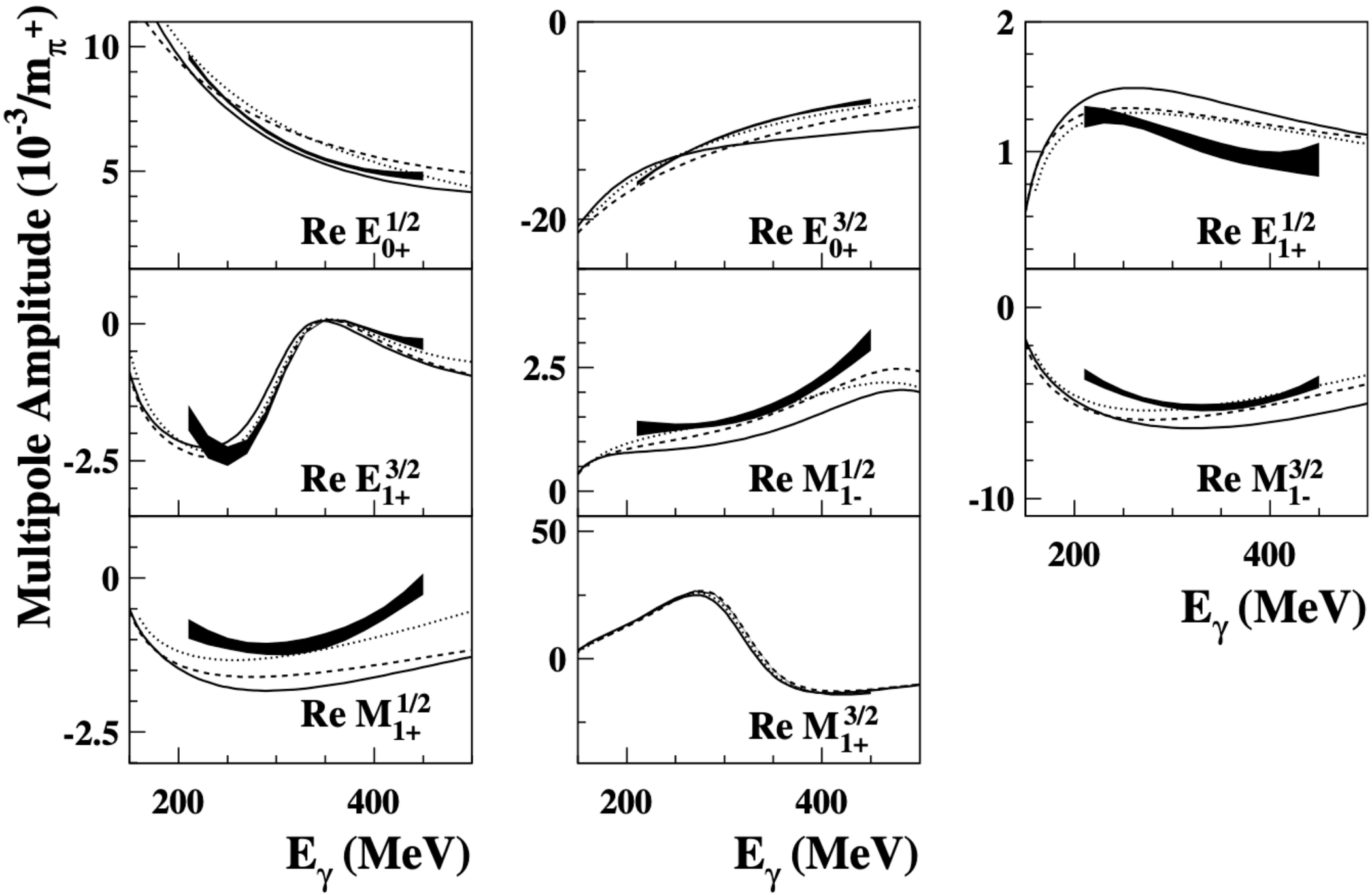
Multipole Amplitude ($10^{-3}/m_{\pi^+}$)
Re $E_{0+}^{1/2}$
Re $E_{0+}^{3/2}$
Re $E_{1+}^{1/2}$
Re $E_{1+}^{3/2}$
Re $M_{1-}^{1/2}$
Re $M_{1-}^{3/2}$
Re $M_{1+}^{1/2}$
Re $M_{1+}^{3/2}$
E_γ (MeV)
E_γ (MeV)
E_γ (MeV)